TECHNISCHE UNIVERSITÄT MÜNCHEN

TUM School of Life Sciences

The potential of extracellular microRNAs as diagnostic biomarkers for acute pulmonary infections

Stefanie Nastasja Hermann

Vollständiger Abdruck der von der TUM School of Life Sciences der Technischen Universität München zur Erlangung des akademischen Grades einer

Doktorin der Naturwissenschaften

genehmigten Dissertation.

Vorsitzende: Prof. Angelika Schnieke, Ph.D.

Prüfende der Dissertation: 1. apl. Prof. Dr. Michael W. Pfaffl

2. apl. Prof. Dr. Gustav Schelling

3. Prof. Dr. Stefan Holdenrieder

Die Dissertation wurde am 26.08.2021 bei der Technischen Universität München eingereicht und durch die TUM School of Life Sciences am 10.03.2022 angenommen.

Table of Contents

Abbreviations

ACE2	Angiotensin-converting enzyme 2
AGO	Argonaute protein
ALIX	ALG-2 interacting protein X
ApoA1	Apolipoprotein A1
APOH	Apolipoprotein H
ARF6	ADP-ribosylation factor 6
CAP	Community-acquired pneumonia
CCR4	Carbon catabolite repressor 4
cDNA	Copy DNA
CNX	Calnexin
CRP	C-reactive protein
CURB-65	Confusion, Blood Urea, Respiratory Rate, Blood Pressure, Age ≥ 65
Cq	Cycle quantification
DAMP	Danger-associated molecular pattern
DCP1/DCP2	MRNA-decapping enzyme 1/2
DDX6	DEAD box helicase DEAD box protein 6
DGCR8	DiGeorge Syndrome Critical Region 8
DGE	Differential gene expression
eIF4F	Eukaryotic translation initiation factor 4F
ESCRT	Endosomal sorting complex required for transport
EV	Extracellular vesicle
Exp5	Exportin 5
IL-6	Interleukin-6
IL-19	Interleukin-19
ILV	Intraluminal vesicle
IPA	Ingenuity Pathway Analysis
ISEV	International Society for Extracellular Vesicles
lncRNA	Long non-coding RNA
MAPK	Mitogen-activated protein kinase
m7G	7-methylguanylate
miRNA	MicroRNA
MISEV	Minimal Information for Studies of Extracellular Vesicles
mRNA	Messenger RNA
MVE	Multivesicular endosome
NF-κB	Nuclear factor-κB
NGS	Next-generation sequencing
NOT	Negative regulator of transcription
ns	Not significant
nt	Nucleotides
NTA	Nanoparticle tracking analysis

ORF	Open reading frame
OR52N2	Olfactory Receptor Family 52 Subfamily N Member 2
PAMPs	Pathogen-associated molecular patterns
PARN2/3	Poly(A)-specific ribonuclease 2/3
P-body	Processing body
PCT	Procalcitonin
piRNA	PIWI-interacting RNA
PLS-DA	Partial-least-squares discriminant analysis
pre-miRNA	Precursor miRNA
pri-miRNA	Primary miRNA
PRR	Pattern-recognition receptor
PS	Phosphatidylserine
RAB	RAS-related protein
RANGTP	GTP-binding nuclear protein Ran
RISC	RNA-induced silencing complex
RNAse	Ribonuclease
RT-qPCR	Reverse transcription real-time PCR
SARS-CoV-2	Severe acute respiratory syndrome coronavirus type 2
SEC	Size-exclusion chromatography
SERPINB8	Serpin Peptidase Inhibitor, Clade B (Ovalbumin), Member 8
small RNA-seq	Small RNA sequencing
SNARE	Soluble N-ethylmaleimide-sensitive fusion attachment protein receptor
sPLS-DA	Sparse partial-least-squares discriminant analysis
TEM	Transmission electron microscopy
TNRC6	Trinucleotide repeat containing gene 6
TRBP	Trans-activation-responsive RNA-binding protein
UTR	Untranslated region
WB	Western blotting

Abstract

As means of intercellular communication, cells release extracellular vesicles (EVs) into the extracellular space. EVs encapsulate specific biomolecular cargoes by a protective lipid bilayer, important for signal transfer during physiological and pathological processes. The short regulatory microRNAs (miRNAs) mainly play a decisive role here, as they regulate gene expression in a highly specific manner on the post-transcriptional level. Disease-related changes in EV miRNA expression profiles in minimally invasive liquid biopsies make them promising candidates for use as biomarkers in clinical practice. Within the scope of this work, the suitability of blood-derived EV miRNAs for the early detection of acute pulmonary infections was investigated. In order to create the basis for these investigations, an optimized and MISEV-compliant workflow was developed. First, various methods for the isolation of EVs were tested to evaluate the ideal method for analyzing EV miRNAs by next-generation sequencing. Each method separated unique EV preparations, demonstrating the strong influence of sample preparation on downstream analysis. The precipitation method was particularly suitable due to its substantial miRNA yield, which precisely grouped healthy controls and sepsis patients. In addition, arterial and venous EV miRNA profiles were examined to compare their joint applicability in biomarker studies. Since, additionally to standard venous blood sampling in healthy controls or less severely ill patients, the collection takes place via existing arterial access in intensive care patients. The marginal differences between arterial and venous EV miRNA profiles suggest equivalent suitability. Finally, based on findings from the preliminary studies, a comprehensive human study was conducted. In this framework, an EV miRNA signature was developed and validated to enable the early detection of community-acquired pneumonia and sepsis as a severe secondary complication. Furthermore, EV-miRNAs were investigated as regulators in the pathophysiology of COVID-19. To prove the actual validity and applicability of EV miRNA biomarkers, the performance of multicenter studies in increasing cohorts is incessant. However, fundamental challenges in EV research currently still stand in the way of the clinical implementation of these promising biomarker candidates.

Zusammenfassung

Zur Steuerung der interzellulären Kommunikation setzen Zellen extrazelluläre Vesikel (EVs) in den extrazellulären Raum frei. EVs enthalten spezifische Biomoleküle, welche durch eine Doppellipidschicht geschützt für die Signalübertragung während physiologischer und pathologischer Prozesse dienen. Hierbei sind die kurzen regulatorischen miRNAs bedeutend, da diese hochspezifisch die Genexpression auf post-transkriptionaler Ebene regulieren. Krankheitsbedingte Veränderungen der EV-miRNA-Expressionsprofile in minimalinvasiven Flüssigbiopsien machen diese zu zukunftsträchtigen Biomarker-Kandidaten für die Anwendung in der klinischen Praxis. In dieser Arbeit wurde die Eignung aus Blut isolierter EV-miRNAs zur Früherkennung akuter pulmonaler Infektionen untersucht. Um die Basis für diese Untersuchungen zu schaffen, wurde ein optimierter MISEV-konformer Arbeitsablauf entwickelt. Zunächst wurden verschiedene Verfahren für die Isolation von EVs getestet, um die ideale Methode für die Analyse von EV-miRNAs mittels Next-Generation Sequencing zu evaluieren. Mit jedem Verfahren wurden einzigartige EV-Präparate isoliert, was den starken Einfluss der Probenaufbereitung auf die nachgeschaltete Analyse verdeutlicht. Das Präzipitationsverfahren überzeugte durch eine große miRNA-Ausbeute, die eine präzise Gruppierung gesunder Kontrollen und Sepsis-Patienten ermöglichte. Zusätzlich wurden arterielle und venöse EV-miRNA-Profile untersucht, um deren gemeinsame Anwendbarkeit in Biomarker-Studien zu vergleichen, da neben der venösen Standard-Blutgewinnung bei Gesunden oder weniger stark Erkrankten die Abnahme über bereits vorhandene arterielle Zugänge bei Intensivpatienten erfolgt. Die marginalen Unterschiede zwischen arteriellen und venösen EV-miRNA-Profilen sprechen für eine vergleichbare Eignung. Basierend auf den Erkenntnissen der Voruntersuchungen wurde schließlich eine umfassende Humanstudie durchgeführt. Es erfolgte die Entwicklung und Validierung einer EV-miRNA-Signatur, um die Früherkennung der ambulant erworbenen Pneumonie sowie der Sepsis als schwere Folgeerkrankung zu ermöglichen. Darüber hinaus wurden EV-miRNAs als Regulatoren in der COVID-19 Pathophysiologie untersucht. Zur Prüfung der tatsächlichen Validität und Anwendbarkeit von EV-miRNA-Biomarkern, ist die Durchführung multizentrischer Studien in größeren Kohorten unerlässlich. Grundlegende Herausforderungen in der EV-Forschung stehen der klinischen Umsetzung dieser zukunftsträchtigen Biomarker-Kandidaten aktuell noch entgegen.

1 Introduction

1.1 MicroRNAs are gene expression master regulators

MicroRNAs (miRNAs) are short, endogenous, non-coding RNAs of ~22 nucleotides (nt) in length, which regulate gene expression post-transcriptionally. In 1993, the first miRNA was described in the nematode *C. elegans* [1, 2]. Upon discovering miRNAs in other organisms and particularly humans seven years later [3, 4], miRNAs were defined as a separate class of partially highly conserved small gene-regulatory RNAs [5-7]. Since then, in the early 2000s, miRNAs have emerged in diverse research areas.

Currently, this large class of small RNAs comprises 48,860 mature miRNAs from 271 different organisms. Thereof 2,654 mature sequences are found in humans [8]. MiRNAs target approximately > 60 % of human protein-coding genes. Along with the fact that in mammals, most conserved miRNAs have conserved messenger RNA (mRNA) targets [9], it has become evident that miRNAs are fundamentally involved in regulating all biological pathways. In humans, most miRNAs are encoded within the introns (intronic) of protein-coding and non-coding genes, while some are located in protein-coding regions (exonic). MiRNAs are encoded by individual genes (monocistronic) or by gene clusters (polycistronic) that are generally co-transcribed [10].

The canonical pathway of mammalian miRNAs biogenesis (Figure 1) initiates in the nucleus, where mainly RNA polymerase II transcribes the primary miRNA (pri-miRNA) from its gene [11]. The 5' capped and 3' polyadenylated pri-miRNA transcript consists of hundreds of nt and is sequentially processed [12, 13]. The microprocessor complex, assembled by the ribonuclease (RNAse) III enzyme Drosha and cofactors, including the RNA-binding protein DGCR8, converts the pri-miRNA into the precursor miRNA (pre-miRNA) [14]. DGCR8 recognizes the pri-miRNA through specific motifs [15], while Drosha cleaves the pri-miRNA into the ~70 nt pre-miRNA with its characteristic 2 nt 3' overhang [13, 16].

Besides, several pathways of non-canonical miRNA biogenesis exist, e.g., mirtons. Intron lariats are excised from intronic regions of the mRNA via splicing. After linearization by the debranching enzyme, mirtons fold into pre-miRNAs and bypass Drosha processing [17].
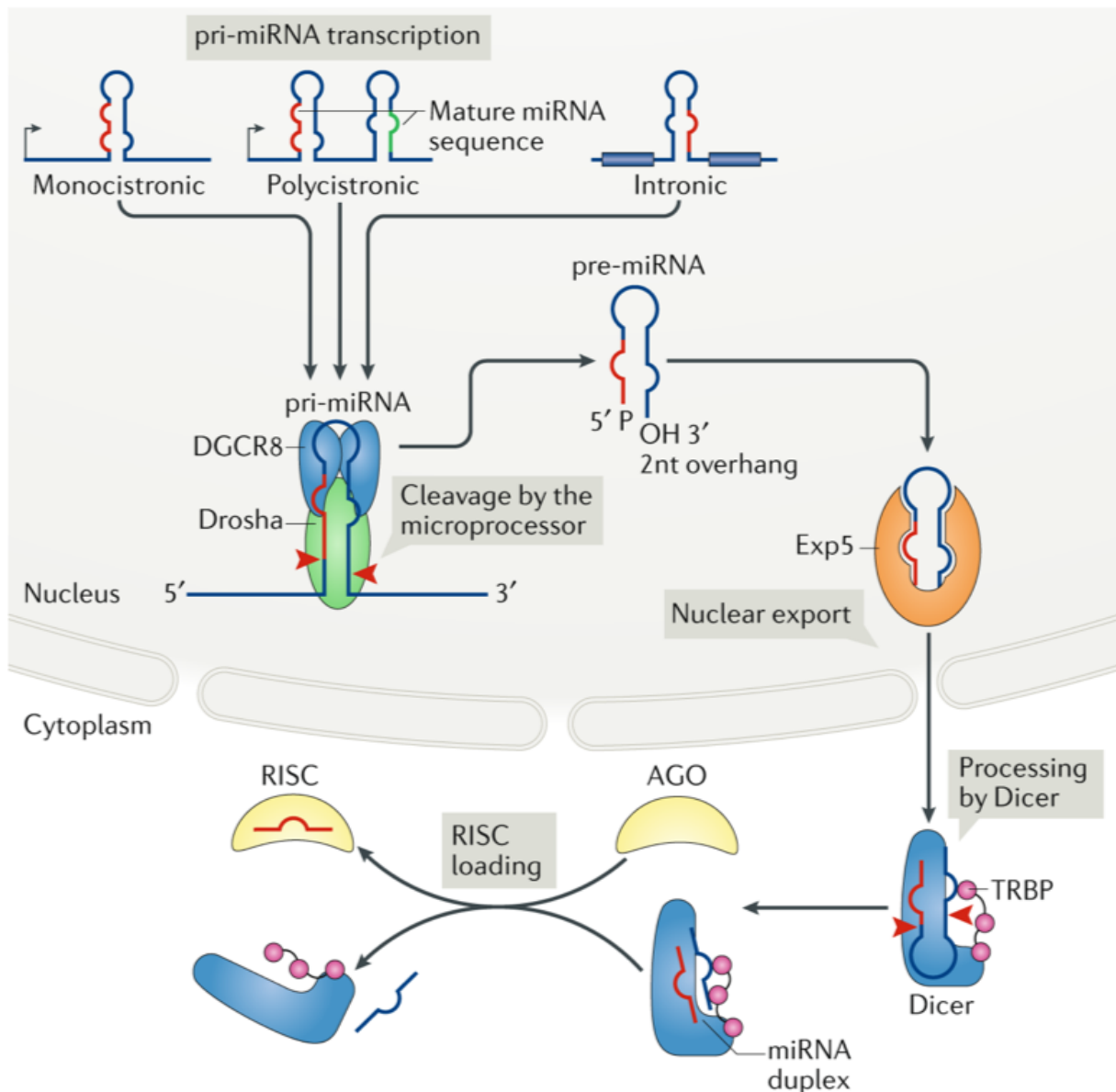
1

Figure 1: Overview of the canonical miRNA biogenesis pathway in mammals. After pri-miRNA transcription in the nucleus, the pri-miRNA transcript is processed into the pre-miRNA, translocated to the cytosol, and catalyzed into the miRNA duplex. The strand loaded into RISC is selected as mature miRNA. pri-miRNA: Primary miRNA; pre-miRNA: Precursor miRNA; DGCR8: DiGeorge Syndrome Critical Region 8; Exp5: Exportin 5; TRBP: Trans-activation-responsive RNA-binding protein; AGO: Argonaute protein; RISC: RNA-induced silencing complex. Figure adapted from [18].

The pre-miRNA from either pathway is translocated to the cytoplasm via the Exp5/RanGTP complex [19, 20]. Then, the RNAse III enzyme Dicer, in coordinated action with the RNA-binding protein TRBP, removes the terminal loop and thereby processes the short ~22 nt mature miRNA duplex from the stem of the pre-miRNA [21, 22].

The miRNA duplex is loaded into an argonaute (AGO) protein (AGO1-4 in humans) to assemble the RNA-induced silencing complex (RISC) [23]. Either strand of the duplex retains as mature miRNA (guide strand), while the other (passenger strand) is degraded. Occasionally both strands may become mature miRNAs [10]. Mature miRNAs from the 5' end of the pre-miRNA hairpin are termed the 5p variant, those from the 3' end the 3p variant. The strand preferred for loading into the pocket within AGO often has a 5' uracil [24] and exhibits less stable base pairing at the 5' end [25].

The miRNA directs RISC to complementary sequences in the 3' untranslated region (UTR) of its target mRNA, which match the seed sequence of the miRNA (nt 2–7) to direct their post-transcriptional repression [26]. In the case of extensive sequence pairing, the endonuclease activity of AGO2 induces mRNA cleavage [27], which rarely occurs in humans and other mammals. Instead, the miRNA only pairs partially to mRNA target transcripts and acts via translational repression or mRNA decay [28].

Upon miRNA–mRNA base pairing, the TNRC6 protein is recruited by AGO to link downstream effector complexes (Figure 2). While tryptophan-containing motifs within the AGO-binding domain of TNRC6 enable interaction with AGO, those within its silencing domain bridge the deadenylase complexes PARN2–PARN3 and CCR4–NOT. The silencing domain of TNRC6 also interacts with Poly(A)-binding proteins that are associated with the mRNA poly(A) tail [18, 29]. The PARN2–PARN3 and CCR4–NOT complexes shorten and remove the mRNA's poly(A) tail. The DCP1–DCP2 complex is recruited to remove the 7-methylguanylate (m7G) cap from the mRNA 5' end. Consequently, the target mRNA is exposed to degradation by 5'–3' exoribonuclease 1 activity [30]. MiRNAs enable translation repression through translation inhibition of the target mRNA by impeding the assembly and/or activity of the eIF4F complex. DDX6 can repress translation, stimulate decapping, and couple the molecular processes of deadenylation and decapping by interacting with the CCR4-NOT complex [18, 29].
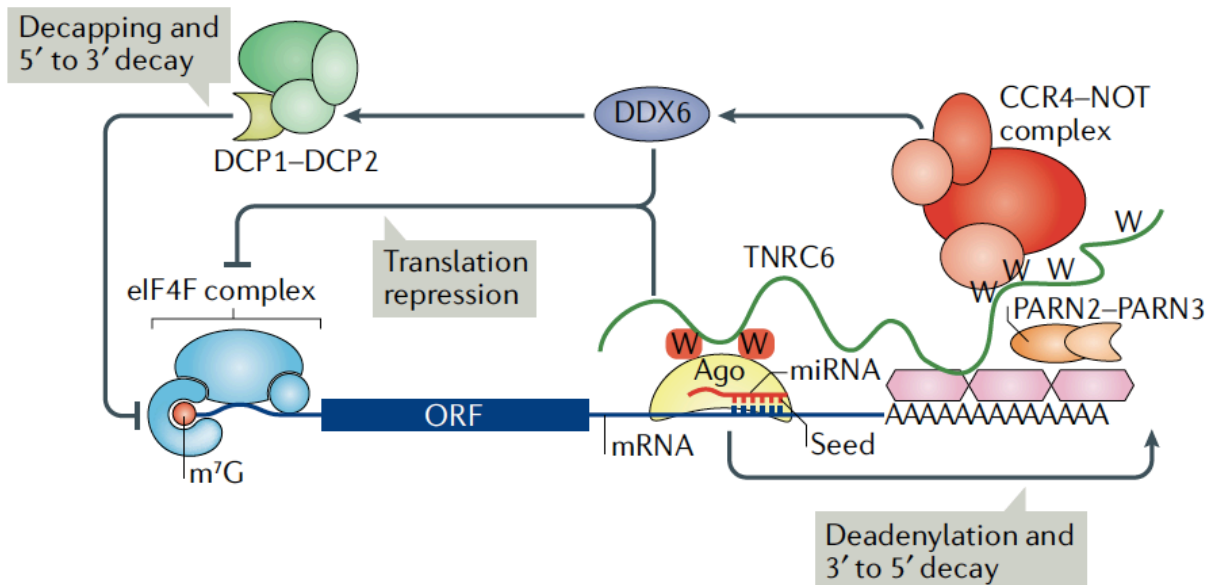
Figure 2: Mechanisms of miRNA-mediated gene silencing in mammals. Upon miRNA–mRNA base pairing, TNRC6 interacts with AGO to couple downstream effector complexes. MRNA silencing can be induced by mRNA decay or translational repression. AGO: Argonaute protein; TNRC6: Trinucleotide repeat containing gene 6; PARN2/3: Poly(A)-specific ribonuclease 2/3; CCR4: Carbon catabolite repressor 4; NOT: Negative regulator of transcription; DCP1/DCP2: MRNA-decapping enzyme 1/2; DDX6: DEAD box helicase DEAD box protein 6; eIF4F: Eukaryotic translation initiation factor 4F; ORF: Open reading frame; W: Tryptophan residues; pink hexagons: Poly(A)-binding proteins. Figure duplicated from [18].

Due to the occurrence of RISC and target mRNAs in distinct cytoplasmic loci termed processing (P)-bodies, also accumulating factors of the mRNA decay machinery, P-bodies were assigned as potential sites for miRNA-mediated gene silencing. However, since miRNA-based target regulation still occurs in the absence of P-bodies, and RISC seems to be distributed throughout the cytoplasm, the fundamental role of P-bodies in miRNA-mediated target regulation remains obscure. Besides their localization in the cytoplasm, mature miRNAs are found in multiple cellular compartments, in the nucleus, and are secreted into extracellular fluids. MiRNAs are protected from endogenous RNase activity by RNA-binding proteins but can also be associated with extracellular vesicles (EVs) [31, 32]. As miRNA expression is specific for different tissues and biofluids, and disease-specific concentration changes are common for many pathologies, liquid biopsy-derived extracellular miRNAs are promising targets for transcriptomic biomarker approaches (as reviewed in Appendix I [33]).

1.2 Extracellular vesicles shuttle intercellular messages

Cells naturally release a heterogeneous group of small-sized, membranous vesicles that cannot replicate, termed extracellular vesicles (EVs) [34]. Their secretion is evolutionarily conserved throughout all kingdoms of life [35]. A lipid bilayer delimits EVs to protect their cargo biomolecules. Eukaryotic cells release EVs that primarily comprise three subtypes, including exosomes, microvesicles, and apoptotic bodies, classified according to their biogenesis (Figure 3) [36].
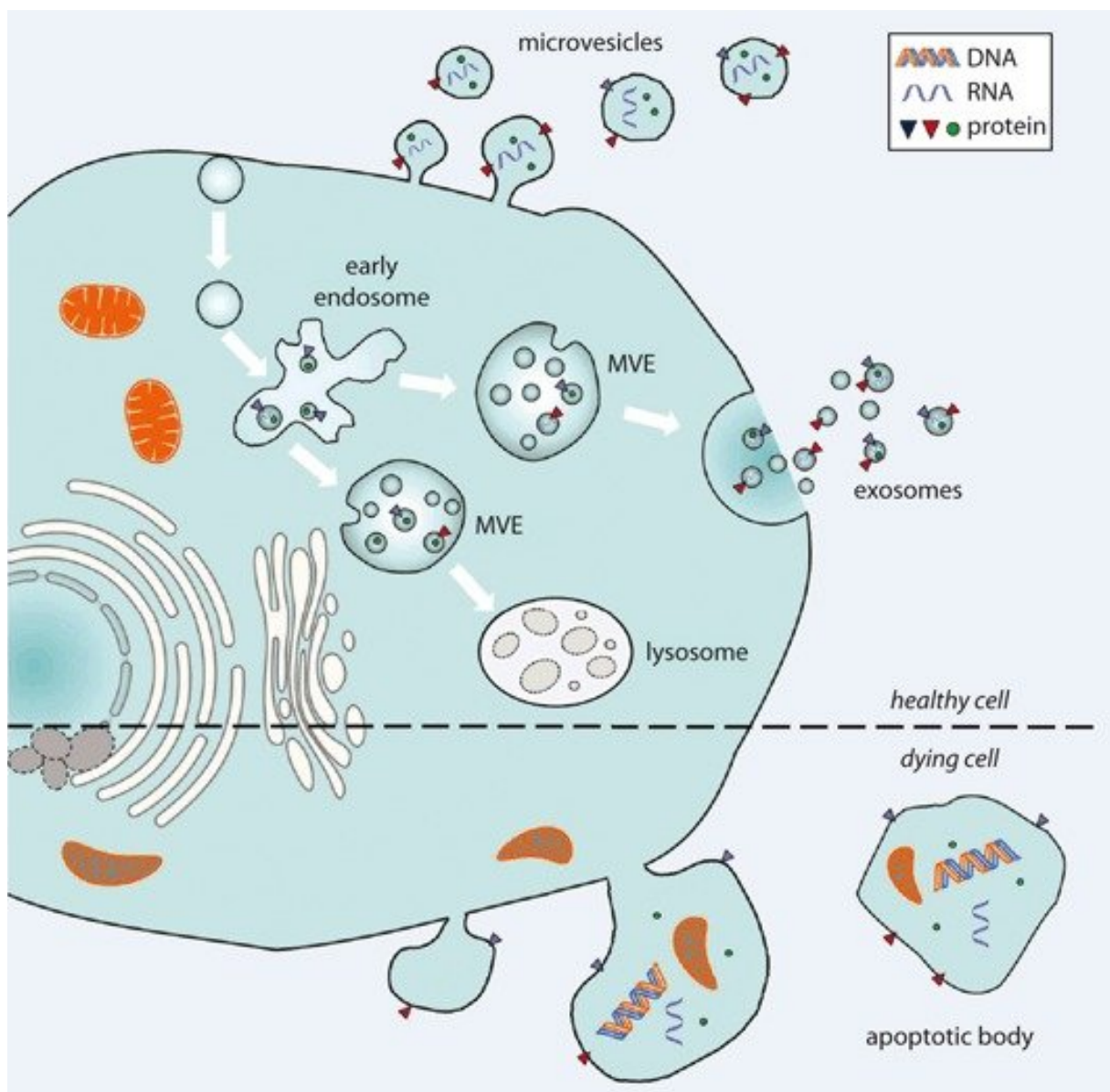

Figure 3: Basic mechanisms of EV biogenesis. MVE: Multivesicular endosome. Figure duplicated from [37].

Exosomes originate from the endosomal system, whereas microvesicles arise from the plasma membrane. Apoptotic bodies emerge by cell fragmentation and blebbing during programmed cell death. While exosomes (~50–150 nm) are generally the smallest EVs, microvesicles (~100–1000 nm) are intermediate-sized, and apoptotic bodies (~100–5000 nm) are the largest. Characteristically vesicles from each subtype have overlapping sizes [38]. Although EVs were formerly deemed cell garbage, several research groups explored significant biological functions contrary [39-42]. With their groundbreaking discovery in 2007, Valadi and colleagues uncovered the exosome-mediated transfer of genetic material as a novel system for short- and long-distance paracrine cell-to-cell communication [43]. With this finding, considerable scientific interest has emerged, and other EV subtypes were reported to transfer intercellular information [44, 45].

Besides the cellular origin, EV composition reflects particular cell type characteristics and the condition of the individual cell. Therefore, specific biomolecules accumulate in different EV subtypes. Common mechanisms involved in the biogenesis of vesicle subtypes often impede correct classification. Exosomes and microvesicles contain cytosolic and transmembrane proteins, lipids, and nucleic acids [36, 46]. Apoptotic bodies additionally enclose fragmented cell organelles and nuclei [47]. Insights into EV biology only recently have started to be revealed and are still incompletely characterized. For example, there are currently many endeavors to uncover the association of EVs with nucleic acids. Besides their intraluminal location, nucleic acids may be located outside EVs [48], likely anchored in the EV membrane or bound by EV surface proteins. The hitherto proposed processes for EV secretion, uptake, and cargo delivery are complex and may depend on specific cell types, conditions, or functions, impacting the molecular mechanisms involved.

Exosome biogenesis (Figure 4) starts within the endosomal system, where lipids and transmembrane proteins segregate on microdomains of the limiting endosomal membrane. These discrete microdomains likely recruit soluble biomolecules, e.g., proteins and RNA classes. The endosomal membrane buds inward to form multivesicular endosomes (MVEs), thereby sequestering cytosolic cargoes into intraluminal vesicles (ILVs) [46]. Various RAB GTPases are involved in sorting cargoes originating from endocytic uptake or the trans-Golgi network [49]. Microtubules transport mature MVEs to the plasma membrane for fusion. Subsequently, MVEs

6

release ILVs as exosomes into the extracellular space [46]. MVE mobility involves RABs, tethering to the plasma membrane RABs and SNARE proteins [49, 50]. Alternately, MVEs are trafficked for enzyme-assisted lysosomal degradation. Different molecular mechanisms regulate the biogenesis of exosomes. Components of the endosomal sorting complex required for transport (ESCRT-0, -I, -II, -III) machinery and accessory proteins act sequentially to promote the formation of ILVs by membrane shaping, vesicle scission, and sorting of cargoes [51, 52]. Syntenin binding to the cytosolic domain of the transmembrane protein syndecan results in ALIX recruitment, bridging cargoes and ESCRT subunits, and supporting endosomal membrane budding [53].
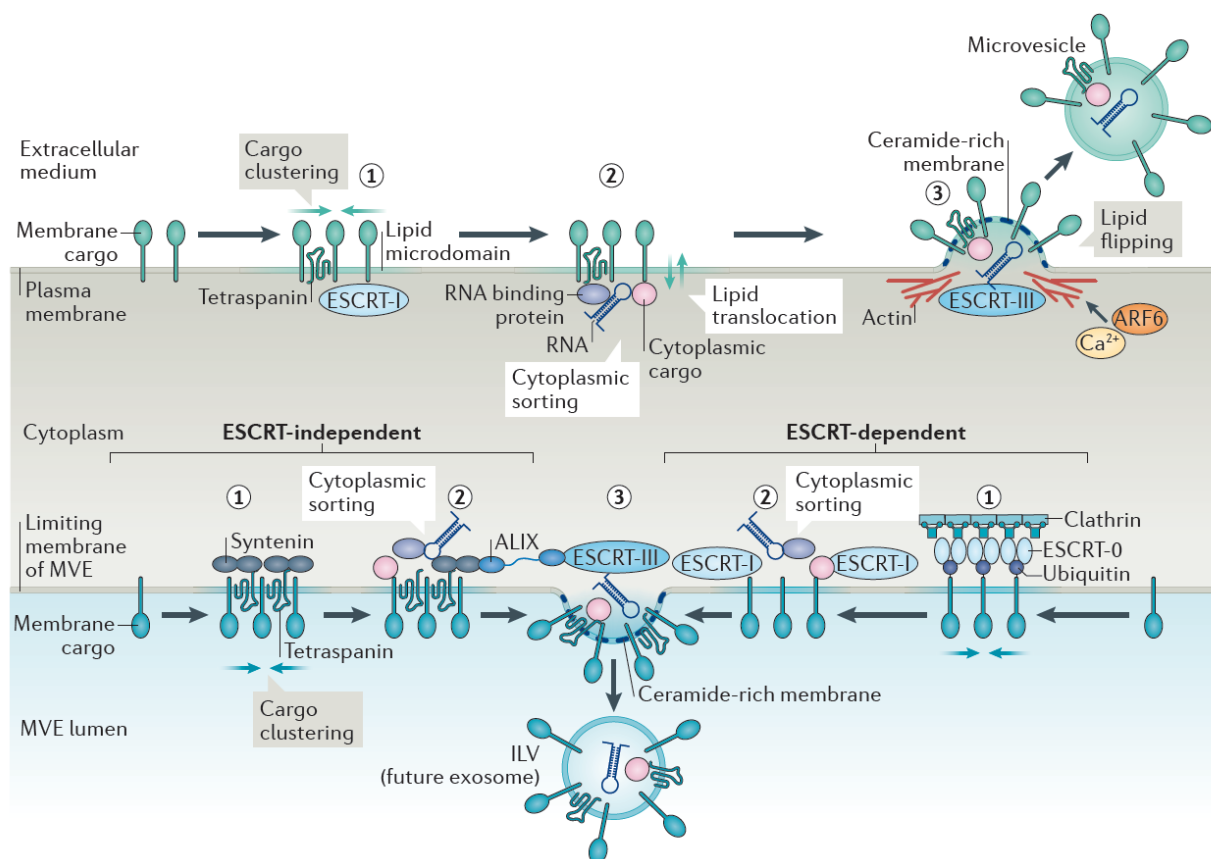

Figure 4: Mechanisms involved in the biogenesis of exosomes and microvesicles. Lipids and transmembrane proteins cluster in distinct membrane microdomains (1) and recruit cytosolic cargo for sorting into EVs (2). Together with other types of machinery, microdomains drive membrane budding and vesicle fission (3). MVE: Multivesicular endosome; ILV: Intraluminal vesicle; ALIX: ALG-2 interacting protein X; ARF6: ADP-ribosylation factor 6; ESCRT: Endosomal sorting complex required for transport. Figure duplicated from [46].

Additionally, exosome secretion occurs after depletion of ESCRT proteins independently via alternative routes [54]. One pathway requires lipid rafts: ceramide-

enriched domains are formed from sphingomyelins via hydrolyses by neutral sphingomyelinase. Small ceramide microdomains coalesce into larger domains and induce a spontaneous negative curvature on the limiting membrane [55, 56]. Tetraspanins such as CD9, CD63, and CD81 regulate cargo sorting into exosomes. Additionally, tetraspanin-enriched microdomains, including other transmembrane and cytosolic proteins, are supposed to initiate budding at the endosomal membrane, possibly via a cone-like tetraspanin structure shown for CD81 [46].

Multiple molecular components and rearrangements within the plasma membrane are essential for forming microvesicles. Similar to exosome biogenesis, the clustering of transmembrane proteins and lipids in distinct membrane microdomains involves cargo sorting. Moreover, ESCRT proteins and ceramide-enriched plasma membrane microdomains promote the biogenesis microvesicle [46]. Additionally, a local cytosolic Ca^{2+} increase activates several Ca^{2+}-dependent enzymes. Calpains destabilize the anchorage of the cytoskeleton to the plasma membrane by disassembling cytoskeletal components. Scramblases and floppases induce the collapse of the phospholipid asymmetry within the lipid bilayer by exposing phosphatidylserine (PS) from the inner to the outer leaflet of the lipid bilayer. These local phospholipid rearrangements cause the outward budding of the plasma membrane [57, 58]. The small GTP-binding protein ARF6 selectively recruits cargo proteins into microvesicles. Moreover, ARF6 activates a signaling cascade that initiates the myosin light chain phosphorylation, resulting in actomyosin contraction and the subsequent release of the microvesicle [59].

Apoptotic bodies emerge during a highly regulated process of programmed cell death. Throughout cell disassembly, apoptotic cells undergo a series of morphological changes, including plasma membrane blebbing, the formation of thin membrane protrusions, and fragmentation into apoptotic bodies. Cytoskeletal dynamics, such as actomyosin contraction and microtubule assembly, foster plasma membrane blebbing. Due to hydrostatic pressure within the dying cell, intracellular fluids are pushed into plasma membrane blebs. Finally, shear forces and interactions with neighboring phagocytes may support the release of apoptotic bodies, which are promptly engulfed by phagocytosis [60, 61].

Once secreted by the donor cell, EVs target the recipient cell to deliver their cargoes and induce a specific cellular response. The unique molecular composition of EV

subtypes defines their path. Docking of EVs with the plasma membrane is mediated through specific ligand-receptor interactions that may activate receptor-mediated signaling. EVs may also fuse with the plasma membrane to directly release their contents into the recipient cell's cytosol. Alternatively, EVs are internalized into the recipient cell through clathrin-mediated endocytosis, endocytosis by caveolae or lipid rafts, as well as phagocytosis and micropinocytosis (Figure 5) [62]. Inside the recipient cell, EVs follow the endocytic pathway by reaching endosomes. EVs either fuse with the limiting endosomal membrane to deliver their cargo or are directed for lysosomal degradation. EVs may also target back from endosomes to the plasma membrane for recycling [38].
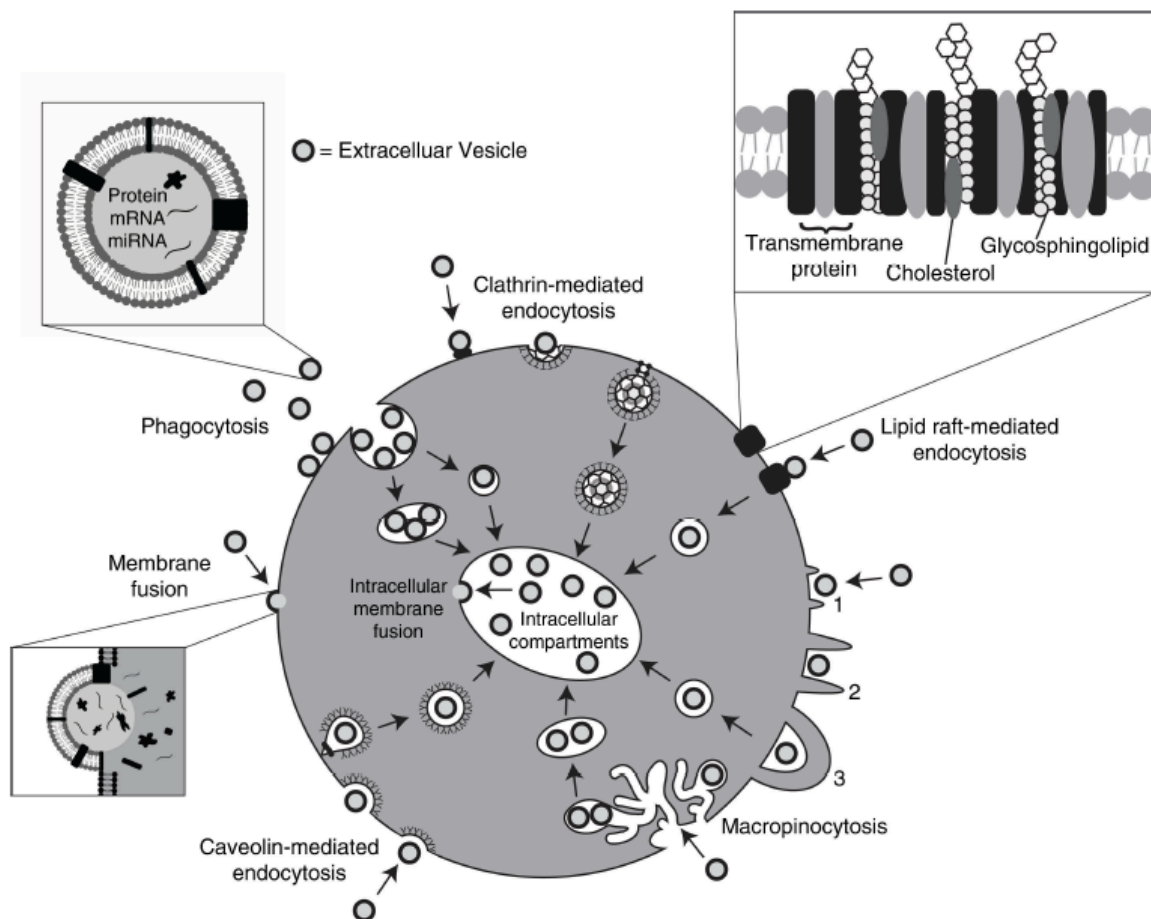

Figure 5: Overview of the molecular mechanisms involved in EV cargo delivery. EVs may release their contents directly into the recipient cell's cytosol by fusion with the plasma membrane or uptake by various endocytic pathways. In addition, internalized EVs may be targeted to endosomes and fuse with the limiting membrane to deliver their contents. Figure duplicated from [62].

Secreted by all cells, EVs regulate physiological pathways, such as embryonic development, immune regulation, angiogenesis, and coagulation. Furthermore, EVs act as mediators in the pathogenesis of various types of cancers, cardiac injury, infectious diseases, neurodegenerative disorders, and numerous others [63-65].

EVs are studied in many research fields, ranging from basic sciences to therapeutic applications and biomarker investigations. Cells release EVs to all tissues and body fluids, e.g., blood, urine, saliva, cerebrospinal fluid, and breast milk [64]. After sampling by minimally invasive liquid biopsies, EVs are isolated from biofluids based on their physical-chemical properties. Differential ultracentrifugation, designated as a gold standard, is a widely used method to isolate EVs [66]. However, the co-isolation of non-EV contaminants desires more pure separation methods [34]. Density gradient centrifugation includes an extra purification step [66], resulting in more pure vesicle subpopulations [67]. However, the time-consuming and labor-intensive characteristics and the low recovery of EVs make this method less practical. Although various commercially available EV separation methods evolved in the last years, none has yet proven to be the benchmark. Therefore, researchers must choose their method based on their requirements on EV sample yield and purity. The sequential use of multiple separation methods has recently become quite popular to obtain more pure vesicle subpopulations [34].

Addressing the challenges in the quickly developing EV field and promoting rigor standardization, the International Society of Extracellular Vesicles (ISEV) developed the Minimal Information for Studies of Extracellular Vesicles (MISEV) guidelines to provide researchers with a guiding standard [34]. Other position statements cover topics such as EV RNA [48]. In addition, the knowledgebase EV-TRACK offers a platform for more transparent reporting by centralizing knowledge and facilitating interpretation and replicating experiments [68].

1.3 Next-generation sequencing: a comprehensive high-throughput method to study microRNA biomarkers

The development of the next-generation sequencing (NGS) technology 15 years ago has revolutionized genomic science. This deep sequencing technology rapidly evolved over the years by realizing speed, read length, and throughput improvements, alongside a substantial reduction in sequencing costs. Nowadays, NGS has become a widely available high-throughput method for sequencing millions of DNA fragments in parallel per run while producing massive data output. Finally, raw reads can be evaluated by specifically adapted downstream bioinformatical pipelines [69, 70].

The translation of NGS technologies in daily routine has enabled meaningful, new diagnostic applications in molecular genetics. In particular, diseases based on mutations in numerous genes have only become diagnostically accessible through their simultaneous analysis [71].

By ongoing investigations in translational research areas, novel classes of analytes such as circulating nucleic acids are likely to develop into molecular biomarkers of clinical relevance prospectively. Molecular biomarkers are, per definition, objectively (1), precisely (2), reproducibly (3), and quickly (4) measurable molecular alterations directly correlating to a specific disease or condition [72]. Deep RNA sequencing technologies are of immense importance in the expanding field of molecular biomarker research since transcriptome profiling uncovers insights into dynamic gene regulatory networks and cellular states [73]. In contrast, DNA profiling provides genetic information exclusively. As reviewed in Hermann et al. 2020 (Appendix I) [33], highly sensitive and specific transcriptomic biomarkers provide early access to data on cellular physiological changes, disease states, or conditions, even at low cellular abundance levels using previously established and relatively cost-efficient methods [73, 74]. Due to their remarkable stability, shorter RNA classes with fewer recognition sites for omnipresent RNAses [75] are favored over longer RNA targets, e.g., mRNAs or long non-coding RNAs (lncRNAs), particularly the extensively studied miRNAs. Compared to other small RNA classes, e.g., PIWI-interacting RNAs (piRNAs), miRNAs are better understood [76], and thus, a significant number of miRNA sequences and annotations are easily accessible on databases such as miRBase [77].

Infectious disease is a typical example, underlining the significant advantages of early detectable diagnostic miRNAs (Figure 6). In the incubation period, pathogen replication starts while patients are still asymptomatic. Ongoing replication of pathogens in the prodromal phase induces immune activation with unspecific symptoms, and finally, clinical illness. With disease progression, treatment options often become limited. However, pathogen detection can be difficult, particularly before the onset of clinical illness. Since cells continuously release miRNAs throughout all stages of infection, these targets provide essential clinical information while reflecting the disease state [78].
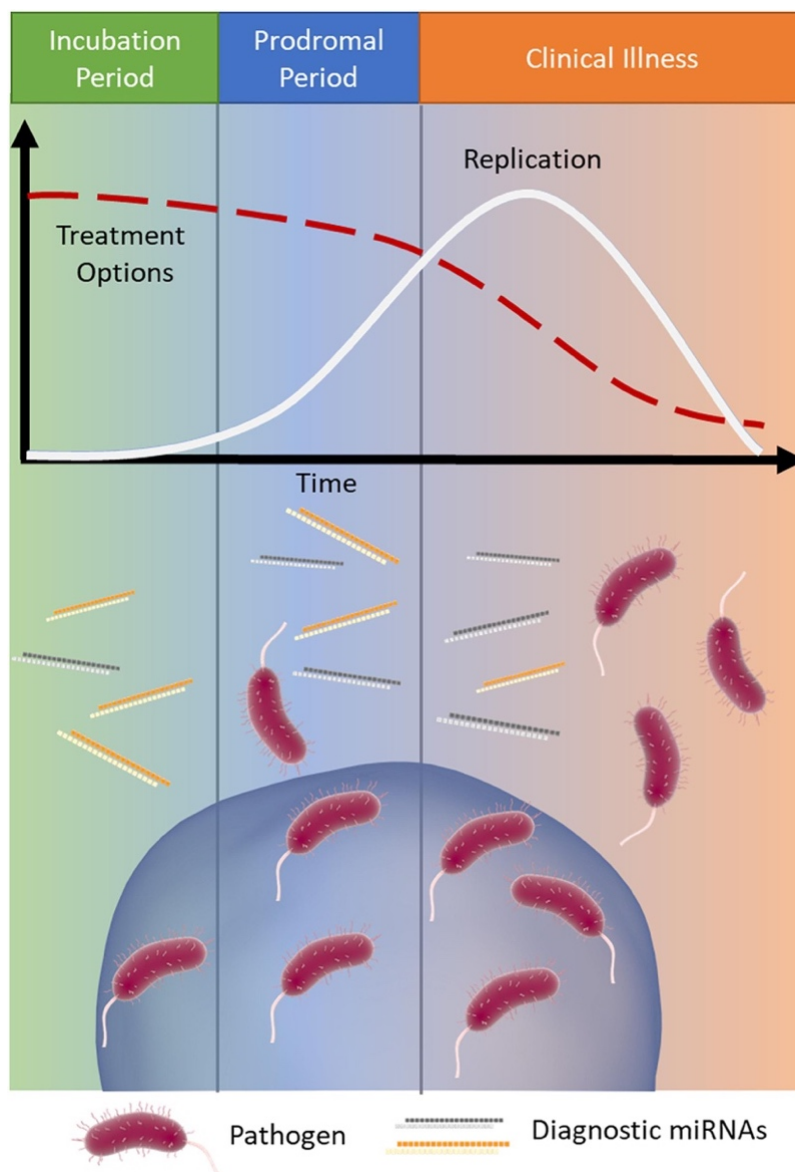

Figure 6: Extracellular miRNAs during infection. Before the onset of clinical illness, pathogen detection can be difficult, while specific miRNA signatures are detectable early on and in each stage of infectious disease. Figure duplicated from [78].

1.4 The unmet need for new clinical biomarkers for community-acquired pneumonia and severe secondary complications

As an acute infection of the pulmonary parenchyma acquired outside of the hospital, community-acquired pneumonia (CAP) remains a major global health threat with the considerable cause of morbidity and mortality in humans of all ages across all populations. The incidence of CAP varies by demographic factors, including country, gender, and age [79], and is significantly highest in low and middle-income countries [80]. CAP varies from mild forms of infections with local inflammation to secondary complications with systemic inflammation present in respiratory distress and sepsis. Sepsis manifests as a serious life-threatening organ dysfunction because of a dysregulated host response to infection. A significant cause of sepsis is CAP since up to half of the cases originate from pulmonary infections [81]. High-risk groups for CAP include, in particular, children younger than five years and adults over the age of 65 years or patients with significant comorbidity. With three million global deaths annually, lower respiratory infections are the most deadly communicable disease and the fourth leading global cause of death worldwide [82].

CAP is mainly caused by microbes including bacteria such as *Streptococcus pneumoniae* and *Mycoplasma pneumoniae*, and respiratory viruses, e.g., *influenza A and B.* Primary viral etiologies may result in secondary bacterial infections. Notably, mixed viral and bacterial infections are likely to induce a more severe disease than bacteria alone [83, 84]. Recently, the newly emerged coronavirus SARS-CoV-2 has caused the pandemic outbreak of hundreds of millions of cases of acute respiratory infections globally. As a consequence, attention to the burden of CAP is evoked throughout the world. Pathogens access the lower airways, e.g., by inhalation of contaminated aerosols or aspiration from the oropharynx. After they accumulate and multiply in the alveoli, an inflammatory host response is induced. This inflammatory response is the leading cause of the pathology of lower respiratory infections [84].

Primary functioning and non-specific innate host defense mechanisms include nasal hairs, nasal turbinates, cought reflexes, and the branching structure of the conducting airways [84]. Impacted particles are cleared away from the bronchioles to the trachea by mucociliary transport, coordinated through ciliary movements of epithelial cells in the mucus of the bronchi. This airway surface liquid, secreted by epithelial cells and

submucosal glands, additionally contains protective macromolecules with anti-microbial, anti-protease, and anti-oxidant activity [85]. Finally, if microbes still manage to reach the alveoli, alveolar macrophages patrolling the alveolar surface are enrolled to kill microbes through phagocytosis directly [84, 85].

Once the infection in the lung is overwhelming and not defended efficiently, the inflammatory host response is initiated. Microbial structures termed pathogen-associated molecular patterns (PAMPs), and host-derived cell damage-related danger-associated molecular patterns (DAMPs) can both activate cell surface and cytosolic pattern-recognition receptors (PRRs). Upon receptor-ligand interactions, intracellular pathways, such as NF-κB and MAPK signaling, are activated, and pro-inflammatory mediators such as cytokines and chemokines are secreted [86]. These inflammatory mediators, primarily released from epithelial cells and alveolar macrophages, rapidly stimulate the accumulation of neutrophils in the lung. Neutrophils are crucially involved in eliminating pathogens by phagocytosis and the release of extracellular traps. Additionally, other leukocytes participate in the host defense of the lung. These include, for example, monocytes that can differentiate into macrophages and dendritic cells, lymphocytes including natural killer cells, T cells, and B cells, as well as mast cells [87]. With inflammatory progress, anti-inflammatory mediators are released to slow or reverse the activation of inflammatory pathways and the infiltration of neutrophils and other inflammatory cells into the lung. Apoptotic neutrophils and other dead or dying inflammatory cells are removed, while specialized anti-inflammatory cells, e.g., regulatory T cells and myeloid-derived suppressor cells, are targeted to the lung to reduce inflammation and injury and enable healing [88]. Exaggerated pro-inflammatory cytokine responses and the overwhelming infiltration of immune cells to the lung may cause sepsis, septic shock, organ failure, as well as death [84].

The diagnosis of CAP is based on an abnormal physical examination along with fever, shortness of breath, cough, sputum production, and pleuritic chest pain. Clinical findings can be supported by lung infiltrates in chest imaging. Pathogen classification by analyzing throat swabs, sputum, or blood cultures enables targeted antibacterial or antiviral treatment. Molecular assays, serology, urine antigen tests, or bronchoscopy can be provided for selected patients [89]. In about half the cases of CAP, however, the causative pathogens remain unidentified [79]. Acute-phase proteins of

inflammation, signaling molecules, and other targets associated with the inflammatory host response may assist in assessing CAP severity [90]. Levels of blood biomarkers, including C-reactive protein (CRP), procalcitonin (PCT), interleukin-6 (IL-6), white blood cell count, and lactate, are evaluated for monitoring the onset and course of the disease [91]. Additionally, scoring systems such as the Confusion, Blood Urea, Respiratory Rate, Blood Pressure, Age ≥ 65 (CURB-65) score may help define CAP severity [92].

High-risk groups, however, frequently present with atypical symptoms. In elderly patients, for example, clinical features and findings from the physical examination can be altered or even absent [89]. Therefore, as an accurate CAP diagnosis can be clinically challenging, misdiagnoses are common and are likely to be followed by inappropriate treatments, such as antibiotic overuse in consequence [93]. In addition, increasing anti-microbial resistance among bacterial pathogens and population aging contribute to the escalating disease burden [94].

To provide more effective treatment with declining proportions of hospitalization and mortality among patients with CAP, on-site diagnosis and risk stratification are essential. Both, however, remain one of the most challenging tasks, as presently no reliable CAP biomarkers are available [95] to enable early diagnosis and prevent disease spread through the detection of patients at risk for progression to severe secondary complications.

1.5 Aim of the thesis

This thesis aimed to establish a viable workflow to study blood-derived EV miRNAs as novel biomarker targets for the early detection of acute pulmonary infections. After optimizing the sample preparation procedure and examining the possibility of an arterial *versus* venous sampling bias, the approved methods were implemented in a large study population of patients with CAP and related progression to sepsis. Furthermore, as the SARS-CoV-2 pandemic emerged, EV-miRNAs were investigated as regulators of pathophysiological processes in patients with COVID-19 pneumonia.

2 Materials and methods

2.1 How to establish a potential extracellular vesicle microRNA biomarker signature?

State-of-the-art technologies for EV-based miRNA biomarker research, as well as potentials and limitations for their application, were examined in a fundamental literature review (Appendix I) [33]. Main findings evaluating the goals and pitfalls of EV miRNA biomarkers are summarized in the discussion of this work. The way discussed and developed in this thesis, studying novel disease-related EV miRNA biomarkers requires a robust and appropriate workflow for commonly low concentrated or low volume patient samples (Figure 7).
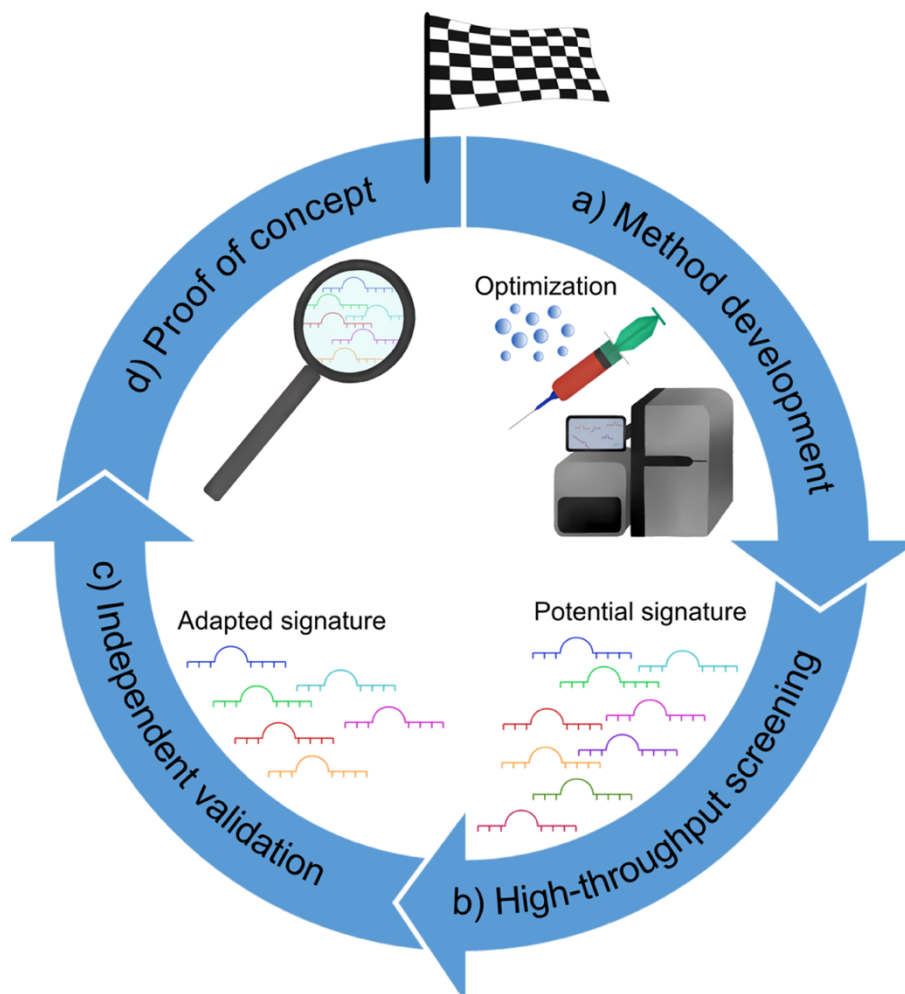

Figure 7: Visualization of the exemplary workflow for the study of EV-based miRNA biomarkers. After method development (a), high-throughput screening is performed (b), following independent validation of the EV miRNA signature (c) and proof of concept (d). Figure duplicated from Appendix I [33].

The first step of this process consists of method development, along with pre-analytical factors, adapted techniques for sample preparation, high-throughput screening (particularly small RNA-seq), and orthogonal validation (particularly RT-qPCR). Additionally, strategies for multivariate data analysis need to be established. Next, researchers can apply these advanced methodologies to a defined cohort of patients to obtain a candidate EV miRNA signature. Additionally, validation needs to be performed in an independent cohort of patients by using the approved methods. Confirming the stability and reproducibility of preliminary findings improves the diagnostic, prognostic, or monitoring value of the candidate biomarker. Finally, the final EV miRNA signature can be further tested by applying the validation method to multiple sample sets across different laboratories.

2.2 Optimization of the extracellular vesicle separation approach for small RNA sequencing applications

As precisely described in Buschmann et al. 2018 (Appendix II) [96], the performance of different EV separation methods was investigated in a study population of healthy controls (n=10) and sepsis patients (n=9). The aim was to determine the optimal approach for small RNA-seq experiments. The workflow included multiple steps: sample preparation, library preparation, small RNA-seq, NGS data analysis, and EV sample characterization.

Precipitation (miRCURY Exosome Isolation Kit, Exiqon), membrane affinity (exoRNeasy Serum-Plasma Midi Kit, Qiagen), size-exclusion chromatography (SEC; Exo-spin Midi Columns, Cell Guidance Systems; qEV Columns, Izon Science), and sedimentation (Beckman Coulter Optima LE-80K, Beckman Coulter) were compared side-by-side. Due to the limited availability of patient sera, the latter method was applied to healthy controls solely. The physicochemical principles of the collated EV separation methods are described in Table 1.

Table 1: Principles of the collated EV separation methods.

Method	Principle
Precipitation	Adding a polymer-based buffer to the biofluid diminishes the hydration envelope of EVs and other particles, allowing for precipitation with low-speed centrifugation.
Membrane affinity	EVs are bound to a membrane by biochemical interactions and elute with a proper buffer subsequently.
SEC*	A matrix with bead pores separates EVs and other particles. While particles larger than the pores (EVs) are the first to elute, smaller particles (proteins) enter the pores and consequently elute delayed.
Sedimentation	Differential ultracentrifugation sequentially separates EVs and other particles with high-speed centrifugal forces according to their sedimentation rate, mainly affected by particle size and density.

*SEC: Size-exclusion chromatography

After separating EVs with either method, total RNA was extracted by employing a column-based extraction method. Eluates were reapplied to the column membrane to maximize the enrichment of EV total RNA.

Small RNA libraries were prepared from six µl of concentrated EV total RNA (NEBNext Multiplex Small RNA Library Prep Set for Illumina, New England BioLabs Inc.) by performing the following steps: 3' adaptor ligation (1), reverse transcription primer hybridization (2), 5' adaptor ligation (3), first-strand copy DNA (cDNA) synthesis (4) and PCR enrichment (5). The protocol was adapted for low quantity EV samples by diluting all adaptors and primers 1:2 in nuclease-free water. CDNA libraries were quantified by capillary electrophoresis (2100 Bioanalyzer, DNA 1000 Kit, Agilent Technologies). If feasible, the same amount of cDNA was pooled from each bar-coded specimen. Alternatively, for low concentrated samples, the whole amount of cDNA was used. Following on 4 % agarose gel electrophoresis, size-selection for cDNA constructs matching small RNAs in size (130–150 bp) was conducted. After purifying cDNA libraries (Monarch DNA Gel Extraction Kit, New England Biolabs Inc) and quality

control (2100 Bioanalyzer, DNA High Sensitivity Kit, Agilent Technologies), single-end small RNA-seq was performed in 50 cycles (HiSeq2500, Illumina Inc.).

Quality control of NGS data was performed using FastQC. After trimming adaptor sequences by Btrim, short reads and reads lacking adaptors were discarded. The remaining reads were mapped to RNAcentral and miRBASe using Bowtie, and read count tables were generated. Finally, differential gene expression (DGE) analysis was performed by DESeq2.

According to the MISEV guidelines, the biological properties of the EV preparations from each separation method were characterized. Following the particles' Brownian motion, the particle size distribution and quantity were determined by nanoparticle tracking analysis (NTA; NanoSight LM10, Malvern). EV preparations were visualized by transmission electron microscopy (TEM; Zeiss EM900, Carl Zeiss Microscopy) after negative staining with uranyl acetate. Western blotting assessed pan-EV protein markers and potential contaminants (WB; XCell SureLock Mini-Cell Electrophoresis System, Thermo Fisher Scientific).

2.3 Control for possible blood sampling differences in arterial *versus* venous blood

As published extensively in Hermann et al. 2019 (Appendix III) [97], arteriovenous differences in the composition of blood-derived EVs still have to be explored. According to the patient's health status and the type of vascular access, blood samples may derive from arterial or venous sampling sites. For example, in daily hospital routine, healthy controls and patients with less severe disease (e.g., CAP) are sampled by venipuncture. In contrast, specimens from critically ill intensive care unit patients (e.g., sepsis) are usually drawn via arterial lines inserted to monitor patients. Currently, various biomarker studies use EV miRNA as starting material.

To control for sampling bias, matched arterial and venous crude (miRCURY Exosome Isolation Kit, Qiagen) and additionally by SEC-purified EVs (miRCURY Exosome Isolation Kit, Qiagen, and qEV Columns, Izon Science) isolated from sera were

compared. The study included patients with severe heart disease (n=20). Blood was preoperatively drawn from the radial artery and the internal jugular vein.

After column-based RNA extraction, small RNA-seq and subsequent DGE analysis were performed as mentioned above. In addition, evaluation of arteriovenous differential expressed miRNAs from the crude EV NGS data set was performed by RT-qPCR (miRCURY LNA SYBR Green PCR Kit, Qiagen) in the same study population.

Crude and purified EVs were analyzed by NTA (ZetaView PMX 110, Particle Metrix) and TEM (Zeiss EM900, Carl Zeiss Microscopy), while WB (XCell SureLock Mini-Cell Electrophoresis System, Thermo Fisher Scientific) was solely performed for purified preparations.

2.4 Extracellular microRNAs as biomarkers in community-acquired pneumonia and sepsis as a secondary complication

As depicted comprehensively in Hermann et al. 2020 (Appendix IV) [98], crude EV miRNAs were studied as biomarker candidates in patients with severe pulmonary disorders. The objective was to develop an innovative approach that may facilitate the often time-consuming and challenging diagnosis of CAP and indicate the risk of sepsis progression.

The study population comprised 142 individuals and was separated into a training (n=67) and a validation cohort (n=75). Patients with CAP (training cohort n=12, validation cohort n=18), sepsis (training cohort n=28, validation cohort n=37), and healthy controls (training cohort n=27, validation cohort n=20) were included.

MiRNAs were quantified by applying the established small RNA-seq procedure to crude EV samples from sera of the training cohort. A candidate biomarker signature was developed by combining DGE analysis (DESeq2) and sparse partial-least-squares discriminant analysis (sPLS-DA, miXOmics). Subsequently, these extracellular miRNAs were evaluated by RT-qPCR (miRCURY LNA SYBR Green PCR Kit, Qiagen) technically in the training cohort and additional in the biologically independent validation cohort.

2.5 Extracellular microRNAs in the pathophysiology of COVID-19

Crude EV miRNAs were studied in patients with acute SARS-CoV-2 infection (manuscript under review). The purpose of this study was to identify a possible role of extracellular miRNAs as regulators of pathophysiological changes in COVID-19.

The study included symptomatic patients with confirmed COVID-19 pneumonia (n=15) and healthy controls (n=18).

Extracellular miRNAs from crude EV samples precipitated from sera were analyzed by the established methods, including small RNA-seq, DGE analysis (DESeq2), and technical RT-qPCR validation (miRCURY LNA SYBR Green PCR Kit, Qiagen). In addition, based on small RNA-seq expression data, gene targets and causal networks were identified by Ingenuity Pathway Analysis (IPA, version 57662101, autumn release 2020, Qiagen Digital Insights).

3 Results and Discussion

3.1 Precipitation is a favorable method for extracellular microRNA biomarker studies

EV separation was compared side-by-side for precipitation, membrane affinity, and SEC in sera from critically ill sepsis patients and healthy controls.

In agreement with isolation-specific differences in RNA quantity and size distribution, total library sizes and mapping frequencies varied between EV separation methods. MiRNA mapping was manifold-higher for precipitates when compared to other sample types. Additionally, the number of miRNAs with an altered expression between sepsis patients and healthy controls was 90, considerably highest for precipitated specimens.

According to grouping, membrane affinity and precipitation separated groups by miRNA expression, while SEC failed to form accurate clusters (Figure 8).
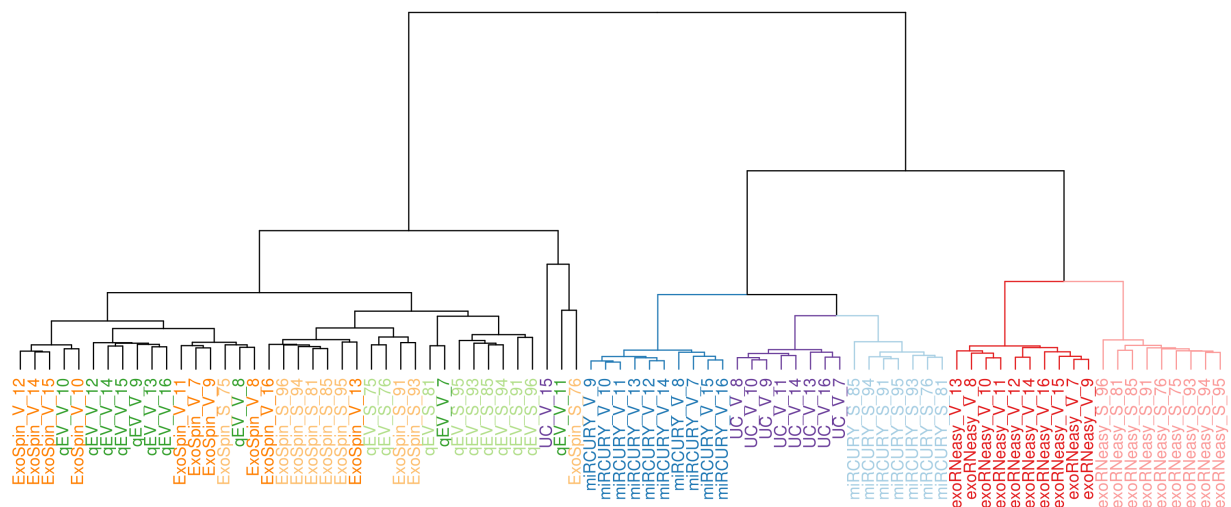

Figure 8: Hierarchical clustering analysis of different EV separation methods by miRNA expression. According to grouping, precipitation (miRCURY, blue) and membrane affinity (exoRNeasy, red) formed accurate clusters. SEC methods (Exo-spin, orange; qEV, green) showed a high degree of heterogeneity with less precise clustering. As the availability of sera was limited, ultracentrifugation (UC, purple) was only performed for healthy controls. Volunteer: V, dark color; Sepsis: S, bright color. Figure duplicated from Appendix II [96].

As outlined in our study, each separation method recovered divergent EV subpopulations with specific biological properties that diverged in particle size, yield,

22

and purity. In addition, pan-EV protein markers and non-EV impurities were detectable to varying degrees in different EV preparations.

In conclusion, the choice of the EV separation approach highly affects results of downstream RNA analysis, e.g., when performing small RNA-seq experiments (Appendix II) [96]. Precipitation, for example, co-isolates high levels of non-EV miRNA carriers, e.g., high- and low-density lipoproteins, AGO proteins, and others [99, 100]. This approach, however, seems to be a feasible option to enrich extracellular miRNA from crude EVs for small RNA-seq, while cleaner separation methods, e.g., SEC, tend to perform poorly (Appendix II) [96].

Up to now, several researchers have systematically studied the applicability of different EV separation methods to various types of starting material, as well as diverse approaches of downstream analyses of EVs and their molecular cargoes [101-103]. In line with our data (Appendix II) [96], findings from these studies clearly show that each separation method results in individual EV preparations. Depending on the research question and the specific approach used for downstream analyses, EVs isolated by different separation methods may be suitable to varying extents.

3.2 Arterial *versus* venous blood sampling has a minor impact on extracellular vesicle microRNA expression profiles and their biological properties

The possibility of an arteriovenous sampling bias was investigated in each crude and additionally by SEC-purified EVs of patients scheduled for cardiac surgery.

RNA yields, total library sizes, and relative miRNA frequencies were equivalent for arterial and venous EVs from either preparation. MiRNA expression broadly overlapped in crude and purified EVs isolated from arterial and venous sampling sites (Figure 9A + C). In addition, all arterial and venous miRNAs from both crude and purified EVs correlated to a high degree.

Additionally, crude and purified EVs did not systematically form consistent clusters but tended to group by individuals rather than sampling site (Figure 9B + D). Overall, this finding was revealed, as the variability of the most abundant transcripts within

23

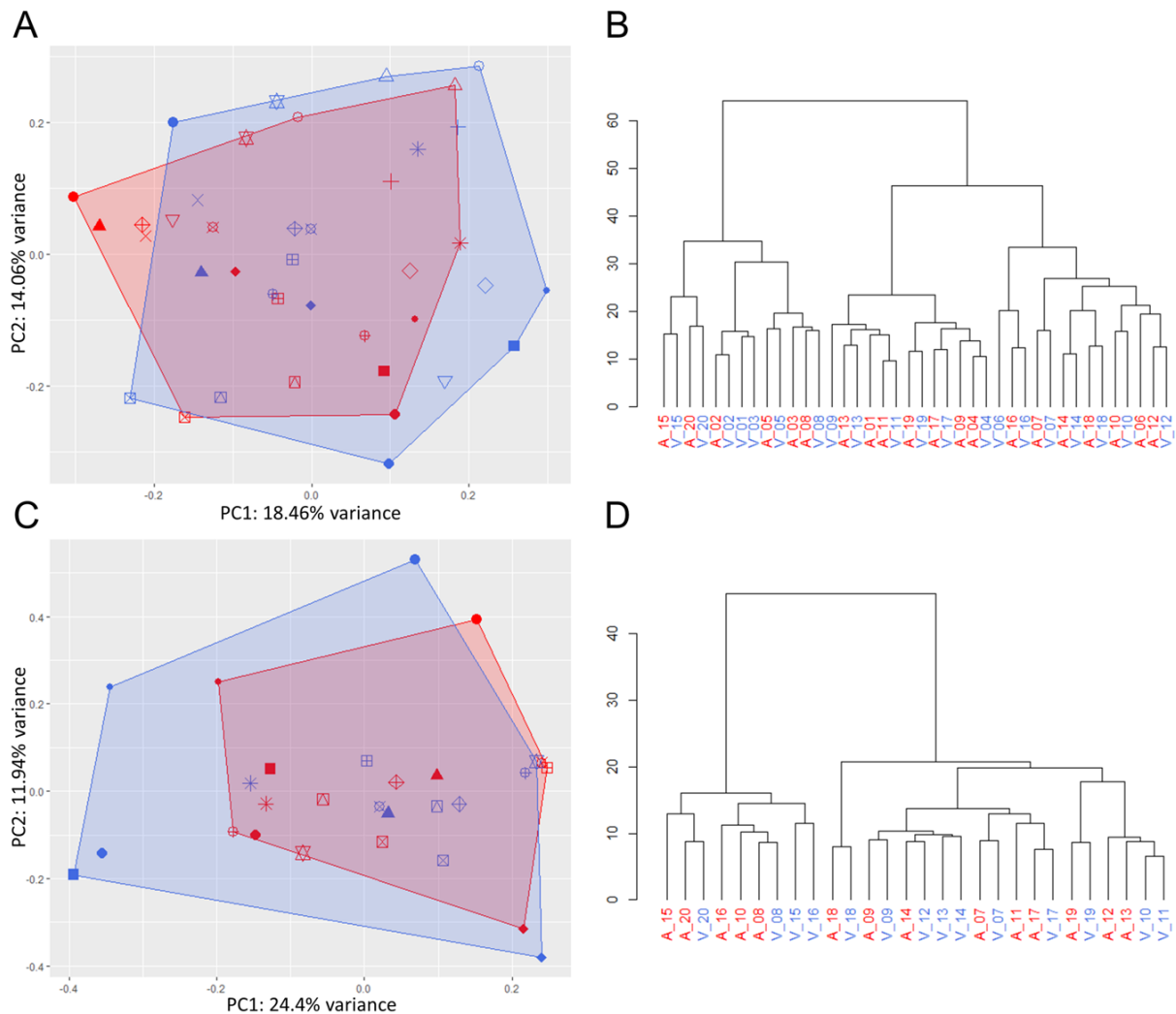individuals was lower than their variability in arterial and venous specimens across individuals.

Figure 9: Visualization of arterial (red) and venous (blue) miRNA expression. Principal component analysis from crude (A) and purified (C) EVs. Arterial and venous preparations generally displayed overlapping miRNA expression profiles. Hierarchical clustering analysis from crude (B) and purified EVs (D). Crude specimens tended to cluster by individuals rather than sampling site, purified EVs clustered by individuals to a lower extent. A: Arterial, V: Venous. Figure duplicated from Appendix III [97].

Four miRNAs displayed a marginal tendency towards arterial up-regulation in crude EVs by setting a less stringent threshold for filtering NGS data than commonly used for DGE analysis. This finding, however, only proved for miR-493-5p in the subsequent RT-qPCR validation, while the other three miRNAs exhibited comparable arteriovenous expression patterns.

On the contrary, in SEC-purified EVs, miRNA expression changes between arterial and venous specimens were not detected at all.

Moreover, arterial and venous EVs from either preparation had similar morphologies with no considerable difference in size and yield. Pan-EV protein markers were enriched in purified EVs (Figure 10).
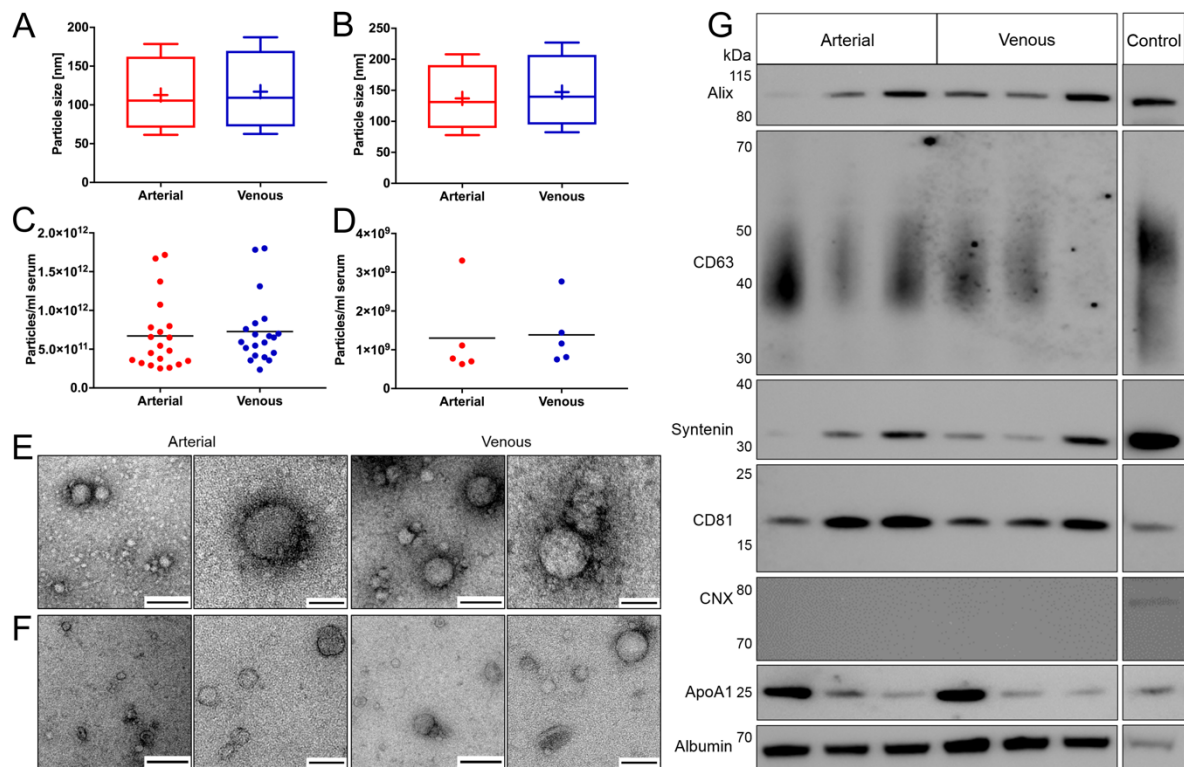

Figure 10: Characterization of crude and purified arterial and venous EVs. NTA revealed comparable particle size and concentration for crude (A + C) and purified (B + D) specimens. Particle size is depicted by boxplots from the 10th to the 90th percentile with median (line) and mean (+) diameters. Spherical particles of about 100 nm were illustrated by TEM for crude (E) and purified (F) preparations. Scale bar first and third column: 250 nm; Scale bar second and fourth column: 100 nm. Immunoblotting in purified EVs (G) detected pan-EV markers (ALIX, CD63, Syntenin, and CD81) in the absence of the negative control (calnexin, CNX). Samples were positive for other non-EV contaminants (Apolipoprotein A1, ApoA1; serum albumin). Figure duplicated from Appendix III [97].

To summarize, expression alterations between arterial and venous preparations are marginal and seem not to be the primary cause for different miRNA content when comparing crude or purified EV miRNA profiles. Therefore, minor arterial *versus* venous sampling bias is expected when studying EVs and their associated miRNAs to discover biomarkers from sera. However, this finding may not apply to all individuals

25

and diseases. Therefore, further arteriovenous comparison studies are necessary to evaluate these findings under different pathophysiological conditions, e.g., severe cardiopulmonary disorders (Appendix III) [97].

To the best of our knowledge, this was the first study to collate the composition of matched human arterial and venous blood compartments concerning miRNA expression. By now, only a few studies aligned matched arterial and venous specimens from different sampling sites. Researchers detected similar levels of protein biomarkers by ELISA in human arterial *versus* venous sera [104]. The study of whole porcine blood by small RNA-seq identified 12 miRNAs with arterial *versus* venous expression alteration [105]. Though miRNA expression was broadly similar, researchers detected 24 differentially expressed miRNAs by microarray when comparing arterial *versus* venous rat plasma specimens [106]. In accordance with our study (Appendix III) [97], these findings indicate that protein and miRNA content of arterial and venous blood may have many similarities. However, in the same way, differences may exist in specific blood components.

3.3 Extracellular microRNAs are innovative biomarker candidates for community-acquired pneumonia and sepsis as a secondary complication

Extracellular miRNAs, extracted from crude EV preparations, were studied as biomarker candidates to assist in the CAP diagnosis and detect patients at risk for progression to sepsis.

Expression profiles of extracellular miRNAs separated patients with CAP and sepsis from healthy controls using an unsupervised or a supervised clustering approach. Patients with CAP and less severe disease to sepsis tended to localize closer to healthy controls, and critically ill sepsis patients were located more distantly (Figure 11A). Supervised clustering of all groups was realized by sPLS-DA based on the expression levels of 12 miRNAs (Figure 11B).
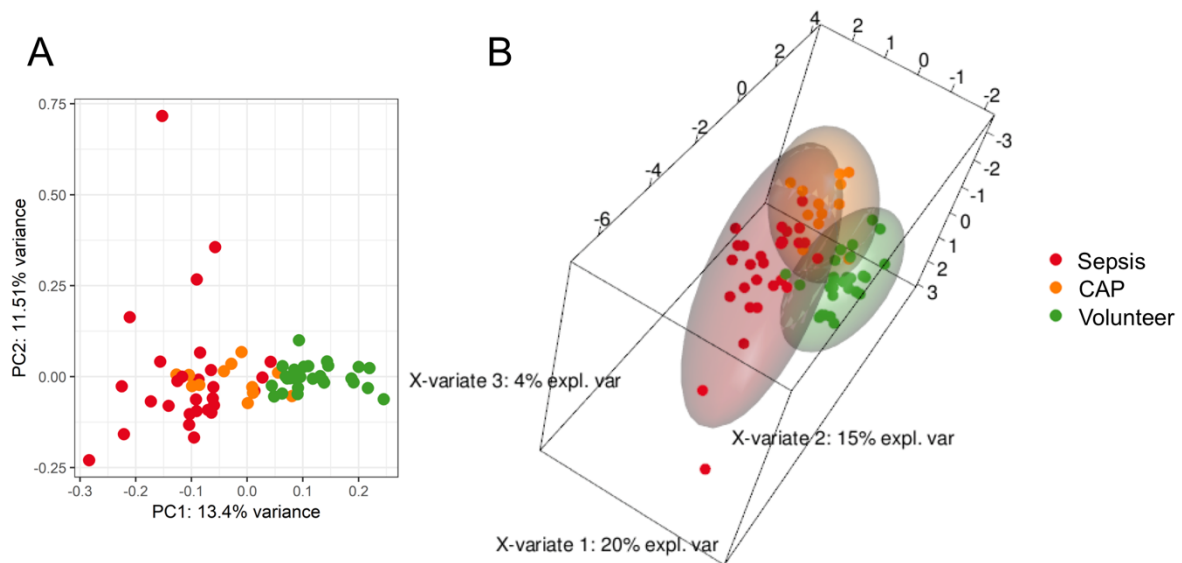
Figure 11: Multivariate NGS data analyses by unsupervised and supervised clustering. Principal component analysis (A) and sparse partial-least-squares discriminant analysis (B) separated groups, which partially had slight overlaps. Figure duplicated from Appendix IV [98].

DGE analysis identified 29 significantly regulated miRNAs differentiating CAP and healthy controls and 25 miRNAs distinguishing CAP and sepsis. Based on DGE and sPLS-DA data, a miRNA subset was selected as a potential biomarker.

When analyzing data from the technical RT-qPCR validation in the training cohort by partial-least-squares discriminant analysis (PLS-DA), groups were separated and comparably distributed to the small RNA-seq data. Additionally, a multitude of samples from the validation cohort could be assigned to the correct groups by PLS-DA.

In the subsequent RT-qPCR validation, a three miRNA signature, including miR-193a-5p, miR-542-3p, and miR-1246, proved significantly for either the training or the biologically independent validation cohort. The expression of miR-1246 increased from healthy controls to CAP and sepsis patients according to the severity of the disease, while miR-193a-5p and miR-542-5p distinguished patients with an infectious disease (CAP or sepsis) from healthy controls (Figure 12).
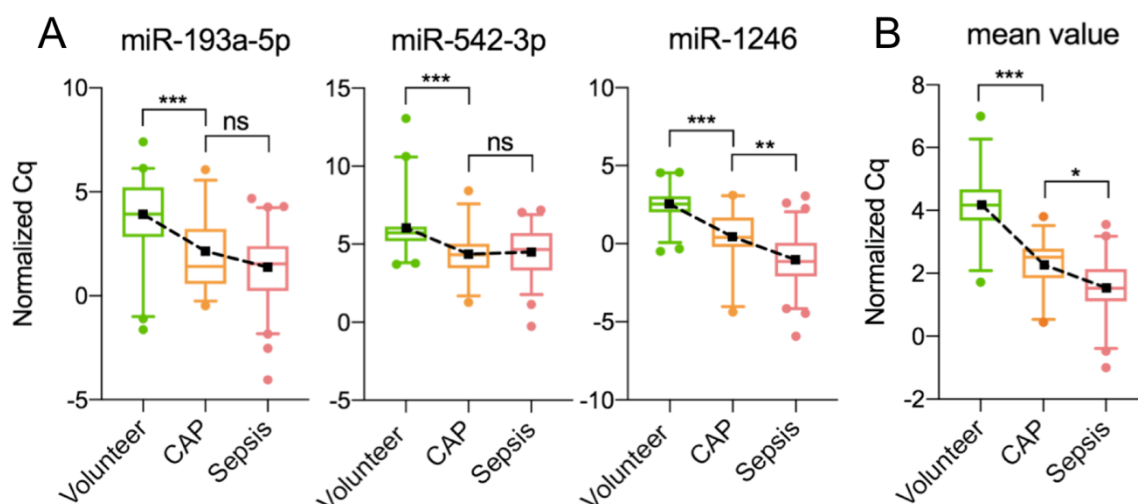
Figure 12: Depiction of miRNAs from the RT-qPCR validation in the whole study population for each miRNA (A) and the mean value of all miRNAs (B) by cycle quantification values (Cq). Normalized Cq values are displayed by boxplots from the 5th to the 95th percentile with median (line) and mean (square). Lower ΔCq values indicate higher miRNA expression. *$p < 0.05$; **$p = 0.005$; ***$p < 0.001$; ns: Not significant. Figure duplicated from Appendix IV [98].

In summary, crude EV miRNAs are innovative biomarker candidates that may prospectively assist in diagnosing CAP and the risk stratification for progression to sepsis. Further studies in increasing patient cohorts across different laboratories will be required to prove the applicability of our biomarker signature under clinical settings (Appendix IV) [98].

Many researchers have studied miRNA expression in acute inflammation, while some reported a contributing role of miR-193a-5p, miR-542-3p, and miR-1246. In a previous study from our group, miR-193a-5p expression correlated with sepsis severity [107]. By mediating mitochondrial dysfunction, miR-542-3p/5p may cause muscle atrophy in intensive care unit patients [108]. Elevated expression levels of miR-1246 may regulate lipopolysaccharide-induced apoptosis of pulmonary endothelial cells and acute lung injury by targeting angiotensin-converting enzyme 2 [109]. Many biomarker studies have investigated extracellular miRNAs to elucidate new targets for severe pulmonary disorders. Several have studied patients with CAP [110-113] and those with CAP and severe secondary complications [114, 115]. Extracellular miRNAs have great potential and are promising diagnostic and prognostic biomarker candidates. As discussed in this work, significant challenges remain, as the minority of extracellular miRNA biomarkers is reported consistently across different investigations [116]. Much

research is yet to accomplish to evolve extracellular miRNAs into clinically applicable biomarkers for routine testing.

3.4 Extracellular microRNAs are regulators in the pathophysiology of COVID-19

This study aimed to identify a possible role of extracellular miRNAs from crude EVs in the pathophysiology of COVID-19.

Out of 43 significantly regulated miRNAs in patients with COVID-19 pneumonia *versus* healthy controls, differential miRNA expression was further analyzed by a bioinformatically constructed regulatory network including only transcripts with the highest level of significant expression alterations (Figure 13).
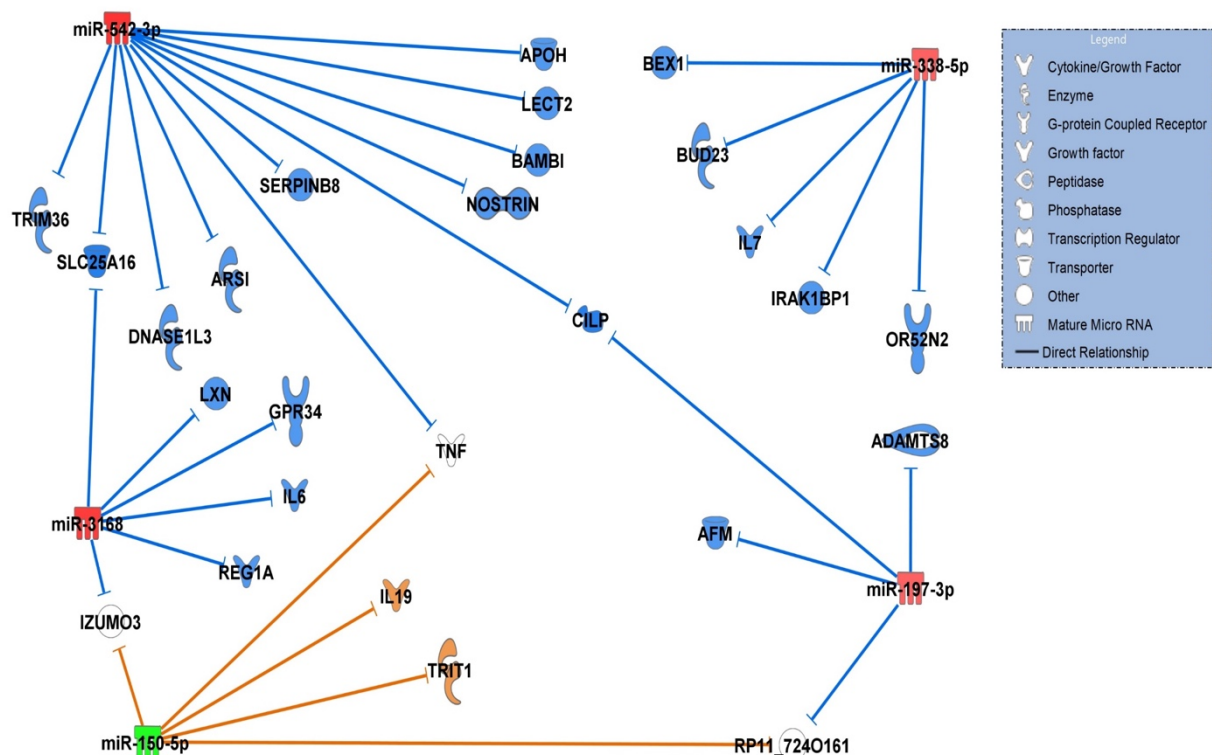

Figure 13: Comparison of significantly regulated miRNAs between patients with COVID-19 pneumonia and healthy controls and their predicted targets by *in silico* analysis. Upregulated miRNAs are colored red, their predicted and presumably inhibited targets blue. Downregulated miRNAs are colored green, their activated targets orange. IL-6: Interleukin-6; OR52N2: Olfactory Receptor Family 52 Subfamily N Member 2; IL-19: Interleukin-19; SERPINB8: Serpin Peptidase Inhibitor, Clade B (Ovalbumin), Member 8; APOH: Apolipoprotein H.

Upregulated miRNAs, miR-338-5p, miR-542-3p, and miR-197-3p, were essential regulators in the network, targeting most mRNAs.

Interestingly, miR-338-5p inhibited the olfactory smell receptor OR52N2 triggering the perception of smell in the nose. This finding may help explain a prominent clinical COVID-19 symptom, the decrease or loss of smell (hyposmia or anosmia), frequently observed in the early phase of SARS-CoV-2 infection [117].

Furthermore, miR-542-3p was identified as a negative regulator for APOH, which inhibits coagulation factors, and SERPINB8, which promotes fibrinolysis. This negative regulation of anticoagulant targets may be an additional risk factor for thromboembolic complications, present in about 30 % of COVID-19 cases [118]. Additionally, as SERPINB8 inhibits the protease furin [119], SERPINB8 inhibition by miR-542-3p was predicted to increase furin activity. Interestingly, SARS-CoV-2 binding to its host cell receptor ACE2 for cellular entry requires cleavage of the viral spike protein by furin [120].

Moreover, upregulated miR-3168 inhibited IL-6, a key mediator of the SARS-CoV-2-induced pro-inflammatory cytokine storm observed in severe COVID-19 cases [121].

The only downregulated miR-150-5p in this regulatory network induced the upregulation of the immunosuppressive cytokine IL-19, elevated in SARS-CoV-2-infected patients in association with increased disease severity [122].

In conclusion, amongst others [123, 124], this study indicates essential functions of extracellular miRNAs as regulators in the pathophysiology of COVID-19. Thus, once significant challenges in miRNA biomarker research are solved, these targets may also serve as COVID-19 biomarkers.

With the outbreak of the COVID-19 pandemic, significant research efforts are carried out to reach scientific progress to further understand SARS-CoV-2 and the associated COVID-19 disease. Hence, it is no surprise that miRNAs are currently studied extensively, e.g., as therapeutic targets for COVID-19 treatment or biomarkers [124, 125].

3.5 Potentials and limitations of extracellular vesicle microRNA biomarkers

With the discovery of functional RNA in exosomes [43], the EV field has started to evolve more than one decade ago. Current research demonstrated that human biofluid-derived EV preparations have great potential as early, minimal invasive disease biomarkers. Therefore, EV-associated miRNAs are often preferred over other compartments [126]. While relatively stable, EVs protect their miRNA cargoes from RNAse degradation in the extracellular space [127]. Loaded with specific information from their releasing cells and for transfer to their target cells, EVs may reflect the patients' actual health status. While the specific patterns of miRNA expression changes may be overwhelmed and undetectable in unfractionated liquid biopsies, EVs are strikingly reduced in unspecific background noise. For that reason, EV-related miRNA expression data often has a remarkably high power to classify different groups correctly.

Although very promising, significant limitations hamper the applicability of EV miRNA biomarkers. The heterogeneity of EVs, along with the co-isolation of non-vesicular material and the lack of standardization, face challenges to our fundamental understanding [128]. Consequently, little is known about the molecular mechanisms for loading miRNAs into EVs and their actual influence as novel regulators on target gene expression in recipient cells [48]. Current research has demonstrated that most extracellular miRNAs are associated with protein complexes and are not contained in EVs [128]. Low miRNA: EV ratios indicate that only a fraction of EVs seems to carry miRNA as a cargo [129, 130]. Researchers recently queried the relevance of EVs in cell-to-cell communication due to the deficiency in delivering functional miRNAs to target cells [130]. Contrary, functional effects of EVs on recipient cells via small RNA cargoes were reported by others [131, 132].

Since the study of EVs is affected by multiple factors, controversial findings are the subject of current research. Significant challenges about the study of EVs and their cargoes remain to be solved. Pre-analytical factors, including the collecting, handling, and storing of biofluids, introduce huge variability [133]. The small size of EVs and low yields of cargoes demand susceptible and accurate analysis methods [34, 48]. Different EV-separation methods are applied to various biofluids with the diverse

recovery of extracellular compartments and rare comparability between labs [34]. Additionally, a broad range of miRNA analysis platforms with varying settings and overall performance are used for analysis [101]. All these limitations currently hamper reproducibility and lead to relatively non-specific extracellular miRNA biomarkers [116].

4   Conclusion and perspectives

Several classes of biomolecules are currently under investigation to improve diagnostic and prognostic tests and prospectively complement already established clinical markers. Since the EV field exploded in recent years, EVs and their biomolecular cargoes were related to a spectrum of diseases. As stable, specific liquid biopsy biomarkers, EV-associated miRNA expression alterations can be quantified early after disease onset by previously established methods. This thesis and many other studies revealed the potential of extracellular miRNAs as novel molecular biomarkers enabling early intervention and expedient treatment, a critical milestone to limit disease spread.

In this work, a viable workflow was developed to study blood-derived EV miRNAs as potential disease biomarkers in the course of acute pulmonary infections. We demonstrated that sample preparation has a high impact on downstream small RNA-seq experiments. For the specific purpose of biomarker research, miRNA expression data from precipitated EVs outperformed cleaner separation methods in our study. Additionally, EVs and associated miRNA expression from arterial and venous blood were highly comparable for crude and purified EV preparations. Therefore, blood from either sampling site can be used with comparable results to study EV-associated miRNAs as biomarker targets. Finally, based on the established achievements, we developed and validated a three miRNA signature as a potential extracellular disease biomarker to detect patients with CAP and those at risk for the associated progression to sepsis. Furthermore, we identified a possible role of extracellular miRNAs in the pathophysiology of COVID-19.

Even in the presence of continuous progress and next-generation technologies, the translation of EV miRNAs into clinics is hampered since critical milestones still need to be achieved. To overcome current challenges, national and international EV societies work on concepts to enhance transparency, standardization, and reproducibility of EV research. Moreover, the study of biomarker signatures in increasing study populations and across multicenter studies is likely to improve the value of EV miRNAs as reliable, specific, and clinically applicable targets in the future. By translating such scientific innovations in biomarker research into clinical practice, progress in the employment of personalized medicine will become more likely and foster patient-tailored treatment of various diseases, e.g., acute pulmonary infection, prospectively.

5 References

1. Lee RC, Feinbaum RL, Ambros V. The C. elegans heterochronic gene lin-4 encodes small RNAs with antisense complementarity to lin-14. Cell 1993; 75: 843-854. DOI: 10.1016/0092-8674(93)90529-y
2. Wightman B, Ha I, Ruvkun G. Posttranscriptional regulation of the heterochronic gene lin-14 by lin-4 mediates temporal pattern formation in C. elegans. Cell 1993; 75: 855-862. DOI: 10.1016/0092-8674(93)90530-4
3. Reinhart BJ, Slack FJ, Basson M et al. The 21-nucleotide let-7 RNA regulates developmental timing in Caenorhabditis elegans. Nature 2000; 403: 901-906. DOI: 10.1038/35002607
4. Pasquinelli AE, Reinhart BJ, Slack F et al. Conservation of the sequence and temporal expression of let-7 heterochronic regulatory RNA. Nature 2000; 408: 86-89. DOI: 10.1038/35040556
5. Lagos-Quintana M, Rauhut R, Lendeckel W et al. Identification of Novel Genes Coding for Small Expressed RNAs. SCIENCE 2001; 294.
6. Lau NC, Lim LP, Weinstein EG et al. An abundant class of tiny RNAs with probable regulatory roles in Caenorhabditis elegans. Science 2001; 294: 858-862. DOI: 10.1126/science.1065062
7. Lee RC, Ambros V. An extensive class of small RNAs in Caenorhabditis elegans. Science 2001; 294: 862-864. DOI: 10.1126/science.1065329
8. Kozomara A, Birgaoanu M, Griffiths-Jones S. miRBase: from microRNA sequences to function. Nucleic Acids Res 2019; 47: D155-D162. DOI: 10.1093/nar/gky1141
9. Friedman RC, Farh KK, Burge CB et al. Most mammalian mRNAs are conserved targets of microRNAs. Genome Res 2009; 19: 92-105. DOI: 10.1101/gr.082701.108
10. Ha M, Kim VN. Regulation of microRNA biogenesis. Nat Rev Mol Cell Biol 2014; 15: 509-524. DOI: 10.1038/nrm3838
11. Lee Y, Kim M, Han J et al. MicroRNA genes are transcribed by RNA polymerase II. EMBO J 2004; 23: 4051-4060. DOI: 10.1038/sj.emboj.7600385
12. Lee Y, Jeon K, Lee JT et al. MicroRNA maturation: stepwise processing and subcellular localization. EMBO J 2002; 21: 4663-4670. DOI: 10.1093/emboj/cdf476
13. Lee Y, Ahn C, Han J et al. The nuclear RNase III Drosha initiates microRNA processing. Nature 2003; 425: 415-419. DOI: 10.1038/nature01957
14. Denli AM, Tops BB, Plasterk RH et al. Processing of primary microRNAs by the Microprocessor complex. Nature 2004; 432: 231-235. DOI: 10.1038/nature03049
15. Alarcon CR, Lee H, Goodarzi H et al. N6-methyladenosine marks primary microRNAs for processing. Nature 2015; 519: 482-485. DOI: 10.1038/nature14281
16. Han J, Lee Y, Yeom KH et al. The Drosha-DGCR8 complex in primary microRNA processing. Genes Dev 2004; 18: 3016-3027. DOI: 10.1101/gad.1262504
17. Okamura K, Hagen JW, Duan H et al. The mirtron pathway generates microRNA-class regulatory RNAs in Drosophila. Cell 2007; 130: 89-100. DOI: 10.1016/j.cell.2007.06.028

18. Treiber T, Treiber N, Meister G. Regulation of microRNA biogenesis and its crosstalk with other cellular pathways. Nat Rev Mol Cell Biol 2019; 20: 5-20. DOI: 10.1038/s41580-018-0059-1

19. Yi R, Qin Y, Macara IG et al. Exportin-5 mediates the nuclear export of pre-microRNAs and short hairpin RNAs. Genes Dev 2003; 17: 3011-3016. DOI: 10.1101/gad.1158803

20. Bohnsack MT, Czaplinski K, Gorlich D. Exportin 5 is a RanGTP-dependent dsRNA-binding protein that mediates nuclear export of pre-miRNAs. RNA 2004; 10: 185-191. DOI: 10.1261/rna.5167604

21. Bernstein E, Caudy AA, Hammond SM et al. Role for a bidentate ribonuclease in the initiation step of RNA interference. Nature 2001; 409: 363-366. DOI: 10.1038/35053110

22. Fareh M, Yeom KH, Haagsma AC et al. TRBP ensures efficient Dicer processing of precursor microRNA in RNA-crowded environments. Nat Commun 2016; 7: 13694. DOI: 10.1038/ncomms13694

23. Hammond SM, Boettcher S, Caudy AA et al. Argonaute2, a link between genetic and biochemical analyses of RNAi. Science 2001; 293: 1146-1150. DOI: 10.1126/science.1064023

24. Frank F, Sonenberg N, Nagar B. Structural basis for 5'-nucleotide base-specific recognition of guide RNA by human AGO2. Nature 2010; 465: 818-822. DOI: 10.1038/nature09039

25. Khvorova A, Reynolds A, Jayasena SD. Functional siRNAs and miRNAs exhibit strand bias. Cell 2003; 115: 209-216. DOI: 10.1016/s0092-8674(03)00801-8

26. Bartel DP. MicroRNAs: target recognition and regulatory functions. Cell 2009; 136: 215-233. DOI: 10.1016/j.cell.2009.01.002

27. Jo MH, Shin S, Jung SR et al. Human Argonaute 2 Has Diverse Reaction Pathways on Target RNAs. Mol Cell 2015; 59: 117-124. DOI: 10.1016/j.molcel.2015.04.027

28. Bartel DP. Metazoan MicroRNAs. Cell 2018; 173: 20-51. DOI: 10.1016/j.cell.2018.03.006

29. Jonas S, Izaurralde E. Towards a molecular understanding of microRNA-mediated gene silencing. Nat Rev Genet 2015; 16: 421-433. DOI: 10.1038/nrg3965

30. Chen CY, Shyu AB. Mechanisms of deadenylation-dependent decay. Wiley Interdiscip Rev RNA 2011; 2: 167-183. DOI: 10.1002/wrna.40

31. Leung AKL. The Whereabouts of microRNA Actions: Cytoplasm and Beyond. Trends Cell Biol 2015; 25: 601-610. DOI: 10.1016/j.tcb.2015.07.005

32. O'Brien J, Hayder H, Zayed Y et al. Overview of MicroRNA Biogenesis, Mechanisms of Actions, and Circulation. Front Endocrinol (Lausanne) 2018; 9: 402. DOI: 10.3389/fendo.2018.00402

33. Hermann S, Grätz C, Kirchner B et al. Extracellular vesicle-derived microRNA biomarkers: goals and pitfalls. Trillium Exctracellular Vesicles 2020; 2: 42-47. DOI: 10.47184/tev.2020.01.04

34. Thery C, Witwer KW, Aikawa E et al. Minimal information for studies of extracellular vesicles 2018 (MISEV2018): a position statement of the International Society for Extracellular Vesicles and update of the MISEV2014 guidelines. J Extracell Vesicles 2018; 7: 1535750. DOI: 10.1080/20013078.2018.1535750

35. Woith E, Fuhrmann G, Melzig MF. Extracellular Vesicles-Connecting Kingdoms. Int J Mol Sci 2019; 20. DOI: 10.3390/ijms20225695

36. Colombo M, Raposo G, Thery C. Biogenesis, secretion, and intercellular interactions of exosomes and other extracellular vesicles. Annu Rev Cell Dev Biol 2014; 30: 255-289. DOI: 10.1146/annurev-cellbio-101512-122326

37. Krämer-Albers EM, Frühbeis C. Delivery on call: exosomes as "care packages" from glial cells for stressed neurons. e-Neuroforum 2013; 19. DOI: 10.1007/s13295-013-0049-x

38. Mathieu M, Martin-Jaular L, Lavieu G et al. Specificities of secretion and uptake of exosomes and other extracellular vesicles for cell-to-cell communication. Nat Cell Biol 2019; 21: 9-17. DOI: 10.1038/s41556-018-0250-9

39. Wolf P. The nature and significance of platelet products in human plasma. Br J Haematol 1967; 13: 269-288. DOI: 10.1111/j.1365-2141.1967.tb08741.x

40. Trams EG, Lauter CJ, Salem N, Jr. et al. Exfoliation of membrane ecto-enzymes in the form of micro-vesicles. Biochim Biophys Acta 1981; 645: 63-70. DOI: 10.1016/0005-2736(81)90512-5

41. Raposo G, Nijman HW, Stoorvogel W et al. B lymphocytes secrete antigen-presenting vesicles. J Exp Med 1996; 183: 1161-1172. DOI: 10.1084/jem.183.3.1161

42. Bergsmedh A, Szeles A, Henriksson M et al. Horizontal transfer of oncogenes by uptake of apoptotic bodies. Proc Natl Acad Sci U S A 2001; 98: 6407-6411. DOI: 10.1073/pnas.101129998

43. Valadi H, Ekstrom K, Bossios A et al. Exosome-mediated transfer of mRNAs and microRNAs is a novel mechanism of genetic exchange between cells. Nat Cell Biol 2007; 9: 654-659. DOI: 10.1038/ncb1596

44. Al-Nedawi K, Meehan B, Micallef J et al. Intercellular transfer of the oncogenic receptor EGFRvIII by microvesicles derived from tumour cells. Nat Cell Biol 2008; 10: 619-624. DOI: 10.1038/ncb1725

45. Zernecke A, Bidzhekov K, Noels H et al. Delivery of microRNA-126 by apoptotic bodies induces CXCL12-dependent vascular protection. Sci Signal 2009; 2: ra81. DOI: 10.1126/scisignal.2000610

46. van Niel G, D'Angelo G, Raposo G. Shedding light on the cell biology of extracellular vesicles. Nat Rev Mol Cell Biol 2018; 19: 213-228. DOI: 10.1038/nrm.2017.125

47. Battistelli M, Falcieri E. Apoptotic Bodies: Particular Extracellular Vesicles Involved in Intercellular Communication. Biology (Basel) 2020; 9. DOI: 10.3390/biology9010021

48. Mateescu B, Kowal EJ, van Balkom BW et al. Obstacles and opportunities in the functional analysis of extracellular vesicle RNA - an ISEV position paper. J Extracell Vesicles 2017; 6: 1286095. DOI: 10.1080/20013078.2017.1286095

49. Stenmark H. Rab GTPases as coordinators of vesicle traffic. Nat Rev Mol Cell Biol 2009; 10: 513-525. DOI: 10.1038/nrm2728

50. Jahn R, Scheller RH. SNAREs--engines for membrane fusion. Nat Rev Mol Cell Biol 2006; 7: 631-643. DOI: 10.1038/nrm2002

51. Henne WM, Buchkovich NJ, Emr SD. The ESCRT pathway. Dev Cell 2011; 21: 77-91. DOI: 10.1016/j.devcel.2011.05.015

52. Hurley JH. ESCRTs are everywhere. EMBO J 2015; 34: 2398-2407. DOI: 10.15252/embj.201592484

53. Baietti MF, Zhang Z, Mortier E et al. Syndecan-syntenin-ALIX regulates the biogenesis of exosomes. Nat Cell Biol 2012; 14: 677-685. DOI: 10.1038/ncb2502

54. Stuffers S, Sem Wegner C, Stenmark H et al. Multivesicular endosome biogenesis in the absence of ESCRTs. Traffic 2009; 10: 925-937. DOI: 10.1111/j.1600-0854.2009.00920.x

55. Trajkovic K, Hsu C, Chiantia S et al. Ceramide triggers budding of exosome vesicles into multivesicular endosomes. Science 2008; 319: 1244-1247. DOI: 10.1126/science.1153124

56. Goni FM, Alonso A. Effects of ceramide and other simple sphingolipids on membrane lateral structure. Biochim Biophys Acta 2009; 1788: 169-177. DOI: 10.1016/j.bbamem.2008.09.002

57. Hugel B, Martinez MC, Kunzelmann C et al. Membrane microparticles: two sides of the coin. Physiology (Bethesda) 2005; 20: 22-27. DOI: 10.1152/physiol.00029.2004

58. Piccin A, Murphy WG, Smith OP. Circulating microparticles: pathophysiology and clinical implications. Blood Rev 2007; 21: 157-171. DOI: 10.1016/j.blre.2006.09.001

59. Muralidharan-Chari V, Clancy J, Plou C et al. ARF6-regulated shedding of tumor cell-derived plasma membrane microvesicles. Curr Biol 2009; 19: 1875-1885. DOI: 10.1016/j.cub.2009.09.059

60. Atkin-Smith GK, Poon IKH. Disassembly of the Dying: Mechanisms and Functions. Trends Cell Biol 2017; 27: 151-162. DOI: 10.1016/j.tcb.2016.08.011

61. Poon IK, Lucas CD, Rossi AG et al. Apoptotic cell clearance: basic biology and therapeutic potential. Nat Rev Immunol 2014; 14: 166-180. DOI: 10.1038/nri3607

62. Mulcahy LA, Pink RC, Carter DR. Routes and mechanisms of extracellular vesicle uptake. J Extracell Vesicles 2014; 3. DOI: 10.3402/jev.v3.24641

63. Yuana Y, Sturk A, Nieuwland R. Extracellular vesicles in physiological and pathological conditions. Blood Rev 2013; 27: 31-39. DOI: 10.1016/j.blre.2012.12.002

64. Yanez-Mo M, Siljander PR, Andreu Z et al. Biological properties of extracellular vesicles and their physiological functions. J Extracell Vesicles 2015; 4: 27066. DOI: 10.3402/jev.v4.27066

65. Shah R, Patel T, Freedman JE. Circulating Extracellular Vesicles in Human Disease. N Engl J Med 2018; 379: 958-966. DOI: 10.1056/NEJMra1704286

66. Thery C, Amigorena S, Raposo G et al. Isolation and characterization of exosomes from cell culture supernatants and biological fluids. Curr Protoc Cell Biol 2006; Chapter 3: Unit 3 22. DOI: 10.1002/0471143030.cb0322s30

67. Arab T, Raffo-Romero A, Van Camp C et al. Proteomic characterisation of leech microglia extracellular vesicles (EVs): comparison between differential ultracentrifugation and Optiprep density gradient isolation. J Extracell Vesicles 2019; 8: 1603048. DOI: 10.1080/20013078.2019.1603048

68. Consortium E-T, Van Deun J, Mestdagh P et al. EV-TRACK: transparent reporting and centralizing knowledge in extracellular vesicle research. Nat Methods 2017; 14: 228-232. DOI: 10.1038/nmeth.4185

69. van Dijk EL, Auger H, Jaszczyszyn Y et al. Ten years of next-generation sequencing technology. Trends Genet 2014; 30: 418-426. DOI: 10.1016/j.tig.2014.07.001

70. Goodwin S, McPherson JD, McCombie WR. Coming of age: ten years of next-generation sequencing technologies. Nat Rev Genet 2016; 17: 333-351. DOI: 10.1038/nrg.2016.49

71.   Qin D. Next-generation sequencing and its clinical application. Cancer Biol Med 2019; 16: 4-10. DOI: 10.20892/j.issn.2095-3941.2018.0055

72.   Strimbu K, Tavel JA. What are biomarkers? Curr Opin HIV AIDS 2010; 5: 463-466. DOI: 10.1097/COH.0b013e32833ed177

73.   Xi X, Li T, Huang Y et al. RNA Biomarkers: Frontier of Precision Medicine for Cancer. Noncoding RNA 2017; 3. DOI: 10.3390/ncrna3010009

74.   Condrat CE, Thompson DC, Barbu MG et al. miRNAs as Biomarkers in Disease: Latest Findings Regarding Their Role in Diagnosis and Prognosis. Cells 2020; 9. DOI: 10.3390/cells9020276

75.   Becker C, Hammerle-Fickinger A, Riedmaier I et al. mRNA and microRNA quality control for RT-qPCR analysis. Methods 2010; 50: 237-243. DOI: 10.1016/j.ymeth.2010.01.010

76.   Liu Y. MicroRNAs and PIWI-interacting RNAs in oncology. Oncol Lett 2016; 12: 2289-2292. DOI: 10.3892/ol.2016.4996

77.   Griffiths-Jones S, Grocock RJ, van Dongen S et al. miRBase: microRNA sequences, targets and gene nomenclature. Nucleic Acids Res 2006; 34: D140-144. DOI: 10.1093/nar/gkj112

78.   Tribolet L, Kerr E, Cowled C et al. MicroRNA Biomarkers for Infectious Diseases: From Basic Research to Biosensing. Front Microbiol 2020; 11: 1197. DOI: 10.3389/fmicb.2020.01197

79.   Welte T, Torres A, Nathwani D. Clinical and economic burden of community-acquired pneumonia among adults in Europe. Thorax 2012; 67: 71-79. DOI: 10.1136/thx.2009.129502

80.   Zar HJ, Madhi SA, Aston SJ et al. Pneumonia in low and middle income countries: progress and challenges. Thorax 2013; 68: 1052-1056. DOI: 10.1136/thoraxjnl-2013-204247

81.   Ceccato A, Torres A. Sepsis and community-acquired pneumonia. Annals of Research Hospitals 2018; 2: 7-7. DOI: 10.21037/arh.2018.06.01

82.   Global Health Estimates 2016. Disease burden by Cause, Age, Sex,by Country and by Region, 2000–2016. Geneva, World Health Organization; 2018.

83.   Tarsia P, Aliberti S, Pappalettera M et al. Mixed community-acquired lower respiratory tract infections. Curr Infect Dis Rep 2007; 9: 14-20. DOI: 10.1007/s11908-007-0017-0

84.   Mandell LA. Community-acquired pneumonia: An overview. Postgrad Med 2015; 127: 607-615. DOI: 10.1080/00325481.2015.1074030

85.   Nicod LP. Lung defences: an overview. European Respiratory Review 2005; 14: 45-50. DOI: 10.1183/09059180.05.00009501

86.   Raymond SL, Holden DC, Mira JC et al. Microbial recognition and danger signals in sepsis and trauma. Biochim Biophys Acta Mol Basis Dis 2017; 1863: 2564-2573. DOI: 10.1016/j.bbadis.2017.01.013

87.   Moldoveanu B, Otmishi P, Jani P et al. Inflammatory mechanisms in the lung. J Inflamm Res 2009; 2: 1-11.

88.   Mizgerd JP. Inflammation and Pneumonia: Why Are Some More Susceptible than Others? Clin Chest Med 2018; 39: 669-676. DOI: 10.1016/j.ccm.2018.07.002

89.   Mandell LA, Wunderink RG, Anzueto A et al. Infectious Diseases Society of America/American Thoracic Society consensus guidelines on the management of community-acquired pneumonia in adults. Clin Infect Dis 2007; 44 Suppl 2: S27-72. DOI: 10.1086/511159

90. Savvateeva EN, Rubina AY, Gryadunov DA. Biomarkers of Community-Acquired Pneumonia: A Key to Disease Diagnosis and Management. Biomed Res Int 2019; 2019: 1701276. DOI: 10.1155/2019/1701276

91. Shaddock EJ. How and when to use common biomarkers in community-acquired pneumonia. Pneumonia (Nathan) 2016; 8: 17. DOI: 10.1186/s41479-016-0017-7

92. Lim WS, van der Eerden MM, Laing R et al. Defining community acquired pneumonia severity on presentation to hospital: an international derivation and validation study. Thorax 2003; 58: 377-382. DOI: 10.1136/thorax.58.5.377

93. Kanwar M, Brar N, Khatib R et al. Misdiagnosis of community-acquired pneumonia and inappropriate utilization of antibiotics: side effects of the 4-h antibiotic administration rule. Chest 2007; 131: 1865-1869. DOI: 10.1378/chest.07-0164

94. Peyrani P, Mandell L, Torres A et al. The burden of community-acquired bacterial pneumonia in the era of antibiotic resistance. Expert Rev Respir Med 2019; 13: 139-152. DOI: 10.1080/17476348.2019.1562339

95. Karakioulaki M, Stolz D. Biomarkers in Pneumonia-Beyond Procalcitonin. Int J Mol Sci 2019; 20. DOI: 10.3390/ijms20082004

96. Buschmann D, Kirchner B, Hermann S et al. Evaluation of serum extracellular vesicle isolation methods for profiling miRNAs by next-generation sequencing. J Extracell Vesicles 2018; 7: 1481321. DOI: 10.1080/20013078.2018.1481321

97. Hermann S, Buschmann D, Kirchner B et al. Transcriptomic profiling of cell-free and vesicular microRNAs from matched arterial and venous sera. J Extracell Vesicles 2019; 8: 1670935. DOI: 10.1080/20013078.2019.1670935

98. Hermann S, Brandes F, Kirchner B et al. Diagnostic potential of circulating cell-free microRNAs for community-acquired pneumonia and pneumonia-related sepsis. J Cell Mol Med 2020. DOI: 10.1111/jcmm.15837

99. Arroyo JD, Chevillet JR, Kroh EM et al. Argonaute2 complexes carry a population of circulating microRNAs independent of vesicles in human plasma. Proc Natl Acad Sci U S A 2011; 108: 5003-5008. DOI: 10.1073/pnas.1019055108

100. Karttunen J, Heiskanen M, Navarro-Ferrandis V et al. Precipitation-based extracellular vesicle isolation from rat plasma co-precipitate vesicle-free microRNAs. J Extracell Vesicles 2019; 8: 1555410. DOI: 10.1080/20013078.2018.1555410

101. Van Deun J, Mestdagh P, Sormunen R et al. The impact of disparate isolation methods for extracellular vesicles on downstream RNA profiling. J Extracell Vesicles 2014; 3. DOI: 10.3402/jev.v3.24858

102. Takov K, Yellon DM, Davidson SM. Comparison of small extracellular vesicles isolated from plasma by ultracentrifugation or size-exclusion chromatography: yield, purity and functional potential. J Extracell Vesicles 2019; 8: 1560809. DOI: 10.1080/20013078.2018.1560809

103. Brennan K, Martin K, FitzGerald SP et al. A comparison of methods for the isolation and separation of extracellular vesicles from protein and lipid particles in human serum. Sci Rep 2020; 10: 1039. DOI: 10.1038/s41598-020-57497-7

104. Kelly E, Owen CA, Abraham A et al. Comparison of arterial and venous blood biomarker levels in chronic obstructive pulmonary disease. F1000Res 2013; 2: 114. DOI: 10.12688/f1000research.2-114.v1

105. Bai L, Ma J, Wang Y et al. MicroRNAomes of Porcine Arterial and Venous Blood. J Anim Vet Adv 2014; 13: 21-27.

106. Xu W, Zhou Y, Xu G et al. Transcriptome analysis reveals non-identical microRNA profiles between arterial and venous plasma. Oncotarget 2017; 8: 28471-28480. DOI: 10.18632/oncotarget.15310

107. Reithmair M, Buschmann D, Marte M et al. Cellular and extracellular miRNAs are blood-compartment-specific diagnostic targets in sepsis. J Cell Mol Med 2017; 21: 2403-2411. DOI: 10.1111/jcmm.13162

108. Garros RF, Paul R, Connolly M et al. MicroRNA-542 Promotes Mitochondrial Dysfunction and SMAD Activity and Is Elevated in Intensive Care Unit-acquired Weakness. Am J Respir Crit Care Med 2017; 196: 1422-1433. DOI: 10.1164/rccm.201701-0101OC

109. Fang Y, Gao F, Hao J et al. microRNA-1246 mediates lipopolysaccharide-induced pulmonary endothelial cell apoptosis and acute lung injury by targeting angiotensin-converting enzyme 2. Am J Transl Res 2017; 9: 1287-1296.

110. Huang S, Feng C, Zhai YZ et al. Identification of miRNA biomarkers of pneumonia using RNA-sequencing and bioinformatics analysis. Exp Ther Med 2017; 13: 1235-1244. DOI: 10.3892/etm.2017.4151

111. Huang F, Bai J, Zhang J et al. Identification of potential diagnostic biomarkers for pneumonia caused by adenovirus infection in children by screening serum exosomal microRNAs. Mol Med Rep 2019; 19: 4306-4314. DOI: 10.3892/mmr.2019.10107

112. Zhang X, Huang F, Yang D et al. Identification of miRNA-mRNA Crosstalk in Respiratory Syncytial Virus- (RSV-) Associated Pediatric Pneumonia through Integrated miRNAome and Transcriptome Analysis. Mediators Inflamm 2020; 2020: 8919534. DOI: 10.1155/2020/8919534

113. Galvan-Roman JM, Lancho-Sanchez A, Luquero-Bueno S et al. Usefulness of circulating microRNAs miR-146a and miR-16-5p as prognostic biomarkers in community-acquired pneumonia. PLoS One 2020; 15: e0240926. DOI: 10.1371/journal.pone.0240926

114. Zhang W, Jia J, Liu Z et al. Circulating microRNAs as biomarkers for Sepsis secondary to pneumonia diagnosed via Sepsis 3.0. BMC Pulm Med 2019; 19: 93. DOI: 10.1186/s12890-019-0836-4

115. Wu X, Wu C, Gu W et al. Serum Exosomal MicroRNAs Predict Acute Respiratory Distress Syndrome Events in Patients with Severe Community-Acquired Pneumonia. Biomed Res Int 2019; 2019: 3612020. DOI: 10.1155/2019/3612020

116. Witwer KW. Circulating microRNA biomarker studies: pitfalls and potential solutions. Clin Chem 2015; 61: 56-63. DOI: 10.1373/clinchem.2014.221341

117. Gupta K, Mohanty SK, Mittal A et al. The Cellular basis of loss of smell in 2019-nCoV-infected individuals. Brief Bioinform 2021; 22: 873-881. DOI: 10.1093/bib/bbaa168

118. Liu Y, Cai J, Wang C et al. Incidence, prognosis, and laboratory indicators of venous thromboembolism in hospitalized patients with coronavirus disease 2019: a systematic review and meta-analysis. J Vasc Surg Venous Lymphat Disord 2021. DOI: 10.1016/j.jvsv.2021.01.012

119. Leblond J, Laprise MH, Gaudreau S et al. The serpin proteinase inhibitor 8: an endogenous furin inhibitor released from human platelets. Thromb Haemost 2006; 95: 243-252. DOI: 10.1160/TH05-08-0561

120. Shang J, Wan Y, Luo C et al. Cell entry mechanisms of SARS-CoV-2. Proc Natl Acad Sci U S A 2020; 117: 11727-11734. DOI: 10.1073/pnas.2003138117

121. Herold T, Jurinovic V, Arnreich C et al. Elevated levels of IL-6 and CRP predict the need for mechanical ventilation in COVID-19. J Allergy Clin Immunol 2020; 146: 128-136 e124. DOI: 10.1016/j.jaci.2020.05.008

122. Sims JT, Krishnan V, Chang CY et al. Characterization of the cytokine storm reflects hyperinflammatory endothelial dysfunction in COVID-19. J Allergy Clin Immunol 2021; 147: 107-111. DOI: 10.1016/j.jaci.2020.08.031

123. Li C, Hu X, Li L et al. Differential microRNA expression in the peripheral blood from human patients with COVID-19. J Clin Lab Anal 2020; 34: e23590. DOI: 10.1002/jcla.23590

124. McDonald JT, Enguita FJ, Taylor D et al. The Great Deceiver: miR-2392's Hidden Role in Driving SARS-CoV-2 Infection. bioRxiv 2021. DOI: 10.1101/2021.04.23.441024

125. El-Nabi SH, Elhiti M, El-Sheekh M. A new approach for COVID-19 treatment by micro-RNA. Med Hypotheses 2020; 143: 110203. DOI: 10.1016/j.mehy.2020.110203

126. Nik Mohamed Kamal N, Shahidan WNS. Non-Exosomal and Exosomal Circulatory MicroRNAs: Which Are More Valid as Biomarkers? Front Pharmacol 2019; 10: 1500. DOI: 10.3389/fphar.2019.01500

127. Keller S, Ridinger J, Rupp AK et al. Body fluid derived exosomes as a novel template for clinical diagnostics. J Transl Med 2011; 9: 86. DOI: 10.1186/1479-5876-9-86

128. Jeppesen DK, Fenix AM, Franklin JL et al. Reassessment of Exosome Composition. Cell 2019; 177: 428-445 e418. DOI: 10.1016/j.cell.2019.02.029

129. Lai RC, Tan SS, Yeo RW et al. MSC secretes at least 3 EV types each with a unique permutation of membrane lipid, protein and RNA. J Extracell Vesicles 2016; 5: 29828. DOI: 10.3402/jev.v5.29828

130. Albanese M, Chen Y-FA, Hüls C et al. 2020. DOI: 10.1101/2020.05.20.106393

131. de Jong OG, Murphy DE, Mager I et al. A CRISPR-Cas9-based reporter system for single-cell detection of extracellular vesicle-mediated functional transfer of RNA. Nat Commun 2020; 11: 1113. DOI: 10.1038/s41467-020-14977-8

132. Tapparo M, Pomatto MAC, Deregibus MC et al. Serum Derived Extracellular Vesicles Mediated Delivery of Synthetic miRNAs in Human Endothelial Cells. Front Mol Biosci 2021; 8: 636587. DOI: 10.3389/fmolb.2021.636587

133. Clayton A, Buschmann D, Byrd JB et al. Summary of the ISEV workshop on extracellular vesicles as disease biomarkers, held in Birmingham, UK, during December 2017. J Extracell Vesicles 2018; 7: 1473707. DOI: 10.1080/20013078.2018.1473707

6 Acknowledgements

List of scientific communications

Peer-reviewed publications

Buschmann D, Kirchner B, <u>Hermann S</u>, et al. Evaluation of serum extracellular vesicle isolation methods for profiling miRNAs by next-generation sequencing. J Extracell Vesicles. 2018; 7: 1481321.

<u>Hermann S</u>, Buschmann D, Kirchner B, et al. Transcriptomic profiling of cell-free and vesicular microRNAs from matched arterial and venous sera. J Extracell Vesicles. 2019; 8: 1670935.

<u>Hermann S</u>, Grätz C, Kirchner B, et al. Extracellular vesicle-derived microRNA biomarkers: goals and pitfalls. Trillium Extracellular Vesicles 2020; 2: 42-7.

<u>Hermann S</u>, Brandes F, Kirchner B, et al. Diagnostic potential of circulating cell-free microRNAs for community-acquired pneumonia and pneumonia-related sepsis. J Cell Mol Med. 2020.

Book chapters

Mussack V, <u>Hermann S</u>, Buschmann D, et al. MIQE-Compliant Validation of MicroRNA Biomarker Signatures Established by Small RNA Sequencing. Methods Mol Biol. 2020; 2065: 23-38.

Poster presentations

<u>Hermann S</u>, Buschmann D, Kirchner B, et al. ISEV 2018, Barcelona, Spain: Comparative analysis of extracellular vesicles from arterial and venous blood reveals only minor differences in vesicle composition.

<u>Hermann S</u>, Kirchner B, Buschmann D, et al. ISEV 2019, Kyoto, Japan: Diagnostic microRNA biomarkers from circulating extracellular vesicles for early detection of pneumonia and severe secondary complications.

Hermann S, Buschmann D, Kirchner B, et al. qPCR, dPCR & NGS Symposium 2019, Freising, Germany: Systematic comparison of extracellular vesicles from human arterial and venous blood: highly identical microRNA expression indicates equal use for biomarker applications.

Hermann S, Kirchner B, Buschmann D, et al. GSEV Autumn Meeting 2019, Marburg, Germany: Distinct miRNA profiles in circulating EVs from critically ill patients with lung damage.

Oral presentations

Hermann S, Kirchner B, Buschmann D, et al. ISEV 2019, Kyoto, Japan: Diagnostic microRNA biomarkers from circulating extracellular vesicles for early detection of pneumonia and severe secondary complications.

Appendix

Appendix I

Hermann S, Grätz C, Kirchner B, et al. Extracellular vesicle-derived microRNA biomarkers: goals and pitfalls. Trillium Extracellular Vesicles 2020; 2: 42-7.

Appendix II

Buschmann D, Kirchner B, Hermann S, et al. Evaluation of serum extracellular vesicle isolation methods for profiling miRNAs by next-generation sequencing. J Extracell Vesicles. 2018; 7: 1481321.

Appendix III

Hermann S, Buschmann D, Kirchner B, et al. Transcriptomic profiling of cell-free and vesicular microRNAs from matched arterial and venous sera. J Extracell Vesicles. 2019; 8: 1670935.

Appendix IV

Hermann S, Brandes F, Kirchner B, et al. Diagnostic potential of circulating cell-free microRNAs for community-acquired pneumonia and pneumonia-related sepsis. J Cell Mol Med. 2020.

Appendix I

Contribution by Stefanie Hermann:

- Project administration
- Manuscript conceptualization
- Writing – original draft
- Investigation – literature review
- Visualization

Stefanie Hermann

Prof. Dr. Michael W. Pfaffl

Extracellular vesicle-derived microRNA biomarkers: goals and pitfalls

Stefanie Hermann, Christian Grätz, Benedikt Kirchner and Michael W. Pfaffl

Liquid biopsy-derived extracellular vesicles (EVs) are an auspicious source for transcriptomic biomarker studies. Here, we review the potential of EV microRNAs (miRNAs) biomarkers, exemplary outline commonly used methods to elucidate new biomarker signatures, and pivotally discuss their applicability at present.

Keywords: *Liquid biopsies, transcriptomic biomarkers, microRNAs*

Molecular biomarkers

A biomarker is a "defined characteristic that is measured as an indicator of normal biological processes, pathogenic processes, or responses to an exposure or intervention, including therapeutic interventions" [1]. Biomarkers should be directly associated to a certain disease state or condition, allowing for precise, reproducible and fast evaluation of molecular alterations in an objective manner [2, 3]. Multiple marker signatures are preferred over single biomarkers [4], as analytical specificity strengthens the diagnostic, prognostic or monitoring potential.

The development towards the routine use of high-throughput molecular techniques, like next generation sequencing (NGS) or proteome profiling, led to a massive increase in potentially valuable molecular biomarkers [2]. But up to now, their clinical implementation is still limited. More than 150,000 biomarker studies have been published by 2011 from which only around 100 reliable biomarkers have been successfully transferred for clinical routine use to the hospitals [5].

In this review, we want to address the goals and pitfalls of extracellular vesicle (EV)-derived microRNA (miRNA) biomarkers in the context of molecular diagnostics.

Transcriptomic biomarkers

Why do we focus on RNA – also referred to as transcriptomic – biomarkers? As compared to DNA, besides genetic insights, the transcriptome provides dynamic information on cellular states and regulatory processes [6]. First early response genes, like transcription factors, are activated within 10 to 20 minutes, after hours mid to late response genes are transcribed. Thus, quantifying RNA biomarkers enables an earlier evaluation of cellular physiological changes, disease states or conditions than measuring proteins.

Moreover, transcriptomic biomarkers show higher sensitivity and specificity, and are more cost-efficient than proteomic markers. Nucleic acid biomarkers are easy to quantify at very low cellular abundance levels by either polymerase chain reaction (PCR) [6, 7], such as reverse transcription real-time PCR (RT-qPCR), or RNA sequencing (RNA-Seq). RNA-Seq analyses can be performed comprehensively, since all transcripts are measurable

in parallel in one run [8], thereby reducing possible batch effects. Additionally, good pathway and network interaction tools are available for the RNA world, e. g. DIANA tools [9] (www.microrna.gr).

But what are the advantages of miRNAs over other transcriptomic biomarkers? Short is better – miRNAs have exceptional high stability [10], unlike longer RNA classes, as for example messenger RNAs (mRNAs) or long non-coding RNAs (lncRNAs). The potential of other small regulatory RNA classes, such as piwi-interacting RNAs (piRNAs) have not yet been thoroughly investigated and only few biomarker relevant articles have been published so far [11]. Although miRNAs and lncRNAs have both been discovered almost 30 years ago [7, 12], miRNAs have been studied more extensively as potential biomarkers than lncRNAs [13], and therefore more extensive miRNA databases are currently available, e. g. miRBase [14] (www.miRbase.org) and miRDB [15] (www.miRDB.org). Additionally, miRNAs are protected from endogenous RNase activity by being encapsulated in EVs or by forming complexes with different kinds of RNA-binding proteins, such as Argonaute proteins or high-density lipoproteins [7, 16].

Liquid biopsies

The availability of high-throughput and highly sensitive methods enables the detection of nucleic acid biomarkers even in low concentrated or low volume patient samples. This allows for minimally invasive sampling of body fluids like blood, urine and saliva amongst others [17]. Liquid biopsies, as these sampling methods are called, offer the possibility to detect diseases in very early stages or in patients where conventional tissue biopsies cannot be performed [17–19]. Furthermore, liquid biopsies make it possible to take multiple samples at any point of time in one patient, to monitor the stage or progress of the disease or follow the therapy success [17, 18]. Because these are crucial advantages for the successful treatment of numerous diseases, e. g. in most types of cancer, liquid biopsies have become quite popular in recent years.

In liquid biopsy samples different targets can be used for molecular diagnostics (Table 1), e. g. circulating cell-free DNA (ccfDNA), circulating RNA, circulating tumor cells (CTCs), and EVs [17].

EVs and more specifically their miRNA content, being present in all kinds of body fluids, are an excellent and often chosen target for liquid biopsy analysis [17, 20]. While circulating nucleic acids are relatively easy to purify from blood samples, EVs are not. EV isolation methods often co-isolate contaminants, most notably various lipoproteins, which are similar to EVs in size and density [21] and may interfere with downstream analysis. Although the choice of purification method can influence the results of EV analysis, a consensus on EV isolation has not yet been established [22, 23].

However, circulating free RNA or DNA is rapidly degraded by nucleases in the extracellular space [19]. Although ccfDNA is more stable than RNA, due to its protection by nucleosomes or other proteins, it is also subject to degradation and fragmentation [17, 24]. Inside EVs, however, nucleic acids are protected from nucleases by the vesicle membrane [20]. Furthermore, the EV cargo is similar in composition to the original cell, meaning that EVs shed by cells involved in a certain disease contain a biomarker signature closely related to the disease [25].

CTCs, on the other hand, are cells that disassociated from the original tumor and therefore carry its mutations and biomarkers [18, 19]. However, they are primarily found in blood and urine and only focus on tumor diagnosis [17]. Furthermore, few CTCs are found in early stage tumor patients, limiting their potential for early diagnosis [26].

EV miRNAs as new avenues for transcriptomic biomarker studies

EVs participate in cell-cell communication amongst others by transferring miRNAs [25]. The discovery of functional mRNA and miRNA in EVs [29] opened

Table 1: Comparison of targets to be analyzed in liquid biopsies.

Target	Source [27]	Advantages	Disadvantages
EVs	All body fluids	Protection of (RNA) cargo from degradation [20], cargo resembles cell of origin [25]	Difficult to purify, isolation method may influence results [28]
ccfDNA	All body fluids	Relatively easy to purify	Fragmented [17, 24]
Circulating RNA	All body fluids	Relatively easy to purify	Fragmented, fast degradation [19]
CTCs	Blood, urine	Whole tumor cell with all information [18,19]	Limited to tumor diagnosis, low abundance in early-stage tumors [26]

EVs: extracellular vesicles; ccfDNA: circulating cell-free DNA; CTCs: circulating tumor cells.

up new avenues for transcriptomic biomarker studies that offer definite advantages. EVs are isolated from non-invasive liquid biopsies (I), are relatively stable (II), protect miRNAs from degradation (III), and are specifically loaded with miRNAs (IV) [30, 31]. EV-based RNA biomarkers would frequently be undetectable in unfractionated or unprocessed biofluids due to high, unspecific background signals. However, one must be aware that different purification methods may result in distinct EV subpopulations and may therefore effect the results of downstream RNA profiling [22, 23].

Liquid biopsies from blood appear to be a robust source for EV RNA research, as storage of plasma samples for up to 12 years at -80°C, two weeks at 4°C, two days at room temperature, and multiple cycles of thawing and refreezing, all resulted in intact, non-degraded EV RNA [32, 33].

Long-term storage and freeze-thaw cycles of EVs themselves seem to only marginally impact their amounts [34]. Additionally, EV-derived nucleic acids imply to be stable under various conditions, as for example storage of EVs for one week at 4°C, one day at room temperature and repeated freeze-thawing, only minorly impact the stability of EV DNA [35].

Hence using EV-related miRNA for molecular diagnostics has major advantages over other target molecules [36]. A PubMed (www.pubmed.ncbi.nlm.nih.gov) search for "extracellular vesicle, microRNA biomarker" identified more than 1,200 publications (May 2020) related to various disorders including diverse types of cancers, neurodegenerative diseases and sepsis, indicative for the innovative exploration of EV miRNAs as biomarker source.

By now, a vast number of EV-related miRNAs has been associated with numerous diseases, one example being cancer. Many potential EV-associated miRNA biomarkers have been discovered for various types of tumors . To name just a few examples, the exosomal miRNAs miR-486-5p, miR-181a-5p and miR-30d-5p have recently been identified as circulating markers of high-risk rectal cancer [37]. Another example is miR-21, which has been shown to be involved in many types of cancer [38], e. g. glioblastoma [39], non-small-cell lung cancer [40] or hepatocellular carcinoma [41].

How to elucidate potential EV miRNA biomarkers

Molecular profiling of EV miRNAs from non-invasive liquid biopsies by high-throughput technologies, in particular small RNA-Seq, is a powerful platform to comprehensively screen for new disease-related miRNA biomarker candidates (Figure 1) [8].

Although EVs are enriched for miRNAs in various physiological or pathophysiological conditions [20] and library preparations for small RNA-Seq typically include a size selection step to exclude larger RNA fragments (>200 nucleotides). NGS data from EV isolations can still include a considerable amount of non-miRNA sequences that need to be removed to reduce background noise and strengthen miRNA-specific disease- or treatment-related signals. Origins of these unspecific RNA fragments can be manifold and range from library preparation artefacts like sequencing adapter dimers to degradation products caused by handling or storage [8]. Furthermore, significant variance is also added to EV
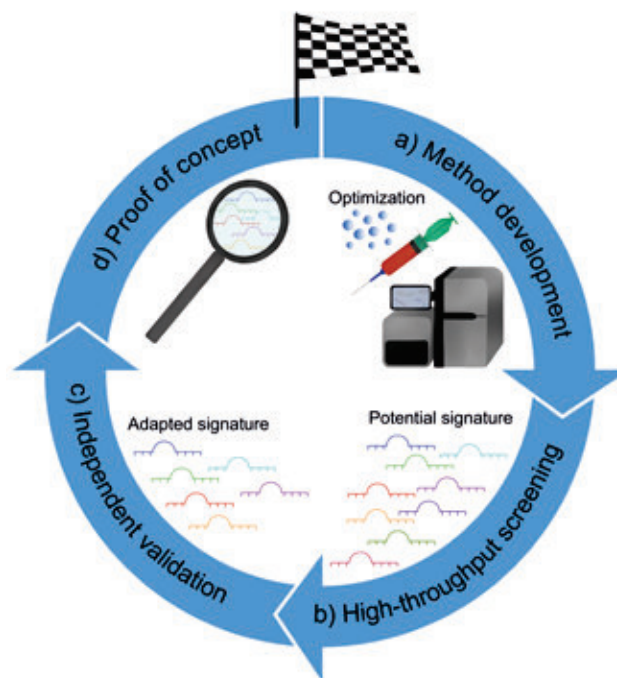

Figure 1: Exemplary workflow on how to elucidate potential EV miRNA biomarkers. a) Method development: After controlling for pre-analytical variables, optimization of methods for sample preparation, high-throughput screening and orthogonal validation takes place, prior to the development of a strategy for multivariate data analysis. b) High-throughput screening: Optimized methods are applied to a defined training set (Cohort 1) to obtain a candidate EV miRNA biomarker signature. c) Independent validation: Methods are applied to a defined validation set (Cohort 2) to confirm and optimize the EV miRNA biomarker signature. d) Proof of concept by applying the approved validation method to various sample sets.

biomarker studies by vesicle isolation methods and the resulting prevalent subpopulations of EVs [42]. Researchers need to pay special attention during experimental setup to consider possible consequences on required sample sizes or sequencing depths arising from less pure but highly concentrated EV preparations such as precipitation methods compared to for instance size-exclusion chromatography [22].

Having navigated these pitfalls, researchers are rewarded with an extensive miRNA profile from EVs that often display much higher discriminatory power than comparable data sets from unfractionated and unprocessed liquid biopsies. By using different bioinformatical approaches of multivariate data analyses, or combinations thereof, a candidate biomarker signature is developed from miRNA expression data in a training set of individuals. Outliers or dominant batch effects can be visualized by unsupervised clustering methods such as hierarchical clustering analysis (HCA) and especially principal component analysis (PCA) or t-distributed stochastic neighbor embedding [43]. Differential gene expression (DGE) analysis detects the most drastically dysregulated transcripts between treatment groups [44], while sparse partial least squares discriminant analysis (sPLS-DA) reveals a subset of EV miRNAs efficient to discriminate all the available groups [45]. Resulting potential biomarker patterns can be cross-referenced with results from pre-existing studies collated in databases such as Vesiclepedia [46] or EVmiRNA [47] to validate specificity for tissues or diseases not included in the experimental setup. By expanding potential miRNA biomarker sets with their corresponding mRNA targets, func-

tional and biological relevance can be assessed through gene enrichment analysis of disease-associated pathways. Databases for mRNA targets include computational prediction models [48] as well as repositories of experimentally validated mRNAs [49]. If available, integrated analyses of miRNA with mRNA or protein information can also be incorporated by directly obtaining data sets of comparable studies from publicly available data repositories like the European Nucleotide Archive [50] or the Sequence Read Archive [51].

Subsequently, the candidate biomarker signature is quantified in a validation trial, to proof for stability and reproducibility, and hence improve the diagnostic, prognostic or monitoring value of the EV miRNA profiles. Ideally, the EV miRNA signature is quantifiable in the same training set by using an orthogonal miRNA analysis platform, particularly RT-qPCR, and additionally confirmable in a larger, biologically independent validation set of individuals. Outsourcing of validation experiments to external laboratories allows for independent proof of validity of the EV miRNA biomarker signature [52].

A long and stony road to the applicability of EV miRNA biomarkers

Although we assume the transfer of EV miRNAs as messages from the "releasing cells" to the "target cells" in intercellular communication, there is a considerable knowledge gap. Cells secrete different subtypes of EVs with varying sizes and compositions, some of which are believed to not even contain RNA as a cargo [53]. The mechanisms which actu-

ally regulate miRNA loading into EVs and how these information influence recipient cells are still poorly understood. Whether these miRNAs are exclusively intraluminal, or maybe located at the outer EV membrane, is yet uncertain [54].

Affected by an irreproducibility problem [52], circulating miRNA biomarkers are currently rather non-specifically related to a multitude of disorders and outcomes, with few accordance between equal studies of even the same disease [55]. But what are the obstacles in the path generating this enormous diversity?

There is mostly an insufficiency of control for pre-analytical variables including collection, handling and storage of human biofluids, affecting both their quality and consistency, and in the same way the recovery of EVs, as well as the grade of potential EV miRNA biomarkers. Thus it is essential to process all samples identically and report all known pre-analytical parameters [52, 56].

The comparability between labs is often limited, as different miRNA analysis platforms with divergent sensitivities, settings and overall performance are available, thereby highly impacting results [57]. Additionally, diverse biofluids and starting volumes are the basis for a multitude of EV separation and RNA extraction protocols resulting in divergent EV miRNA expression profiles [22, 23].

To facilitate and improve standardization in the EV field, the MISEV guidelines were published and provide recommendations with regard to the minimal information for studies of EVs [56]. Other position statements from the International Society of Extracellular Vesicles (ISEV) focus on EV subtopics, for instance EV-associated RNA [54]. EV-

TRACK offers a platform for transparent reporting and centralizing knowledge in EV research [28].

Now the question comes up: what is the best strategy for normalization? While some researchers apply a definite starting volume of the respective biofluid and thereof extracted EV total RNA, others consider EV numbers or RNA concentrations for their assays [58, 59]. However, as EVs are nanosized and carry only limited quantities of RNA, accurate quantification of EVs themselves and their RNA cargo by highly specific and sensitive techniques still remains challenging [54, 56]. Moreover, different amounts of miRNAs in EV subtypes might hamper normalization based on the vesicle level.

Currently, most EV miRNA biomarker studies are conducted in fairly small study populations, while generating truly homogenous cohorts can be challenging. It is well-known that miRNA expression is affected by biological properties such as sex, age or body mass index [60], and it is obvious that EV composition is influenced by demographics as well [61, 62]. As each patient represents an individual medical condition, prescribed treatments and medications may lead to distinct outcomes due to heterogeneous patient responses to therapy. Profiling of EV miRNAs is therefore recommended in large cohorts, to minimize the confounding effects of differential expression due to individual variability in both patients and healthy controls.

Conclusion

Despite the tremendous effort in EV miRNA biomarker research, there are currently no specific and validated targets with real potential for clinic routine settings available. High inter-lab variability is introduced by divergent pre-processing approaches of multiple human biofluids, various combinations of EV separation and RNA extraction methods, added by different miRNA analysis platforms, normalization, and data evaluation strategies.

A future focus on standardization of the EV-based transcriptomic biomarker workflow is urgently required. Increased efforts aiming to solve the challenges related to EV research are essential, filling the knowledge gaps by strengthening research, to exploit the opportunity of a new innovative approach of clinically applicable and non-invasive molecular biomarkers. Since single miRNAs are involved in many different pathogenic pathways, diagnostic strategies should focus on patterns of up- and downregulated miRNAs that are specific for certain diseases.

References

1. FDA-NIH Biomarker Working Group. BEST (Biomarkers, EndpointS, and other Tools) Resource. Silver Spring (MD): Food and Drug Administration (US); Bethesda (MD): National Institutes of Health (US). 2016.

2. Pfaffl MW. Transcriptional biomarkers. Methods. 2013; 59: 1-2.

3. Strimbu K, Tavel JA. What are biomarkers? Curr Opin HIV AIDS. 2010; 5: 463-6.

4. Alhasan AH, Scott AW, Wu JJ, et al. Circulating microRNA signature for the diagnosis of very high-risk prostate cancer. Proc Natl Acad Sci U S A. 2016; 113: 10655-60.

5. Poste G. Bring on the biomarkers. Nature. 2011; 469 (7329): 156-7.

6. Xi X, Li T, Huang Y, et al. RNA Biomarkers: Frontier of Precision Medicine for Cancer. Noncoding RNA. 2017; 3.

7. Condrat CE, Thompson DC, Barbu MG, et al. miRNAs as Biomarkers in Disease: Latest Findings Regarding Their Role in Diagnosis and Prognosis. Cells. 2020; 9.

8. Buschmann D, Haberberger A, Kirchner B, et al. Toward reliable biomarker signatures in the age of liquid biopsies - how to standardize the small RNA-Seq workflow. Nucleic Acids Res. 2016; 44: 5995-6018.

9. Vlachos IS, Hatzigeorgiou AG. Functional Analysis of miRNAs Using the DIANA Tools Online Suite. In: Schmidt M (eds) Drug Target miRNA Methods in Molecular Biology, vol 1517 Humana Press, New York, NY. 2017.

10. Becker C, Hammerle-Fickinger A, Riedmaier I, et al. mRNA and microRNA quality control for RT-qPCR analysis. Methods. 2010; 50: 237-43.

11. Maleki Dana P, Mansournia MA, Mirhashemi SM. PIWI-interacting RNAs: new biomarkers for diagnosis and treatment of breast cancer. Cell Biosci. 2020; 10: 44.

12. Bonetti A, Carninci P. From bench to bedside: The long journey of long non-coding RNAs. Current Opinion in Systems Biology. 2017; 3: 119-24.

13. Finotti A, Fabbri E, Lampronti I, et al. MicroRNAs and Long Non-coding RNAs in Genetic Diseases. Mol Diagn Ther. 2019; 23: 155-71.

14. Griffiths-Jones S, Grocock RJ, van Dongen S, et al. miRBase: microRNA sequences, targets and gene nomenclature. Nucleic Acids Res. 2006; 34: D140-4.

15. Wang X. miRDB: a microRNA target prediction and functional annotation database with a wiki interface. RNA. 2008; 14: 1012-7.

16. Mitchell PS, Parkin RK, Kroh EM, et al. Circulating microRNAs as stable blood-based markers for cancer detection. Proc Natl Acad Sci U S A. 2008; 105: 10513-8.

17. Poulet G, Massias J, Taly V. Liquid Biopsy: General Concepts. Acta Cytol. 2019; 63: 449-55.

18. Mader S, Pantel K. Liquid Biopsy: Current Status and Future Perspectives. Oncol Res Treat. 2017; 40: 404-8.

19. Molina-Vila MA, Mayo-de-Las-Casas C, Gimenez-Capitan A, et al. Liquid Biopsy in Non-Small Cell Lung Cancer. Front Med (Lausanne). 2016; 3: 69.

20. Cheng L, Sharples RA, Scicluna BJ, et al. Exosomes provide a protective and enriched source of miRNA for biomarker profiling compared to intracellular and cell-free blood. J Extracell Vesicles. 2014; 3.

21. Karimi N, Cvjetkovic A, Jang SC, et al. Detailed analysis of the plasma extracellular vesicle proteome after separation from lipoproteins. Cell Mol Life Sci. 2018; 75: 2873-86.

22. Buschmann D, Kirchner B, Hermann S, et al. Evaluation of serum extracellular vesicle isolation methods for profiling miRNAs by next-generation sequencing. J Extracell Vesicles. 2018; 7: 1481321.

23. Van Deun J, Mestdagh P, Sormunen R, et al. The impact of disparate isolation methods for extracellular vesicles on downstream RNA profiling. J Extracell Vesicles. 2014; 3.

24. Kustanovich A, Schwartz R, Peretz T, et al. Life and death of circulating cell-free DNA. Cancer Biol Ther. 2019; 20: 1057-67.

25. Yanez-Mo M, Siljander PR, Andreu Z, et al. Biological properties of extracellular vesicles and their physiological functions. J Extracell Vesicles. 2015; 4: 27066.

26. Zhang W, Xia W, Lv Z, et al. Liquid Biopsy for Cancer: Circulating Tumor Cells, Circulating Free DNA or Exosomes? Cell Physiol Biochem. 2017; 41: 755-68.

27. Bronkhorst AJ, Ungerer V, Holdenrieder S. The emerging role of cell-free DNA as a molecular marker for cancer management. Biomol Detect Quantif. 2019; 17: 100087.

28. Consortium E-T, Van Deun J, Mestdagh P, et al. EV-TRACK: transparent reporting and centralizing knowledge in extracellular vesicle research. Nat Methods. 2017; 14: 228-32.

29. Valadi H, Ekstrom K, Bossios A, et al. Exosome-mediated transfer of mRNAs and microRNAs is a novel mechanism of genetic exchange between cells. Nat Cell Biol. 2007; 9: 654-9.

30. Keller S, Ridinger J, Rupp AK, et al. Body fluid derived exosomes as a novel template for clinical diagnostics. J Transl Med. 2011; 9: 86.

31. Jeyaram A, Jay SM. Preservation and Storage Stability of Extracellular Vesicles for Therapeutic Applications. AAPS J. 2017; 20: 1.

32. Enderle D, Spiel A, Coticchia CM, et al. Characterization of RNA from Exosomes and Other Extracellular Vesicles Isolated by a Novel Spin Column-Based Method. PLoS One. 2015; 10: e0136133.

33. Ge Q, Zhou Y, Lu J, et al. miRNA in plasma exosome is stable under different storage conditions. Molecules. 2014; 19: 1568-75.

34. Baek R, Sondergaard EK, Varming K, et al. The impact of various preanalytical treatments on the phenotype of small extracellular vesicles in blood analyzed by protein microarray. J Immunol Methods. 2016; 438: 11-20.

35. Jin Y, Chen K, Wang Z, et al. DNA in serum extracellular vesicles is stable under different storage conditions. BMC Cancer. 2016; 16: 753.

36. Nik Mohamed Kamal N, Shahidan WNS. Non-Exosomal and Exosomal Circulatory MicroRNAs: Which Are More Valid as Biomarkers? Front Pharmacol. 2019; 10: 1500.

37. Bjornetro T, Redalen KR, Meltzer S, et al. An experimental strategy unveiling exosomal microRNAs 486-5p, 181a-5p and 30d-5p from hypoxic tumour cells as circulating indicators of high-risk rectal cancer. J Extracell Vesicles. 2019; 8: 1567219.

38. Pfeffer SR, Yang CH, Pfeffer LM. The Role of miR-21 in Cancer. Drug Dev Res. 2015; 76: 270-7.

39. Masoudi MS, Mehrabian E, Mirzaei H. MiR-21: A key player in glioblastoma pathogenesis. J Cell Biochem. 2018; 119: 1285-90.

40. Bica-Pop C, Cojocneanu-Petric R, Magdo L, et al. Overview upon miR-21 in lung cancer: focus on NSCLC. Cell Mol Life Sci. 2018; 75: 3539-51.

41. Cao LQ, Yang XW, Chen YB, et al. Exosomal miR-21 regulates the TETs/PTENp1/PTEN pathway to promote hepatocellular carcinoma growth. Mol Cancer. 2019; 18: 148.

42. Willms E, Cabanas C, Mager I, et al. Extracellular Vesicle Heterogeneity: Subpopulations, Isolation Techniques, and Diverse Functions in Cancer Progression. Front Immunol. 2018; 9: 738.

43. van der Maaten L, Hinton G. Visualizing Data using t-SNE. Journal of Machine Learning Research. 2008; 9: 2579-605.

44. Love MI, Huber W, Anders S. Moderated estimation of fold change and dispersion for RNA-seq data with DESeq2. Genome Biol. 2014; 15: 550.

45. Chun H, Keles S. Sparse partial least squares regression for simultaneous dimension reduction and variable selection. J R Statist Soc B. 2010; 72: 3–25.

46. Pathan M, Fonseka P, Chitti SV, et al. Vesiclepedia 2019: a compendium of RNA, proteins, lipids and metabolites in extracellular vesicles. Nucleic Acids Res. 2019; 47: D516-D9.

47. Liu T, Zhang Q, Zhang J, et al. EVmiRNA: a database of miRNA profiling in extracellular vesicles. Nucleic Acids Res. 2019; 47: D89-D93.

48. Agarwal V, Bell GW, Nam JW, et al. Predicting effective microRNA target sites in mammalian mRNAs. Elife. 2015; 4.

49. Chou CH, Shrestha S, Yang CD, et al. miRTarBase update 2018: a resource for experimentally validated microRNA-target interactions. Nucleic Acids Res. 2018; 46: D296-D302.

50. Leinonen R, Akhtar R, Birney E, et al. The European Nucleotide Archive. Nucleic Acids Res. 2011; 39: D28-31.

51. Leinonen R, Sugawara H, Shumway M, et al. The sequence read archive. Nucleic Acids Res. 2011; 39: D19-21.

52. Clayton A, Buschmann D, Byrd JB, et al. Summary of the ISEV workshop on extracellular vesicles as disease biomarkers, held in Birmingham, UK, during December 2017. J Extracell Vesicles. 2018; 7: 1473707.

53. Lai RC, Tan SS, Yeo RW, et al. MSC secretes at least 3 EV types each with a unique permutation of membrane lipid, protein and RNA. J Extracell Vesicles. 2016; 5: 29828.

54. Mateescu B, Kowal EJ, van Balkom BW, et al. Obstacles and opportunities in the functional analysis of extracellular vesicle RNA - an ISEV position paper. J Extracell Vesicles. 2017; 6: 1286095.

55. Witwer KW. Circulating microRNA biomarker studies: pitfalls and potential solutions. Clin Chem. 2015; 61: 56-63.

56. Thery C, Witwer KW, Aikawa E, et al. Minimal information for studies of extracellular vesicles 2018 (MISEV2018): a position statement of the International Society for Extracellular Vesicles and update of the MISEV2014 guidelines. J Extracell Vesicles. 2018; 7: 1535750.

57. Git A, Dvinge H, Salmon-Divon M, et al. Systematic comparison of microarray profiling, real-time PCR, and next-generation sequencing technologies for measuring differential microRNA expression. RNA. 2010; 16: 991-1006.

58. Hermann S, Buschmann D, Kirchner B, et al. Transcriptomic profiling of cell-free and vesicular microRNAs from matched arterial and venous sera. J Extracell Vesicles. 2019; 8: 1670935.

59. Moloney BM, Gilligan KE, Joyce DP, et al. Investigating the Potential and Pitfalls of EV-Encapsulated MicroRNAs as Circulating Biomarkers of Breast Cancer. Cells. 2020; 9.

60. Ameling S, Kacprowski T, Chilukoti RK, et al. Associations of circulating plasma microRNAs with age, body mass index and sex in a population-based study. BMC Med Genomics. 2015; 8: 61.

61. Baek R, Varming K, Jorgensen MM. Does smoking, age or gender affect the protein phenotype of extracellular vesicles in plasma? Transfus Apher Sci. 2016; 55: 44-52.

62. Jayachandran M, Lugo G, Heiling H, et al. Extracellular vesicles in urine of women with but not without kidney stones manifest patterns similar to men: a case control study. Biol Sex Differ. 2015; 6: 2.

Correspondence
Stefanie Hermann
stefanie.hermann@tum.de

Christian Grätz

Benedikt Kirchner

Michael W. Pfaffl

Animal Physiology & Immunology,
Technical University of Munich,
School of Life Sciences,
85354 Freising-Weihenstephan, Germany

Appendix II

Contribution by Stefanie Hermann:

- Writing – review and editing
- Investigation – laboratory experiments
- Formal analysis and data curation

Stefanie Hermann

Prof. Dr. Michael W. Pfaffl

Taylor & Francis
Taylor & Francis Group

RESEARCH ARTICLE

OPEN ACCESS ⓡ Check for updates

Evaluation of serum extracellular vesicle isolation methods for profiling miRNAs by next-generation sequencing

Dominik Buschmann ⓘ[a,b], Benedikt Kirchner ⓘ[b,c], Stefanie Hermann ⓘ[b], Melanie Märte ⓘ[d], Christine Wurmser ⓘ[e], Florian Brandes ⓘ[d], Stefan Kotschote[f], Michael Bonin[f], Ortrud K. Steinlein ⓘ[a], Michael W. Pfaffl ⓘ[b], Gustav Schelling ⓘ[d] and Marlene Reithmair ⓘ[a]

aInstitute of Human Genetics, University Hospital, LMU Munich, Munich, Germany; bDivision of Animal Physiology and Immunology, TUM School of Life Sciences Weihenstephan, Technical University of Munich, Freising, Germany; cDr. von Hauner Children's Hospital, LMU Munich, Munich, Germany; dDepartment of Anesthesiology, University Hospital, LMU Munich, Munich, Germany; eChair of Animal Breeding, TUM School of Life Sciences Weihenstephan, Technical University of Munich, Freising, Germany; fIMGM Laboratories GmbH, Planegg, Germany

ABSTRACT

Extracellular vesicles (EVs) are intercellular communicators with key functions in physiological and pathological processes and have recently garnered interest because of their diagnostic and therapeutic potential. The past decade has brought about the development and commercialization of a wide array of methods to isolate EVs from serum. Which subpopulations of EVs are captured strongly depends on the isolation method, which in turn determines how suitable resulting samples are for various downstream applications. To help clinicians and scientists choose the most appropriate approach for their experiments, isolation methods need to be comparatively characterized. Few attempts have been made to comprehensively analyse vesicular microRNAs (miRNAs) in patient biofluids for biomarker studies. To address this discrepancy, we set out to benchmark the performance of several isolation principles for serum EVs in healthy individuals and critically ill patients. Here, we compared five different methods of EV isolation in combination with two RNA extraction methods regarding their suitability for biomarker discovery-focused miRNA sequencing as well as biological characteristics of captured vesicles. Our findings reveal striking method-specific differences in both the properties of isolated vesicles and the ability of associated miRNAs to serve in biomarker research. While isolation by precipitation and membrane affinity was highly suitable for miRNA-based biomarker discovery, methods based on size-exclusion chromatography failed to separate patients from healthy volunteers. Isolated vesicles differed in size, quantity, purity and composition, indicating that each method captured distinctive populations of EVs as well as additional contaminants. Even though the focus of this work was on transcriptomic profiling of EV-miRNAs, our insights also apply to additional areas of research. We provide guidance for navigating the multitude of EV isolation methods available today and help researchers and clinicians make an informed choice about which strategy to use for experiments involving critically ill patients.

Introduction

A multitude of isolation methods for extracellular vesicles (EVs) has been developed and commercialized in the last decade. Many methods claim rapid, reliable and highly efficient isolation from serum, yet there is no consensus on each method's suitability for scientific and clinical applications. Comparative data on methods for isolating EVs from patient biofluids are scarce, despite clear interest in utilizing EVs and their miRNA cargo for biomarker studies. Further, few attempts have been made to comprehensively analyse vesicular miRNAs in biofluid samples from critically ill patients, a population highly relevant to many clinical situations.

This work compares five different methods of EV isolation and their suitability for miRNA-based biomarker discovery. We isolated serum EVs from sepsis patients and healthy volunteers, sequenced their small RNA cargo and performed differential miRNA expression analysis. Additional experiments assessed method-specific differences in vesicle composition and morphology. Our data reveal that precipitation and membrane affinity are highly suitable for both small RNA-Seq and patient classification based on cell-free miRNAs. Comparative evaluation demonstrates that miRNA yield correlates with robust separation of sepsis patients and healthy individuals, while vesicle purity seems less

relevant for RNA-based biomarker applications. Differences in size, quantity and composition of isolated vesicles indicate that each method captures distinctive, but partially overlapping EV populations accompanied by varying degrees of contamination with non-EV material.

EVs are intercellular communicators with key functions in physiological and pathological processes and have recently garnered significant interest as potential diagnostic and therapeutic agents. Rapidly increasing research in this field is accompanied by the demand for reproducible, time-efficient and economic isolation methods. A recent survey conducted by Gardiner et al. revealed that although ultracentrifugation (UC) remains the most commonly used isolation method, other approaches have gained preference when starting volume is limited [1]. Capturing EVs from blood-based biofluids such as serum and plasma is of particular interest for clinical applications. As a consequence, manufacturers offer a wide array of commercial isolation kits. These rely on principles ranging from filtration, precipitation and sedimentation to size-exclusion chromatography (SEC) and immunocapture.

One of the most important aspects of EV research is analysing their nucleic acid cargo, particularly small RNAs. These are commonly quantified by RT-qPCR or, increasingly, comprehensive transcriptomic profiling by next-generation sequencing (NGS, small RNA-Seq). Applications of EV transcriptomics range from basic research to biomarker discovery and drug development, making use of EVs as an easily accessible, enriched sampling fraction [2,3]. Inferring credible information from the transcriptome relies on precise quantification of target RNA, which in turn requires samples of high quality and integrity [4]. Additionally, methods for RNA extraction itself influence downstream analyses by yielding non-identical, kit-specific isolates [5]. This holds true particularly for extracellular RNA, which bears additional challenges such as low concentrations, diminished RNA integrity and high variability between individuals. Indeed, recent publications have highlighted the impact of cell-free RNA extraction strategies on small RNA-Seq, reporting quantitative and qualitative differences in resulting sequencing libraries [6,7].

Similarly, the impact of EV isolation strategies on RNA quantification assays has been demonstrated for cell culture supernatant [8], urine [9,10], milk [11] and serum [12]. Depending on the respective isolation principle, different populations of EVs with varying degrees of contamination seem to be isolated, resulting in only partially overlapping RNA profiles. Being able to detect specific RNA patterns in bulk populations of blood-derived EVs is challenging due to the vesicular secretome's complexity. Although most EVs in blood are secreted by erythrocytes, platelets and endothelial cells, various other tissues also secrete vesicles into the circulation, further complicating analysis [13,14]. Multiple classes of EVs are secreted from even one specific cell type, each carrying its individual RNA signature [15]. Beyond RNA profiles, kit-specific isolates also differ in EV composition, size, concentration, purity and functionality [16–20]. Selecting appropriate isolation methods is therefore a critical step in all areas of EV research.

There are excellent publications comparing different strategies of isolating EVs from human serum for RNA analyses. Rekker et al., Andreu et al. and Crossland et al. relied on RT-qPCR to profile vesicular miRNAs, comparing isolation based on UC, precipitation and filtration [12,21,22]. Helwa et al. isolated EVs from different starting volumes by precipitation and UC and quantified associated miRNAs by droplet digital PCR [23]. Analysing EV miRNAs using PCR-based assays is an important and well-established approach supported by excellent protocols and methods [24–26].

However, as NGS has become an increasingly popular downstream application to study miRNAs in EVs, it is crucial to define the EV isolation method most suitable for this particular technique. Several previous publications reported the feasibility and utility of sequencing small RNA in EVs isolated from serum, plasma, urine, and cell culture supernatant [2,27–30]. Small RNA-Seq experiments often focus on valuable applications such as liquid biopsy-based diagnostics and, consequently, clinical samples. Screening potential isolation methods should therefore include samples from healthy individuals as well as diseased patients, who often display severe anomalies in blood parameters. These matrix effects could conceivably interfere with EV isolation and hamper the transfer of methodologies from healthy to diseased subjects. Prime examples of critically ill patients are individuals suffering from sepsis and septic shock. This complex, life-threatening disease comes along with various clinical complications such as multiple organ failure, dysregulated coagulation and altered blood lipid profiles [31,32]. Findings derived from comparing EV isolation strategies for healthy donors, however, might not be readily transferred to such challenging samples. We therefore believe it is important to verify each method's applicability in samples relevant for the respective clinical situation.

The objective of the current study was to compare several methods of isolating EVs from healthy and septic sera and to identify the one most suitable for biomarker-focused small RNA-Seq in this population

of critically ill patients. Routine biomarker applications call for time-efficient, simple and streamlined procedures, ideally provided to clinical laboratories as one-box solutions. We did therefore not screen all potential combinations of EV isolation and RNA extraction methods but focused on either recommended RNA kits by the same manufacturer or combinations commonly used in the EV field. Additionally, isolates from each method were comparatively characterized in order to assess method-specific differences in captured EV populations and potential contaminating material.

Material and methods

Ethics approval and consent to participate

The study was approved by the Ethics Committee of the Medical Faculty of the University of Munich (protocol #551-14). Written informed consent and approval of a patient's legal representative was obtained when the patient lacked capacity to give informed consent for participation in the study. The study was carried out in accordance with approved guidelines, and all study samples were anonymized during analysis. Written informed consent for publication of blinded individual person's data was obtained from each participant or the patient's legal representative.

Patient recruitment

Four patients with sepsis and five patients in septic shock were included in the study and sex-matched to 10 healthy volunteers (Supplemental Table 1). Patients included in the study were >18 years of age and within 24 h of admission to the intensive care unit (ICU). Exclusion criteria were pregnancy, immunosuppression, leukopenia, haematological malignancies or the initiation of palliative care. Healthy volunteers were recruited from hospital personnel and by advertisement. Only volunteers with a Charlson Comorbidity Index [33] of ≤1 were included.

Sample collection

Blood was drawn from 20G catheters within the radial artery of sepsis patients on the day of admission to the ICU (day 0) and 24 h later (day 1). Healthy volunteers were sampled by venipuncture using 20G needles. In order to prevent haemolysis, aspiration was performed slowly and evenly for both procedures. Blood was collected in 9 ml serum tubes (S-Monovette, Sarstedt AG&Co) and centrifuged at 3400 g for 10 min at room temperature (RT) within 10 min of sampling. Resulting serum was aliquoted and stored at −80 °C.

Isolation of extracellular vesicles

EVs were isolated from serum using four commercially available isolation kits as well as differential UC (Table 1). One millilitre serum from each patient and volunteer was used as starting material for all isolation methods. EV isolation was performed as detailed below, following manufacturer's recommendations for pre-clearing of serum and subsequent steps. For all commercial isolation methods, we sequenced vesicular RNA from both patients and volunteers. Small RNA-Seq was performed for all samples except in the case of UC-derived EVs where it was only performed for healthy volunteers, but not for sepsis patients, as serum availability was limited. Serum EVs from day 0 were used for RNA extraction and small RNA-Seq.

Five septic shock patients and five matched volunteers from our small RNA-Seq cohort were selected for additional biological characterization of EVs. In these supplemental experiments, we isolated EVs from 1 ml serum sampled on day 1 of intensive care therapy in patients with sepsis. These day 1 EVs were isolated as described below, concentrated to 50 μl using Amicon Ultra-4 30 kDa NMWL spin filters (Merck Millipore) and split into separate aliquots for protein analysis and particle characterization, respectively. A schematic diagram that summarizes all steps of the EV isolation and characterization workflow is provided in Figure 1.

Precipitation

EVs were precipitated from 1 ml serum using the miRCURY Exosome Isolation Kit (Exiqon) according to the manufacturer's instructions. For RNA extraction, EV pellets were lysed with the provided miRCURY biofluid

Table 1. EV isolation methods and RNA extraction kits utilized in this study.

| Principle of EV isolation	Method	RNA extraction kit
Precipitation	miRCURY Exosome Isolation Kit (Exiqon)	miRCURY RNA Isolation Kit – Biofluids (Exiqon)
Size-exclusion chromatography	Exo-spin Midi Columns (Cell Guidance Systems)	miRCURY RNA Isolation Kit – Biofluids (Exiqon)
Size-exclusion chromatography	qEV Columns (Izon Science)	miRCURY RNA Isolation Kit – Biofluids (Exiqon)
Membrane affinity	exoRNeasy Serum-Plasma Midi Kit (Qiagen)	exoRNeasy Serum/Plasma Midi Kit (Qiagen)
Sedimentation	Differential ultracentrifugation (Beckman Coulter Optima LE-80K)	exoRNeasy Serum/Plasma Midi Kit (Qiagen)
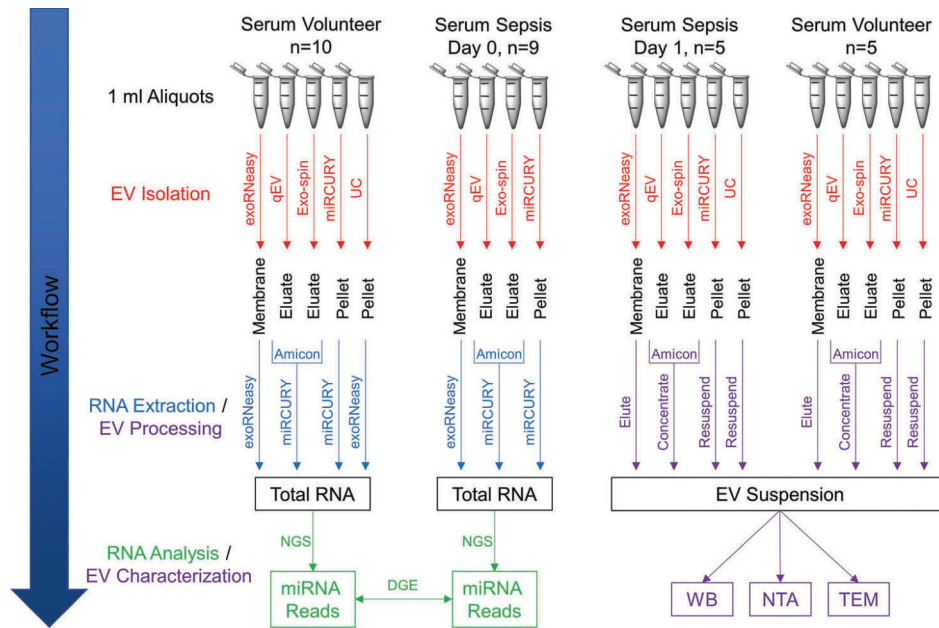
Figure 1. Schematic summary of EV isolation, RNA extraction and downstream analyses. EVs were isolated from human serum using five (healthy donors) or four (sepsis patients) different methods. After extracting total RNA from EV isolates, small RNA species were profiled by NGS. Differential expression of miRNAs between volunteers and patients was assessed to identify potential biomarker candidates. Sera from a subset of volunteers and patients were used to additionally characterize isolates from each method by Western blot (WB), nanoparticle tracking analysis (NTA) and transmission electron microscopy (TEM).

lysis solution. Pellets for biological characterization were resuspended in phosphate-buffered saline (PBS).

Size-exclusion chromatography

For Exo-spin (Cell Guidance Systems), EVs from 1 ml serum were purified on the provided columns and eluted in 3 ml particle-free PBS according to the manufacturer's quick start protocol. For qEV (Izon Science), columns were equilibrated, overlaid with 1 ml serum and flushed with particle-free PBS, collecting sequential fractions of 0.5 ml. Fractions 7–9 were pooled to maximize EV yield.

Membrane affinity

Pre-cleared serum was applied to exoEasy columns (Qiagen) as per the manufacturer's protocol. EVs were captured and washed using reagents provided in the kit. For RNA extraction, EVs bound to the membrane were lysed by adding QIAzol (Qiagen). Intact EVs for biological characterization were eluted from the column by addition of the provided buffer XE (analogous to the procedures in Qiagen's exoEasy kit).

Sedimentation

Serum was diluted 1:4 in PBS and subjected to low-speed centrifugation (12,000 g, 1 h, k-factor: 1401.3). EVs from the pre-cleared supernatant were then pelleted at 120,000 g for 14 h (k-factor: 139.7). All centrifugation steps were carried out at 4°C using an Optima LE-80K ultracentrifuge (Beckman Coulter) and a SW60 rotor. Pellets were lysed in QIAzol for RNA extraction or resuspended in PBS for EV characterization.

RNA extraction and characterization

Total RNA was extracted from day 0 serum EVs using commercial column-based kits listed in Table 1. For all extraction methods, RNA eluates were reapplied to the membrane for a second elution.

Precipitation

RNA was extracted from EV lysates using the corresponding miRCURY RNA Isolation Kit for biofluids. Procedures were carried out according to the manufacturer's protocol, and RNA was eluted in 30 µl nuclease-free water.

Size-exclusion chromatography

Eluted EVs (Exo-spin: 3 ml; qEV: 1.5 ml) were concentrated to 200 µl on Amicon Ultra-4 30 kDa NMWL spin filters. RNA was subsequently extracted from the concentrate using the miRCURY biofluids kit as described above.

Membrane affinity

RNA was extracted from EVs lysed in QIAzol using reagents provided in the exoRNeasy kit. Procedures were carried out according to the manufacturer's protocol, and RNA was eluted in 14 µl nuclease-free water.

Differential UC

Following lysis of pellets in QIAzol, RNA was extracted using the exoRNeasy kit as described above.

In order to compensate for the varying elution volumes, all RNAs were gently dried in a centrifugal evaporator and resuspended in 10 µl nuclease-free water. Yield and size distribution of EV-RNA were assessed by capillary electrophoresis on the 2100 Bioanalyzer (Agilent Technologies). We used the RNA 6000 Pico Assay (Agilent Technologies) to assess the total RNA profile including potential contaminations with cellular RNA.

Next-Generation Sequencing

EV-RNA from sepsis patients and healthy volunteers was profiled by small RNA-Seq. For all isolation methods, we used 60% (6 µl) of eluted total RNA as starting material. Library preparation was performed as described in Reithmair et al. [34], using the NEBNext Multiplex Small RNA Library Prep Set for Illumina (New England BioLabs Inc.). To compensate for the low RNA input, all adaptors and primers were diluted 1:2 in nuclease-free water. Size selection of PCR products was performed by high-resolution 4% agarose gel electrophoresis, selecting bands of 130–150 base pairs. Fragment sizes of purified libraries were assessed using capillary electrophoresis prior to 50 cycles of single-end sequencing on the HiSeq2500 (Illumina Inc.).

Data analysis

Sequencing data were processed as described elsewhere [35]. Briefly, FastQC (version 0.10.1) [36] was used to assess sequence length distribution and quality. Adaptor sequences were trimmed using Btrim [37], and all reads without adaptors were discarded. Additionally, reads shorter than 16 nt, probably degradation products from longer coding and non-coding RNA species, were excluded from the data set before proceeding to alignment [4]. To avoid false-positive hits during miRNA analysis, reads that mapped to sequences from human rRNA, tRNA, snRNA and snoRNA (obtained from RNAcentral) were initially removed from the data set [38]. Remaining reads were then aligned to human

miRNA sequences in the most recent version (21) of miRBase [39]. Mapping was performed using Bowtie [40] and the "best" alignment algorithm, allowing one mismatch for alignment to both RNAcentral and miRBase. For all RNA classes, final read count tables were generated directly from Bowtie output by summing up all hits per sequence. Differential gene expression (DGE) analysis was subsequently performed via the Bioconductor Package DESeq2 (version 1.8.1) [41] using the included normalization strategy based on median ratios of mean miRNA expression and the Benjamini–Hochberg method to correct for false discovery. A $\log_2$ fold change $\geq|1|$ and an adjusted p-value of ≤ 0.05 were set as thresholds to identify significantly regulated miRNAs. Only transcripts with a baseMean ≥ 50 were included in the analysis. Hierarchical clustering (Euclidean distances, Ward's method), principal component analysis (regularized log-transformed, sizefactor-corrected counts obtained from DESeq2) and visualization of significantly regulated miRNAs in Venn diagrams were carried out in R (version 3.4.0) using the packages gplots, ggplots2, RColorBrewer, dendextend, ggfortify and VennDiagram [42–48]. Trimmed sequence reads were deposited in the European Nucleotide Archive under accession number PRJEB24913 (http://www.ebi.ac.uk/ena/data/view/PRJEB24913).

Nanoparticle tracking analysis

EV suspensions were diluted in particle-free PBS (prepared by a 120,000 g spin at 4°C for 14 h, k-factor: 231.6) and analysed using a NanoSight LM10 (Malvern Instruments GmbH) equipped with a 405-nm laser and a high-sensitivity sCMOS camera. Samples were introduced manually, and six videos of 45 s each were captured at a frame rate of 25 frames/second. With sample temperatures monitored manually, individual particles were tracked using NTA 3.0 software (Malvern Instruments GmbH) at camera level 10 and the Finite Track Length Adjustment (FTLA) algorithm. For analysis, we used a conservative detection threshold with blur and minimum track length set to auto and only considered captures with at least 2000 completed tracks. Starting from concentrations measured by NTA, initial particle concentrations in serum were calculated using the respective dilution factors for each sample as described elsewhere [49].

Transmission electron microscopy

EVs were fixed in 2% paraformaldehyde and adsorbed onto formvar/carbon-coated 200-mesh nickel grids (Electron Microscopy Sciences) for 15 min. Grids

were then washed with PBS, fixed in 2.5% glutaraldehyde for 5 min and washed with milliQ water. After performing negative staining with 2% uranyl acetate for 1 min, grids were washed again and air-dried overnight. Images were acquired on a Zeiss EM900 (Carl Zeiss Microscopy GmbH) with a wide-angle dual-speed 2K-CCD camera at 80 kV.

Western blot

EV samples were lysed in ice-cold Radioimmunoprecipitation Assay (RIPA) buffer on ice for 15 min intermitted by three bouts of sonication in a water bath. After centrifugation at 13,000 g for 10 min, protein concentration in the supernatant was analysed using Bicinchoninic Acid (BCA) assay (Sigma Aldrich). Input for exoRNeasy, Exo-spin, miRCURY and UC was normalized to 25 µg total protein. Due to very low protein concentrations, maximum volumes were loaded on the gel for qEV. For electrophoresis, samples were reduced in Laemmli buffer and heated at 70 °C for 10 min. Protein lysates for analysis of CD63 were incubated with non-reducing sample buffer at RT for 20 min. Proteins were separated using NuPAGE 4–12% Bis-Tris Gels (Invitrogen) prior to transfer to a 0.45 µm nitrocellulose membrane (GE Healthcare Life Sciences). Membranes were blocked with 1% non-fat milk powder in Phosphate Buffered Saline with Tween (PBST) for 1 h at RT and incubated with primary antibodies at 4°C overnight. Secondary antibodies were added for 1 h at RT. After washing with blocking buffer, blots were developed using the Clarity Western ECL Blotting Substrate Kit (Bio-Rad). Primary antibodies were from Abcam (mouse anti-TSG101 clone 4A10, ab83, 1:800, rabbit anti-Syntenin clone EPR8102, 1:5000, ab57113, 1:250,

mouse anti-CD63, clone TS63, ab59479, 1:500, mouse anti-Human Serum Albumin clone 1A9, ab37989, 1:250), OriGene (rabbit anti-CD81, TA343598, 1:500) and Biomol (goat anti-Calnexin, WA-AF1179a, 1:2500). All marker proteins except CD63 were analysed using reducing conditions. HRP-conjugated secondary antibodies were purchased from Abcam (goat anti-Mouse, ab97040, 1:10,000, goat anti-Rabbit, ab97080, 1:10,000, rabbit anti-Goat, ab97105, 1:10,000).

Results

Analysis of isolation-specific EV-RNA composition by small RNA-Seq

Total EV-RNA was characterized by capillary electrophoresis, revealing major differences in quantity and size distribution across EV isolation strategies (Supplemental Figure 1). Similarly, sequencing of small RNA resulted in vastly differing total library sizes, ranging from 3.68E6 ± 1.72E6 reads (qEV sepsis) to 1.17E7 ± 3.76E6 reads (UC volunteer). Two EV samples precipitated from sepsis patients did not properly amplify during sequencing and were excluded from subsequent analyses. Method-dependent capture of miRNAs was assessed by aligning reads to miRBase and expressing mapped miRNAs as percentages of library size (Figure 2). miRNA enrichment was highest for precipitation-based EV isolation, followed by UC, membrane affinity and SEC. Even though library sizes were similar for UC, exoRNeasy and miRCURY, the latter displayed a 3.5–5-fold higher percentage of mapped miRNAs, respectively. For all isolation methods, relative frequencies of mapped miRNAs for sepsis patients were slightly lower than for volunteers (Figure 2). The top 10 most highly expressed miRNAs for each method are provided in Supplemental Table 2.
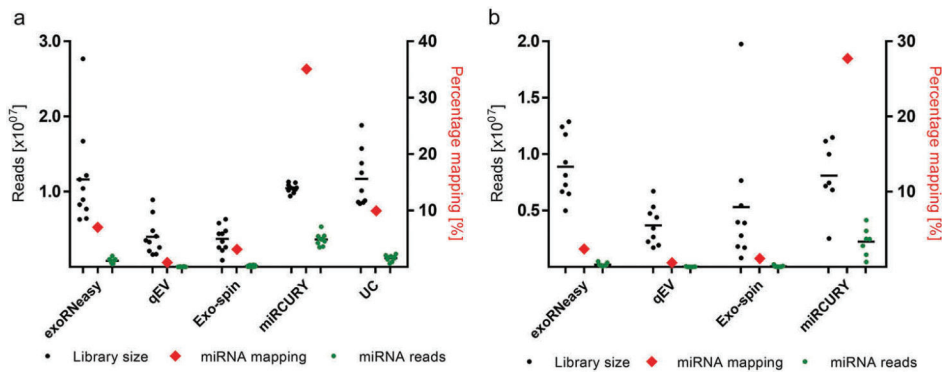

Figure 2. Mean library size and mapped miRNAs for EVs isolated from healthy volunteers (a) and sepsis patients (b). miRNA mapping frequencies (red diamonds) are expressed as percentages of total library size and plotted against the right x-axes. Enrichment of miRNA reads was highest for miRCURY (35.08% and 27.56% for volunteers and patients, respectively) and lowest for qEV (0.79% for volunteers and 0.57% for patients). All data are mean ± SD for 10 volunteers and 9 sepsis patients.

Similar differences were found when mapping reads to further classes of small non-coding RNA (Figure 3). Expressed as the ratio of non-target reads to miRNA reads, both SEC-based methods tended to isolate more rRNA fragments than other methods (Supplemental Figure 2). Increased frequencies of rRNA reads were also observed in sepsis EVs isolated by membrane affinity. Additionally, membrane affinity captured significantly more tRNA fragments than other methods from both septic and healthy EVs. SEC-based methods, particularly qEV, also isolated large numbers of fragments shorter than 15 nt. Mean library sizes, mapped miRNAs and results from DGE are provided in Supplemental Table 3.

EV-miRNAs from precipitation and membrane affinity separate volunteers and patients

DESeq2 was used to assess differential regulation of miRNA levels between sepsis patients and volunteers for commercial isolation kits. After applying stringent filtering criteria (baseMean ≥50, $\log_2$ fold change $\geq|1|$, adjusted p-value ≤0.05), we found 6 (qEV), 14 (Exospin), 60 (exoRNeasy) and 90 (miRCURY) miRNAs to be significantly regulated. While there was minimal overlap between all EV isolation strategies, most regulated miRNAs were unique for a specific isolation method (Figure 4). A common set of two significantly regulated miRNAs was detected for all EV isolation methods. Data for unfiltered differential expression analysis are provided in Supplemental Figure 3.

Similarities between miRNA patterns from each patient and isolation method were assessed by hierarchical clustering analysis (HCA) (Figure 5). Based on all miRNA reads, HCA separated isolation by precipitation, UC and membrane affinity from both SEC-based methods. Within these principal clusters, precipitation and membrane affinity flawlessly separated sepsis patients from healthy volunteers. Even though samples from precipitation and UC showed a high degree of similarity, UC volunteers were more closely related to miRCURY sepsis patients. Clustering of miRNAs from SEC isolation revealed substantial heterogeneity within and overlap between qEV and Exospin. Subsequently, these methods did not accurately distinguish volunteers from patients. This was also demonstrated by principal component analysis (Supplemental Figure 4), where separation of patient groups was achieved exclusively by miRCURY and exoRNeasy.

The number of differentially regulated miRNAs detected in DESeq2 analysis varied significantly
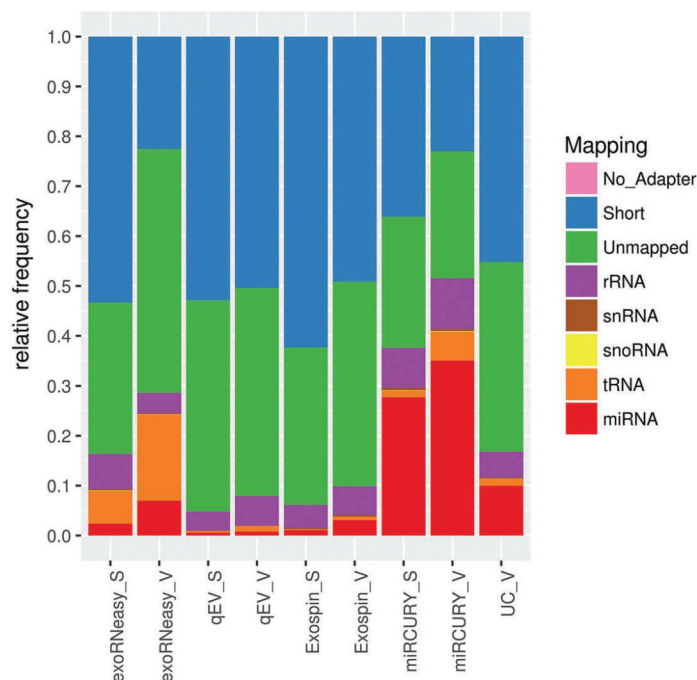

Figure 3. Mapping statistics for various classes of small non-coding RNA. Highest frequencies of miRNA mapping were observed in isolates from precipitation, sedimentation and membrane affinity. Both SEC-based methods were prone to capture short sequences, while libraries from membrane affinity-derived samples contained an increased share of tRNA fragments. Short: sequence is shorter than 15 nt; unmapped: sequence did not align to human rRNA, snRNA, snoRNA, tRNA or miRNA. Data are expressed as mean mapping percentages for 10 volunteers (V) and 9 sepsis patients (S).
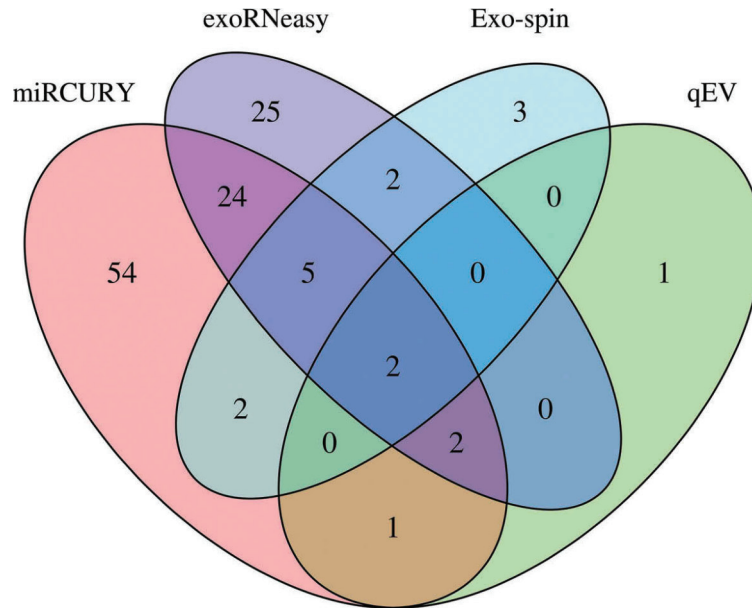
Figure 4. Differential expression of miRNAs in EVs isolated by commercial methods. Precipitation and membrane affinity yielded high numbers of differentially regulated miRNAs (miRCURY: 90; exoRNeasy: 60). Far fewer regulated miRNAs were detected in SEC-derived samples (Exo-spin: 14; qEV: 6). Two differentially regulated miRNAs were detected in EVs isolated by all methods. Data are filtered for baseMean ≥50, $\log_2$ fold change ≥|1| and adjusted p-value ≤0.05.
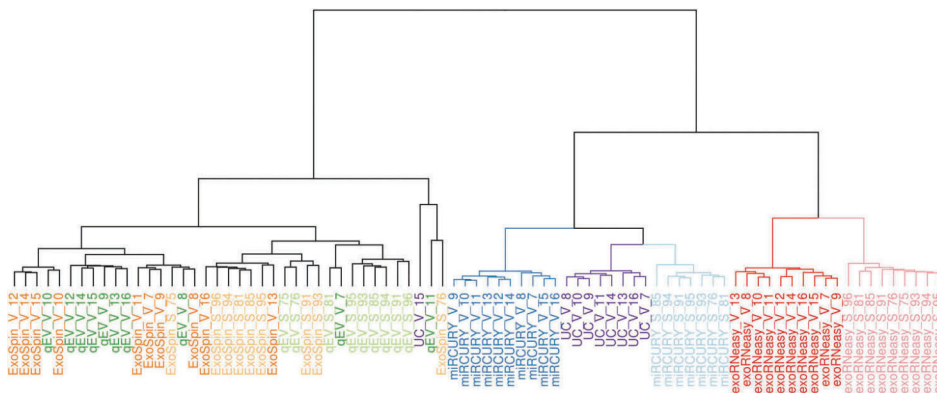

Figure 5. Hierarchical clustering analysis of miRNAs in EVs isolated by commercial methods. Samples split up into two clusters, separating precipitation and membrane affinity from both SEC-based methods. miRCURY (blue) and exoRNeasy (red) accurately distinguished between healthy volunteers (darker shades, V) and sepsis patients (lighter shades, S). miRNAs isolated from SEC-EVs (Exo-spin, qEV) showed noticeable heterogeneity and were less capable of separating volunteers and patients.

between isolation methods (Figure 4). Differentially expressed miRNAs as well as corresponding $\log_2$ fold changes and adjusted p-values for each method are provided in Supplemental Table 4. As predicted by sequencing output, methods yielding larger libraries also tended to result in more dysregulated miRNAs and greater fold changes. A common set of two miRNAs was found to be differentially expressed in EVs isolated by all methods. In EVs from sepsis patients, miR-122-5p was upregulated with $\log_2$ fold changes of 1.86 (Exo-spin) to 4.53 (exoRNeasy). miR-151a-3p, on the other hand, was downregulated in

septic EVs, displaying $\log_2$ fold changes of −1.18 (miRCURY) to −1.65 (exoRNeasy) (Table 2).

EV populations isolated by divergent methods differ in size, concentration and purity

EVs captured by all isolation methods were analysed by NTA. Mean and mode particle diameters ranged from 104.46 ± 11.96 nm and 80.02 ± 10.12 nm (miRCURY volunteer) to 202.86 ± 10.70 nm and 174.48 ± 18.20 nm (exoRNeasy volunteer), respectively (Figure 6(a)). Size distributions for sepsis patients were slightly broader for all

Table 2. Common set of miRNAs differentially regulated between sepsis and healthy controls for all EV isolation methods.

	miR-122-5p	
Isolation method	log$_2$FC	p-adj
exoRNeasy	4.53	6.72E-17
qEV	2.11	2.73E-04
Exo-spin	1.86	2.72E-04
miRCURY	2.88	1.42E-07
	miR-151a-3p	
Isolation method	log$_2$FC	p-adj
exoRNeasy	−1.65	4.61E-10
qEV	−1.55	4.97E-06
Exo-spin	−1.19	3.92E-02
miRCURY	−1.18	5.72E-03

Log$_2$FC: log$_2$ fold change; p-adj: DESeq2-adjusted p-value.
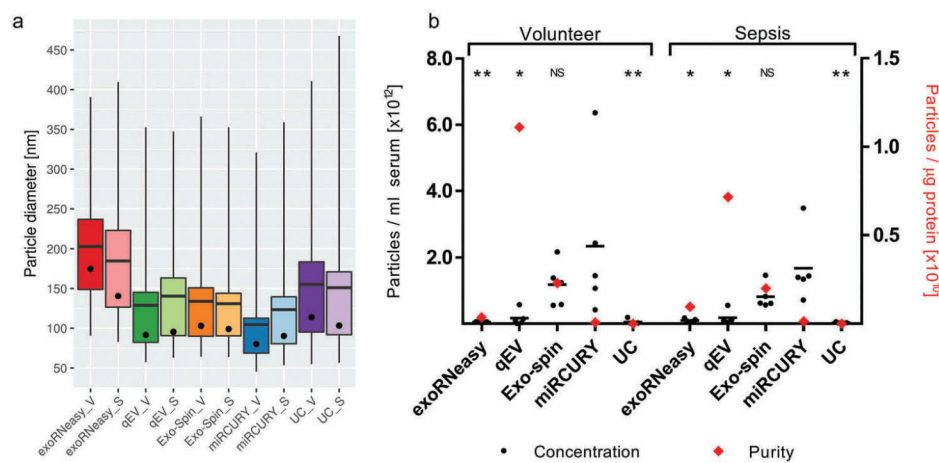
Figure 6. Analysis of EVs by NTA demonstrates differences in size distribution (a). Whiskers indicate 1st and 99th percentiles; line: mean diameter; dot: modal diameter; V: volunteer; S: sepsis patient. Precipitation- and membrane affinity-based methods isolated the smallest and largest EVs, respectively. Concentration and purity of isolated EVs differed depending on isolation strategies (b). Black bars indicate the absolute number of vesicles isolated from 1 ml serum; red diamonds plotted against the right x-axis represent vesicle purity defined as the particle to protein ratio. While precipitation most efficiently isolated EVs from serum, SEC-based isolation yielded fewer but highly pure vesicles. Asterisks indicate significant differences in particle numbers compared to miRCURY. *$p < 0.05$; **$p < 0.01$; NS: not significant. All data are mean ± SD for five volunteers and five sepsis patients.

isolation methods except qEV, but no significant differences in particle diameter were detected between volunteers and patients. The total number of particles isolated from 1 ml serum was highest for miRCURY, followed by Exo-spin, qEV, UC and exoRNeasy (Figure 6(b)). Additional plots for particle diameter and concentration are provided in Supplemental Figure 5.

Estimates for sample purity were calculated as ratios between NTA particle counts and protein concentrations [50]. While calculating these ratios does not necessarily help characterize a sample's EV fraction and their homogeneity, it provides a useful metric for assessing to which degree a sample is contaminated with non-EV protein. SEC-based isolation yielded isolates with significantly higher particle to protein ratios than all other methods, indicating less co-isolation of soluble protein (Figure 6(b)). Isolates derived from

precipitation and UC, on the other hand, displayed the lowest ratios due to increased protein contamination. Additional data on particle size, concentration and purity are included in Supplemental Table 5.

Next, we assessed particle morphology by TEM. Confirming our findings from NTA, we detected particles with EV morphology and size for all isolation methods (Figure 7). While the majority of vesicles were less than 200 nm in diameter for all methods, precipitation-derived EVs seem to be additionally enriched for particles smaller than 100 nm.

Enrichment of contaminating soluble protein in EVs isolated by precipitation and UC

Prior to immunoblotting, total protein in EV lysates from each method was quantified by BCA assay.
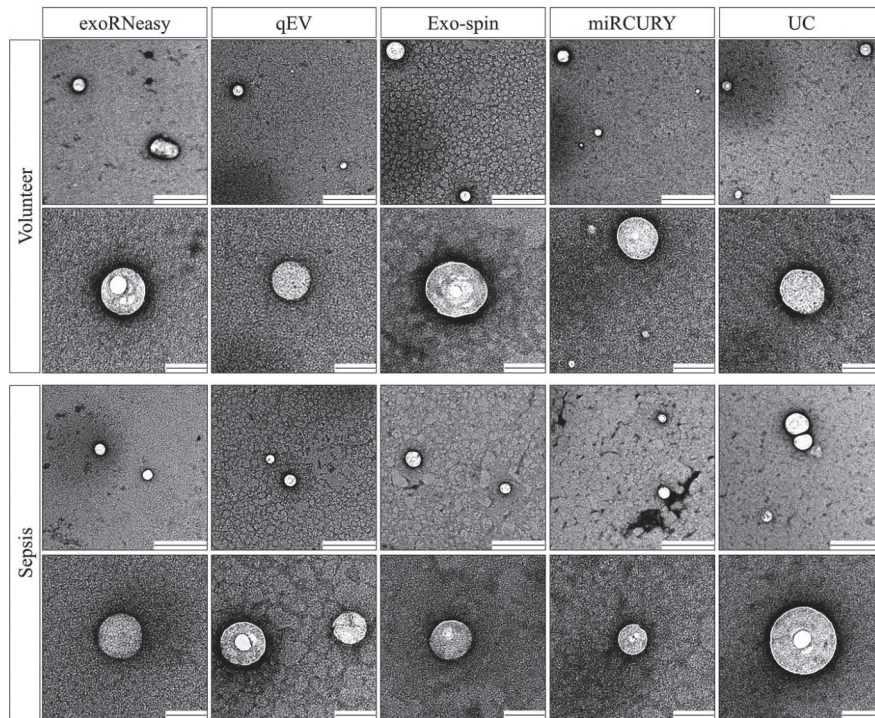
Figure 7. Morphology of serum EVs by transmission electron microscopy. Images are representative for three separate biological replicates for both volunteers (top panel) and sepsis patients (bottom panel). Scale bars are 500 nm (top row) and 100 nm (bottom row).

Similar to initial RNA concentrations and sequencing library sizes, striking differences in protein yield were observed (Supplemental Table 6). The amount of total protein in EV isolates ranged from 11.73 ± 5.18 μg (qEV, volunteer) to $26,202.95 \pm 3904.31$ μg (precipitation, volunteer). On average, precipitation and UC captured 50–80 times the amount of protein derived from SEC and membrane affinity isolations. Protein recovery from volunteer samples was significantly higher ($p < 0.05$) for exoRNeasy, miRCURY and UC, but failed to reach significance for Exo-spin ($p = 0.87$). Isolation by qEV captured significantly more ($p = 0.01$) protein from sepsis patients.

EV-specific proteins as well as negative markers were assessed by Western blot (Figure 8). CD63, a commonly used vesicle marker, was detected as a broad smear between 30 and 60 kDa, indicating differentially glycosylated forms of the protein. EVs isolated by membrane affinity showed high signal intensities for CD63, while both SEC-based methods resulted in weaker bands. No CD63 was detected for isolation by precipitation and UC. A similar pattern was observed for syntenin, showing clear signals for exoRNeasy, qEV and Exo-spin, but not for miRCURY and UC. EV markers CD81 and TSG101 were not detected for any isolation strategy.

Nonspecific staining of total EV protein by Ponceau S revealed a very prominent band at 60–70 kDa for Exo-spin, miRCURY and UC (Supplemental Figure 6), potentially indicating co-isolation of non-vesicular material. Human serum albumin (HSA), the most abundant blood protein, was selected as a likely candidate for protein contamination in EV preparations. Indeed, Western blot analysis revealed extraordinarily high HSA levels for miRCURY and UC, but also exoRNeasy and Exo-spin (Figure 8). Only minor amounts of HSA were detected for qEV isolations.

Protein lysates were also analysed for contamination with cellular fragments as indicated by the endoplasmic reticulum protein calnexin. In contrast to HSA, no calnexin signal was detected for any of the isolation methods. These findings hint at a contamination with soluble proteins, but not with non-vesicular membrane fragments. None of the detected protein markers showed significant enrichment for either volunteers or sepsis patients.

Increased contamination with soluble proteins such as HSA leads to an underrepresentation of marker proteins in EV lysates. As no EV markers were detected for miRCURY and UC, we increased the input for immunoblotting to 50 μg total protein. Additionally, EVs isolated by these techniques were further purified
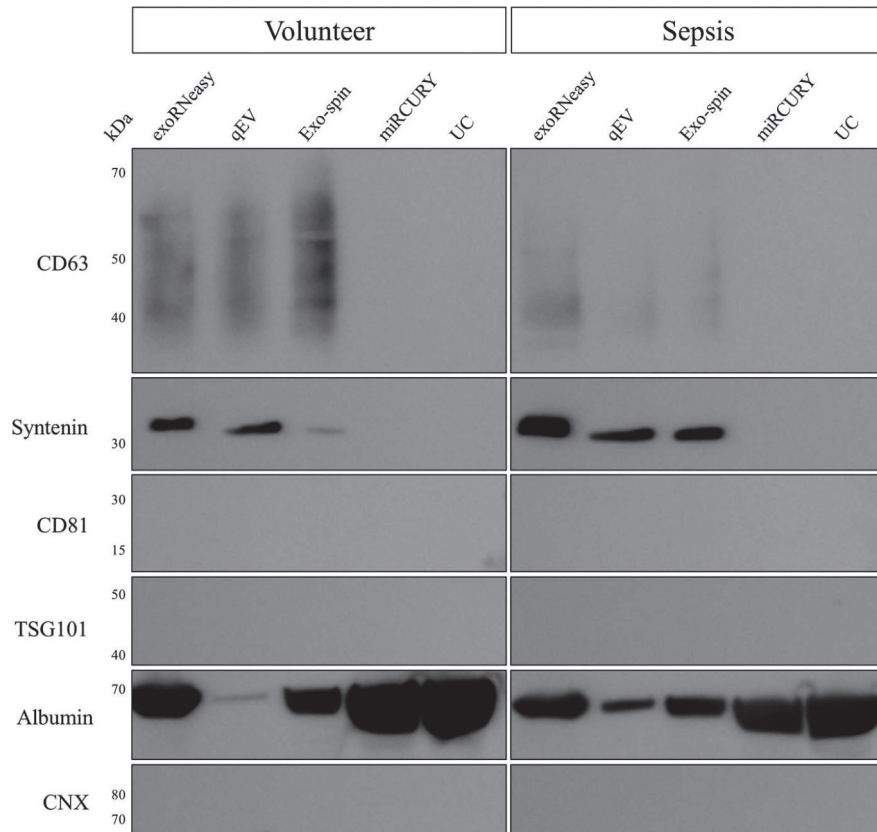
Figure 8. Analysis of marker proteins in EVs from volunteers (left) and sepsis patients (right). EV markers CD63 and syntenin were detected in vesicles isolated by membrane affinity (exoRNeasy) and SEC (qEV, Exo-spin), but not precipitation (miRCURY) and UC. All EV isolates were negative for TSG101, CD81 and calnexin. Significant albumin contamination of EVs was found for non-SEC isolation methods. Results are representative for three separate biological replicates for both volunteers and sepsis patients.

by iodixanol density gradient centrifugation to remove soluble proteins. Even though increasing total protein did not lead to the detection of protein markers (Supplemental Figure 7), floatation into a density gradient effectively separated contaminating HSA from EVs captured by sedimentation and precipitation. While the majority of HSA was retained in fractions of 1.02–1.07 g/ml, EV markers syntenin and CD63 were identified in a fraction of 1.18 g/ml, corresponding to previously reported floatation densities of blood-derived EVs [51] (Figure 9).

Discussion

EVs fascinate researchers in basic science and translational applications alike, but our understanding of EV biogenesis, secretion, tissue retention and potential therapeutic use depends on the ability to isolate and characterize specific, well-defined populations of vesicles. The question as to which EV isolation method to utilize for a given downstream application is a frequent subject of controversial debate that has yet to be settled. In this study, we

qualitatively and quantitatively compared EV isolation strategies based on different physiochemical mechanisms ranging from sedimentation and precipitation to membrane affinity and SEC. Importantly, we used serum as a biofluid relevant to clinical applications and included diseased patients as well as healthy volunteers. As isolation methods need to be validated using clinical samples, we opted for sepsis patients, who represent a prime example for both interindividual variability and complex aberrations in blood parameters.

High-throughput sequencing has evolved into a mainstream method of analysing nucleic acids. It allows precise quantification of miRNAs and sheds light on RNA composition, co-isolation of non-target molecules and novel classes of non-coding RNA. Using Illumina small RNA-Seq, we found that vesicular RNA profiles greatly depend on the respective EV isolation strategy. While the methods less specific for EVs (precipitation, sedimentation and membrane affinity) resulted in higher absolute and relative numbers of mapped miRNAs, a more stringent size selection on EVs (SEC) led to lower mapping rates and an abundance of short RNA fragments in preparations
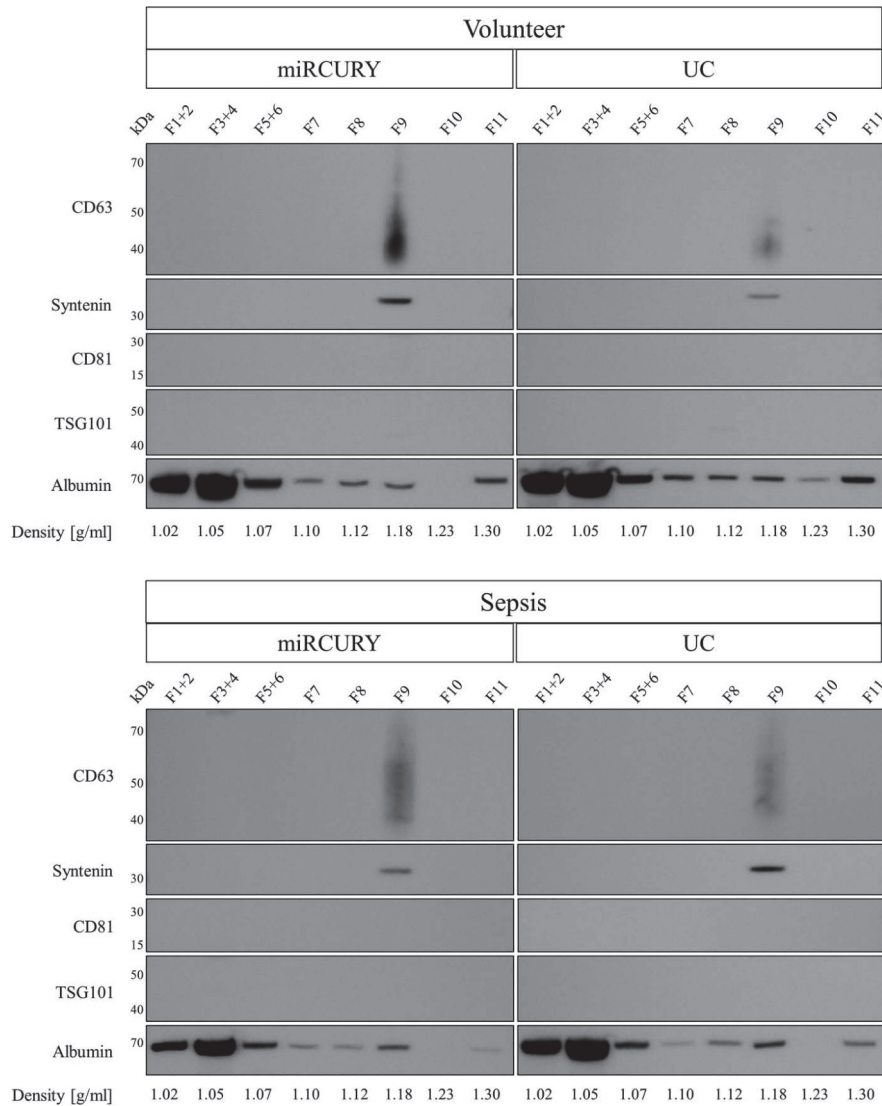
Figure 9. Analysis of EV markers and human serum albumin in EVs isolated by precipitation and sedimentation and further purified by iodixanol density gradient centrifugation. CD63 and syntenin were detected in a density fraction of 1.18 g/ml, while the majority of albumin floated in fractions of 1.02–1.05 g/ml. Results are representative for two separate biological replicates for both volunteers (top panel) and patients (bottom panel).

(Figure 3). Furthermore, isolates from different methods were reproducibly enriched in fragments of additional short non-coding RNA classes such as tRNA. We have used two different RNA extraction kits in this study, and varying combinations of EV isolation and RNA extraction methods might yield slightly different results [5,52]. However, based on the vastly different characteristics of the material captured by each method, we believe that EV isolation itself has a far greater impact on downstream RNA analysis than the respective extraction method (Figure 6).

The prime objective of this study was to assess EV isolation methods regarding their suitability for miRNA-based biomarker studies. In our data, the

ability to separate healthy individuals from diseased patients strongly correlated with sequencing output for a given method: EV isolation based on precipitation and membrane affinity resulted in higher absolute numbers of mapped miRNA reads, more candidates in DGE analysis and enhanced separation of groups in hierarchical clustering. In contrast, low-output methods (SEC) were also able to identify a core set of two miRNAs differentially regulated regardless of isolation strategy but did not reliably assign individual samples to the correct study population (Figure 5). Interestingly, only SEC-based methods generated similar or greater numbers of reads from diseased samples, while precipitation and membrane affinity seemed to

work more effectively for healthy individuals (Supplemental Table 3). This correlated only partially with particle data from NTA, which indicate that both qEV and exoRNeasy recover more particles from sepsis sera. Even though assessing sequencing library size as a standalone metric is of limited use, results from differential expression analysis correlated with higher sequencing output and more diverse libraries in our data. Library composition might, however, differ depending on sample preparation, as demonstrated by Huang et al. [28]. As different library preparation kits tend to preferentially capture specific RNA sequences, NGS data in different experiments might be biased for certain transcripts. Highly abundant miRNAs are less affected by library preparation-induced biases, which might be more problematic for low-abundance transcripts or biomarker studies in diseases with less extreme alterations in miRNA expression. In conclusion, isolation methods less specific for EVs yielded more RNA, better libraries and, therefore, increased separation of patient groups. More specific methods, which purify EVs rather than enrich cell-free material in general, resulted in less complex libraries, fewer miRNA reads and poor performance in clustering. It is worth noting that increasing sequencing depth for RNA associated with pure vesicle preparations might in turn improve results from DGE analysis.

Observed variations in RNA composition could be attributed to a number of factors including a method's efficiency of isolating EVs, isolation of non-overlapping subpopulations of vesicles and co-isolation of non-vesicular RNA. As blood samples from sepsis patients and healthy donors were drawn using slightly different methods, potential sampling-related batch effects might confound genuine disease effects. Yet, as shown in hierarchical clustering (Figure 5), poor separation of sample groups for SEC-based isolation indicates the absence of a systematic batch effect caused by blood sampling. Additionally, in a separate study on paired samples collected by arterial and venous catheters from the same donors, we couldn't detect any significant sampling-dependent differences in EV morphology and associated miRNA profiles (manuscript in preparation). Differential expression of miRNAs in this study is therefore likely to be caused by sepsis itself, rather than by collection methods.

Several of the miRNAs we found to be differentially expressed (Supplemental Table 4) have previously been associated with sepsis and inflammation. Reithmair et al. and Wang et al. reported increased levels of circulating miR-193b-5p in EVs from sepsis patients and a strong association with disease mortality [34,53]. miR-30a-5p, upregulated in samples from exoRNeasy, miRCURY and

Exo-spin, is induced by inflammatory stimuli and discriminates sepsis from non-infectious systemic inflammatory response syndrome [54,55]. Several groups reported that treating macrophages with lipopolysaccharides (LPS) increased expression of miR-155-5p, which, in turn, dampened the immune response, protected septic mice from cardiac dysfunction and improved survival [56–58]. Additionally, circulating levels of miR-155 were shown to correlate with disease severity and poor prognosis in a cohort of 60 sepsis patients [59]. In mice and rats, miR-150-5p, upregulated in samples captured by membrane affinity, was increased by polymicrobial sepsis and LPS treatment, respectively [60,61]. Vasilescu et al. reported plasma levels of miR-150-5p to correlate with sepsis aggressiveness in a cohort of 17 sepsis patients [62]. In concordance with previous findings in critically ill patients, we detected miR-122-5p as upregulated in samples derived from all isolation methods. This miRNA is commonly considered to be liver specific, and increased serum concentrations have been reported in cases of liver injury and hepatotoxicity [63]. Increased serum levels of miR-122-5p were also reported in sepsis patients, correlating with liver damage, coagulation disorders and mortality [53,64,65]. A more recent publication by Roderburg et al., however, demonstrated that miR-122-5p expression in critically ill patients was dysregulated by hepatic injury alone, independent of an infectious state [66]. Exclusively focusing on the septic shock patients in our cohort might have tightened expression patterns of disease-related miRNAs, but as our goal was to assess EV isolation methods capable of also detecting the less severe stage, we did not perform separate analyses on this subgroup. In conclusion, our findings match previous reports about altered profiles of circulating miRNAs in critically ill patients and animal models of sepsis, and crude preparations of cell-free RNA allow for more robust detection of disease-associated differential expression.

In an attempt to shed light on the nature of vesicles isolated by each method, we characterized intact particles using NTA. Unsurprisingly, all methods used in this study isolated particles in the size range of small EVs. Mean particle diameters, however, differed significantly: membrane affinity captured EVs with diameters close to 200 nm, while precipitation isolated vesicles with an exosome-like diameter of 100–120 nm. These differences might be due to capturing different EV populations or manipulation of originally identical EVs during isolation by aggregation [67] or coating with serum proteins [68]. In line with our findings, Stranska et al. recently reported larger particle diameters for EV samples isolated from human plasma by membrane affinity compared to SEC [69]. For most kits, variability of particle

diameters was greater in sepsis samples, indicating disease-specific changes in circulating vesicles, or interferences caused by matrix effects in serum from critically ill patients. It is also conceivable that an increased proportion of immune cell-derived EVs or bacterial outer membrane vesicles, typically ranging from 20 to 300 nm in diameter, might contribute to the broader range of particles recovered from septic sera [70,71].

Quantitative analysis of particles revealed another layer of complexity, as precipitation captured both the smallest and the highest number of EVs, whereas particles isolated by membrane affinity were larger and much less abundant. For a given isolation method, seemingly high standard deviations of particle sizes can most likely be attributed to endogenous variability within patient groups. Recent work by Eitan et al. revealed individual-specific set points for EV concentration and composition, indicating the need for larger cohorts in descriptive and clinical EV studies [49]. The slightly decreased concentration of EVs recovered from sepsis patients by most methods could be due to less efficient capture from patient sera, or genuinely lower EV concentrations in serum caused by decreased secretion, increased clearance from the bloodstream, dilution of EVs by therapeutic blood products administered in the ICU or a combination thereof. It should be noted, however, that lipoproteins such as low-density lipoprotein (LDL) outnumber EVs in cell-free blood by at least one order of magnitude and are known to co-purify with EVs [72]. As LDL and other common contaminants such as protein aggregates mimic characteristics of genuine EVs, particle quantification using NTA might overestimate EV concentrations in low-purity preparations and skew isolation-dependent size profiles [73–75]. Interestingly, the ability of extracellular RNA to separate healthy and diseased individuals did not seem to be tied to the diameter of the corresponding EVs since methods isolating both very small (precipitation) and very large (membrane affinity) EVs performed best in differential expression analysis. As these methods are prone to contamination with soluble material (Figure 8), we cannot rule out the possibility that separation of patient groups is based on RNA not associated with EVs, but co-isolated from the non-vesicular serum compartment. SEC-based methods, on the other hand, isolated EVs contaminated with large quantities of short RNA fragments, rendering them less suitable for robust classification of patient samples. This discovery raises questions about the origin of these fragments and whether they are encapsulated in EVs or co-isolated from non-vesicular blood compartments. While part of the population of short fragments might be derived from RNA degradation and library preparation artefacts such as adaptor dimers, non-human RNA sequences could also contribute to this category. Certain bacteria secrete cell-free

RNA, some of it vesicle-associated, which might have been captured from septic sera by the EV isolation methods used here [76,77]. Additionally, reads categorized as unmapped (Figure 3) might be derived from bacterial RNA, even though the frequency of unmapped reads was not significantly increased in sepsis samples. As differential contamination of libraries with non-human sequences would impair normalization to library size or reads per million, we strictly normalized expression values for confirmed human miRNAs. Analysing particle morphology by TEM demonstrated that all methods isolated vesicles in the 100–200 nm size range. Isolates from precipitation did not display significantly more vesicles than other methods, indicating that non-vesicular particles such as protein aggregates might have contributed to increased particle counts in NTA [78]. The number of particles per field shown in Figure 7 does not necessarily correlate to particle concentrations from NTA since different dilution factors were used for samples from each isolation method in TEM imaging. In accordance with recent reports [79], we also observed double vesicles and vesicles containing two or more smaller vesicles.

Further profiling of EV isolates demonstrated an enrichment in CD63 and syntenin for SEC-based and membrane affinity-based isolations, but not for precipitation and UC. Potentially owing to insufficient starting material or technical factors, and in contrast to preexisting publications [23,34,80], we did not detect TSG101 and CD81 for any isolation method. Similar findings were recently presented in a publication by Stranska et al., which demonstrated the absence of CD81 and TSG101 in plasma EVs isolated by membrane affinity [69]. Additionally, recent advances in the field have demonstrated that so-called exosome markers can also be present on other classes of EVs and that EV isolates are a heterogeneous mixture of various subpopulations with specific protein profiles [81,82]. It is therefore conceivable that isolation methods are biased towards only partially overlapping EV populations, resulting in different protein profiles. Additionally, modifications of EVs during isolation, including coating with precipitation polymers or serum proteins, might mask antigens and impede detection of marker proteins as observed elsewhere [83,84]. Even though increasing the input for protein analysis helped other investigators to detect markers in crude EV samples [23], it was not sufficient for samples from precipitation and sedimentation in our study. Additional purification by density gradient centrifugation, however, established the presence of EV markers syntenin and CD63 in fractions with a density of 1.18 g/ml (Figure 9). While serum albumin and other soluble proteins overpowered EV markers in crude isolates, floatation into a density gradient could be used to specifically purify vesicles from pre-enriched samples. The endoplasmic reticulum marker calnexin could

not be detected in lysates from any of the isolation principles, indicating the absence of contaminating cellular fragments and vesicles not originating from endosomes [85]. Contamination of EV preparations with highly abundant blood proteins is a well-known problem, particularly for proteomic analyses [86]. In line with earlier publications, we demonstrate that precipitation- and sedimentation-based isolations co-fractionate significant amounts of serum albumin that mask genuine EV-enriched proteins. Additionally, we herein confirm previous findings [69,83,87] that SEC-based methods represent an efficient way of removing high-abundance serum proteins (Supplemental Figure 6), trading decreased vesicle yield for higher purity [88].

Highly pure and well-defined populations of EVs, however, might not be prerequisite for all research questions. While mechanistic and descriptive scrutinies are crucial for basic research and developing EV therapeutics, biomarker applications rely heavily on pronounced and reproducible changes in the molecules of interest. A recent publication by Quek et al. suggests that impurities in vesicle preparations have little effect on downstream nucleic acid quantification and states the utility of time-efficient, but rather crude EV isolation methods for biomarker discovery [89]. In line with this, we report precipitation-based isolation to yield samples with lower purity and significant protein contamination, but excellent potential for transcriptomics-driven biomarker discovery. We agree with previous publications stating that enriching serum EVs by precipitation might be a viable strategy for biomarker discovery studies [21,23]. Alvarez et al. presented similar findings for profiling RNA biomarkers in urinary EVs [9]. Decreased purity does not have to be a limitation if the objective is enriching cell-free miRNAs rather than purifying specific EV populations. If researchers strive to identify extracellular miRNA signatures that separate patient populations, these could be analysed regardless of their carriers [90]. As long as samples isolated by a given method reproducibly provide strong divisional capabilities for patient populations of interest, comprehensively characterizing isolated vesicles might not be a mandatory requirement for clinical biomarker applications. Given that precipitation is time efficient, inexpensive and demands no specialized equipment, it also seems to conveniently lend itself to integration into clinical usage. However, in a research field as vibrant and international, standardizing reagents and protocols utilized for EV precipitation and characterization are crucial for generating valid and reproducible data across laboratories [22,85,91].

In conclusion, we herein report that enriching cell-free miRNAs by precipitation allows for reliable separation of sepsis patients and healthy volunteers in sequencing-based analyses. As extracellular RNA can be encapsulated in vesicles or stabilized by binding to circulating proteins such as argonaute 2 (Ago2), further investigations using additional purification steps such as density gradient centrifugation or SEC are needed to conclusively verify if miRNAs dysregulated in this study are genuinely encapsulated in EVs [92]. Based on our experiments, we cannot rule out the possibility that miRNAs separating patients and volunteers are associated with non-vesicular carriers rather than EVs [93]. Should this be the case, additional validation of sepsis-related miRNA signatures might be carried out on total cell-free RNA without prior enrichment of EVs, reducing time and cost of analysis. Even though exosomes have been shown to provide an enriched source of miRNA with higher predictive value than total cell-free blood, miRNAs of diagnostic potential might be associated with different carriers in a disease-specific manner, calling for the careful validation of previous findings in each biomarker discovery process [2,94]. In diseases with less drastic clinical manifestation than sepsis, extracellular signalling could be more clearly detectable in pure EVs as opposed to crude preparations of cell-free RNA. Our findings might therefore not be generalizable to all clinical applications, as a different approach may be more appropriate for diseases other than sepsis.

Even though the focus of this work was on transcriptomic profiling of EVs, our findings could be transferred to different routes of analysis as well. It has become increasingly clear that the optimal method of EV isolation differs depending on the respective research setting and downstream analyses. Both failing to choose appropriate isolation methods for a particular experiment and trying to integrate results from multiple studies conducted with inappropriate or incompatible methodology squander resources decrease experimental validity and hamper translation of research findings into practical applications. This work therefore provides valuable guidance for navigating the wide array of EV isolation methods available today.

Acknowledgements

Disclosure statement

ORCID

Dominik Buschmann   http://orcid.org/0000-0003-0460-6459
Benedikt Kirchner   http://orcid.org/0000-0003-3878-0148
Stefanie Hermann   http://orcid.org/0000-0002-6274-5919
Melanie Märte   http://orcid.org/0000-0002-0741-616X
Christine Wurmser   http://orcid.org/0000-0003-0649-6206
Florian Brandes   http://orcid.org/0000-0003-3741-287X
Ortrud K. Steinlein   http://orcid.org/0000-0003-4311-6276
Michael W. Pfaffl   http://orcid.org/0000-0002-3192-1019
Gustav Schelling   http://orcid.org/0000-0002-6538-0652
Marlene Reithmair   http://orcid.org/0000-0002-9113-9643

References

[1] Gardiner C, Di Vizio D, Sahoo S, et al. Techniques used for the isolation and characterization of extracellular vesicles: results of a worldwide survey. J Extracell Vesicles. 2016;5:32945.

[2] Cheng L, Sharples RA, Scicluna BJ, et al. Exosomes provide a protective and enriched source of miRNA for biomarker profiling compared to intracellular and cell-free blood. J Extracell Vesicles. 2014;3:23743

[3] Mustapic M, Eitan E, Werner JK Jr., et al. Plasma extracellular vesicles enriched for neuronal origin: a potential window into brain pathologic processes. Front Neurosci. 2017;11:278.

[4] Buschmann D, Haberberger A, Kirchner B, et al. Toward reliable biomarker signatures in the age of liquid biopsies – how to standardize the small RNA-Seq workflow. Nucleic Acids Res. 2016;44: 5995–6018. Epub 2016/ 06/19.

[5] El-Khoury V, Pierson S, Kaoma T, et al. Assessing cellular and circulating miRNA recovery: the impact of the RNA isolation method and the quantity of input material. Sci Rep. 2016;6:19529.

[6] Guo Y, Vickers K, Xiong Y, et al. Comprehensive evaluation of extracellular small RNA isolation methods from serum in high throughput sequencing. BMC Genomics. 2017;18:50.

[7] Danielson KM, Rubio R, Abderazzaq F, et al. High throughput sequencing of extracellular RNA from human plasma. PLoS One. 2017;12:e0164644.

[8] Van Deun J, Mestdagh P, Sormunen R, et al. The impact of disparate isolation methods for extracellular vesicles on downstream RNA profiling. J Extracell Vesicles. 2014;3:24858.

[9] Alvarez ML, Khosroheidari M, Kanchi Ravi R, et al. Comparison of protein, microRNA, and mRNA yields using different methods of urinary exosome isolation for the discovery of kidney disease biomarkers. Kidney Int. 2012;82:1024–1032.

[10] Royo F, Diwan I, Tackett MR, et al. Comparative miRNA analysis of urine extracellular vesicles isolated through five different methods. Cancers (Basel). 2016;8:112

[11] Blans K, Hansen MS, Sorensen LV, et al. Pellet-free isolation of human and bovine milk extracellular vesicles by size-exclusion chromatography. J Extracell Vesicles. 2017;6:1294340.

[12] Rekker K, Saare M, Roost AM, et al. Comparison of serum exosome isolation methods for microRNA profiling. Clin Biochem. 2014;47: 135–138. Epub 2013/ 11/05.

[13] Muller L, Hong CS, Stolz DB, et al. Isolation of biologically-active exosomes from human plasma. J Immunol Methods. 2014;411:55–65.

[14] Nielsen MH, Beck-Nielsen H, Andersen MN, et al. A flow cytometric method for characterization of circulating cell-derived microparticles in plasma. J Extracell Vesicles. 2017;3:20795.

[15] Lasser C, Shelke GV, Yeri A, et al. Two distinct extracellular RNA signatures released by a single cell type identified by microarray and next-generation sequencing. RNA Biol. 2017;14:58–72.

[16] Caponnetto F, Manini I, Skrap M, et al. Size-dependent cellular uptake of exosomes. Nanomedicine. 2017;13: 1011–1020.

[17] Zlotogorski-Hurvitz A, Dayan D, Chaushu G, et al. Human saliva-derived exosomes: comparing methods of isolation. J Histochem Cytochem. 2015;63:181–189.

[18] Abramowicz A, Widlak P, Pietrowska M. Proteomic analysis of exosomal cargo: the challenge of high purity vesicle isolation. Mol Biosyst. 2016;12: 1407–1419. Epub 2016/ 04/01.

[19] Royo F, Zuniga-Garcia P, Sanchez-Mosquera P, et al. Different EV enrichment methods suitable for clinical settings yield different subpopulations of urinary extracellular vesicles from human samples. J Extracell Vesicles. 2016;5: 29497. Epub 2016/ 02/20.

[20] Mol EA, Goumans MJ, Doevendans PA, et al. Higher functionality of extracellular vesicles isolated using size-exclusion chromatography compared to ultracentrifugation. Nanomedicine. 2017;13:2061–2065.

[21] Andreu Z, Rivas E, Sanguino-Pascual A, et al. Comparative analysis of EV isolation procedures for miRNAs detection in serum samples. J Extracell Vesicles. 2016;5:31655.

[22] Crossland RE, Norden J, Bibby LA, et al. Evaluation of optimal extracellular vesicle small RNA isolation and qRT-PCR normalisation for serum and urine. J Immunol Methods. 2016;429:39–49.

[23] Helwa I, Cai J, Drewry MD, et al. A comparative study of serum exosome isolation using differential ultracentrifugation and three commercial reagents. PLoS One. 2017;12:e0170628.

[24] Bellingham SA, Shambrook M, Hill AF. Quantitative analysis of exosomal miRNA via qPCR and digital PCR. Methods Mol Biol. 2017;1545: 55–70. Epub 2016/ 12/13.

[25] Zeringer E, Li M, Barta T, et al. Methods for the extraction and RNA profiling of exosomes. World J Methodol. 2013;3: 11–18. Epub 2013/ 03/26.

[26] Takahashi K, Yan IK, Kim C, et al. Analysis of extracellular RNA by digital PCR. Front Oncol. 2014;4: 129. Epub 2014/ 06/14.

[27] Li M, Zeringer E, Barta T, et al. Analysis of the RNA content of the exosomes derived from blood serum and urine and its potential as biomarkers. Philos

Trans R Soc Lond B Biol Sci. 2014;369 (Epub 2014/08/20).

[28] Huang X, Yuan T, Tschannen M, et al. Characterization of human plasma-derived exosomal RNAs by deep sequencing. BMC Genomics. 2013;14: 319. Epub 2013/ 05/15.

[29] Tsang EK, Abell NS, Li X, et al. Small RNA sequencing in cells and exosomes identifies eQTLs and 14q32 as a region of active export. G3 (Bethesda). 2017;7: 31–39. Epub 2016/ 11/04.

[30] Tang YT, Huang YY, Zheng L, et al. Comparison of isolation methods of exosomes and exosomal RNA from cell culture medium and serum. Int J Mol Med. 2017;40: 834–844. Epub 2017/ 07/25.

[31] Nimah M, Brilli RJ. Coagulation dysfunction in sepsis and multiple organ system failure. Crit Care Clin. 2003;19:441–458.

[32] SepNet Critical Care Trials G. Incidence of severe sepsis and septic shock in German intensive care units: the prospective, multicentre INSEP study. Intensive Care Med. 2016;42:1980–1989.

[33] Charlson ME, Pompei P, Ales KL, et al. A new method of classifying prognostic comorbidity in longitudinal studies: development and validation. J Chronic Dis. 1987;40:373–383.

[34] Reithmair M, Buschmann D, Märte M, et al. Cellular and extracellular miRNAs are blood-compartment-specific diagnostic targets in sepsis. J Cell Mol Med. 2017;21:2403–2411.

[35] Spornraft M, Kirchner B, Haase B, et al. Optimization of extraction of circulating RNAs from plasma – enabling small RNA sequencing. PLoS One. 2014;9:e107259.

[36] Andrews S FastQC: a quality control tool for high throughput sequence data; 2010.

[37] Kong Y. Btrim: a fast, lightweight adapter and quality trimming program for next-generation sequencing technologies. Genomics. 2011;98:152–153.

[38] Consortium RN. RNAcentral: an international database of ncRNA sequences. Nucleic Acids Res. 2015;43: D123–D129.

[39] Kozomara A, Griffiths-Jones S. miRBase: annotating high confidence microRNAs using deep sequencing data. Nucleic Acids Research. 2014;42:D68–D73.

[40] Langmead B, Trapnell C, Pop M, et al. Ultrafast and memory-efficient alignment of short DNA sequences to the human genome. Genome Biology. 2009; 10:R25.

[41] Love MI, Huber W, Anders S. Moderated estimation of fold change and dispersion for RNA-seq data with DESeq2. Genome Biology. 2014;15:550.

[42] R Core Team. R: a language and environment for statistical computing. Vienna, Austria; 2017.

[43] Gregory R, Warnes BB, Bonebakker L, et al. Various R Programming Tools for Plotting Data; 2016.

[44] Wickham H ggplot2: Elegant Graphics for data analysis; 2009.

[45] Neuwirth E RColorBrewer: ColorBrewer Palettes. 2014.

[46] Galili T. dendextend: an R package for visualizing, adjusting and comparing trees of hierarchical clustering. Bioinformatics. 2015;31:3718–3720.

[47] Yuan Tang MH, Wenxuan L. ggfortify: unified interface to visualize statistical result of popular R Packages; 2016.

[48] Chen H VennDiagram: generate high-resolution Venn and Euler plots; 2016.

[49] Eitan E, Green J, Bodogai M, et al. Age-related changes in plasma extracellular vesicle characteristics and internalization by leukocytes. Sci Rep. 2017;7:1342.

[50] Webber J, Clayton A. How pure are your vesicles? J Extracell Vesicles. 2013;2:19861.

[51] Kalra H, Adda CG, Liem M, et al. Comparative proteomics evaluation of plasma exosome isolation techniques and assessment of the stability of exosomes in normal human blood plasma. Proteomics. 2013;13: 3354–3364. Epub 2013/ 10/12.

[52] Eldh M, Lotvall J, Malmhall C, et al. Importance of RNA isolation methods for analysis of exosomal RNA: evaluation of different methods. Mol Immunol. 2012;50:278–286.

[53] Wang H, Zhang P, Chen W, et al. Serum microRNA signatures identified by Solexa sequencing predict sepsis patients' mortality: a prospective observational study. PLoS One. 2012;7: e38885. Epub 2012/ 06/22.

[54] Caserta S, Kern F, Cohen J, et al. Circulating plasma microRNAs can differentiate human sepsis and systemic inflammatory response syndrome (SIRS). Sci Rep. 2016;6: 28006. Epub 2016/ 06/21.

[55] Jiang X, Xu C, Lei F, et al. MiR-30a targets IL-1alpha and regulates islet functions as an inflammation buffer and response factor. Sci Rep. 2017;7: 5270. Epub 2017/ 07/15.

[56] Cheng Y, Kuang W, Hao Y, et al. Downregulation of miR-27a* and miR-532-5p and upregulation of miR-146a and miR-155 in LPS-induced RAW264.7. Macrophage Cells Inflammation. 2012;35:1308–1313.

[57] Tili E, Michaille JJ, Cimino A, et al. Modulation of miR-155 and miR-125b levels following lipopolysaccharide/TNF-alpha stimulation and their possible roles in regulating the response to endotoxin shock. J Immunol. 2007;179: 5082–5089. Epub 2007/ 10/04.

[58] Zhou Y, Song Y, Shaikh Z, et al. MicroRNA-155 attenuates late sepsis-induced cardiac dysfunction through JNK and beta-arrestin 2. Oncotarget. 2017;8: 47317–47329. Epub 2017/ 05/20.

[59] Liu J, Shi K, Chen M, et al. Elevated miR-155 expression induces immunosuppression via CD39(+) regulatory T-cells in sepsis patient. Int J Infect Dis. 2015;40: 135–141. Epub 2015/ 10/04.

[60] Tacke F, Roderburg C, Benz F, et al. Levels of circulating miR-133a are elevated in sepsis and predict mortality in critically ill patients. Crit Care Med. 2014;42: 1096–1104. Epub 2014/ 01/15.

[61] Sari AN, Korkmaz B, Serin MS, et al. Effects of 5,14-HEDGE, a 20-HETE mimetic, on lipopolysaccharide-induced changes in MyD88/TAK1/IKKbeta/IkappaB-alpha/NF-kappaB pathway and circulating miR-150, miR-223, and miR-297 levels in a rat model of septic shock. Inflamm Res. 2014;63: 741–756. Epub 2014/ 06/12.

[62] Vasilescu C, Rossi S, Shimizu M, et al. MicroRNA fingerprints identify miR-150 as a plasma prognostic marker in patients with sepsis. PLoS One. 2009;4: e7405. Epub 2009/ 10/14.

[63] Lin H, Ewing LE, Koturbash I, et al. MicroRNAs as biomarkers for liver injury: current knowledge, challenges and future prospects. Food Chem Toxicol. 2017;110: 229–239. Epub 2017/ 10/19.

[64] Wang H, Yu B, Deng J, et al. Serum miR-122 correlates with short-term mortality in sepsis patients. Crit Care. 2014;18: 704. Epub 2015/ 02/13.

[65] Wang HJ, Deng J, Wang JY, et al. Serum miR-122 levels are related to coagulation disorders in sepsis patients. Clin Chem Lab Med. 2014;52: 927–933. Epub 2014/ 01/15.

[66] Roderburg C, Benz F, Vargas Cardenas D, et al. Elevated miR-122 serum levels are an independent marker of liver injury in inflammatory diseases. Liver Int. 2015;35: 1172–1184. Epub 2014/ 07/22.

[67] Linares R, Tan S, Gounou C, et al. High-speed centrifugation induces aggregation of extracellular vesicles. J Extracell Vesicles. 2015;4:29509.

[68] Dominguez-Medina S, McDonough S, Swanglap P, et al. In situ measurement of bovine serum albumin interaction with gold nanospheres. Langmuir. 2012;28:9131–9139.

[69] Stranska R, Gysbrechts L, Wouters J, et al. Comparison of membrane affinity-based method with size-exclusion chromatography for isolation of exosome-like vesicles from human plasma. J Transl Med. 2018;16: 1. Epub 2018/ 01/11.

[70] Kaparakis-Liaskos M, Ferrero RL. Immune modulation by bacterial outer membrane vesicles. Nat Rev Immunol. 2015;15: 375–387. Epub 2015/ 05/16.

[71] Alexander M, Hu R, Runtsch MC, et al. Exosome-delivered microRNAs modulate the inflammatory response to endotoxin. Nat Commun. 2015;6: 7321. Epub 2015/ 06/19.

[72] Sodar BW, Kittel A, Paloczi K, et al. Low-density lipoprotein mimics blood plasma-derived exosomes and microvesicles during isolation and detection. Sci Rep. 2016;6: 24316. Epub 2016/ 04/19.

[73] Gyorgy B, Szabo TG, Turiak L, et al. Improved flow cytometric assessment reveals distinct microvesicle (cell-derived microparticle) signatures in joint diseases. PLoS One. 2012;7: e49726. Epub 2012/ 11/28.

[74] Mork M, Handberg A, Pedersen S, et al. Prospects and limitations of antibody-mediated clearing of lipoproteins from blood plasma prior to nanoparticle tracking analysis of extracellular vesicles. J Extracell Vesicles. 2017;6: 1308779. Epub 2017/ 05/06.

[75] Gardiner C, Ferreira YJ, Dragovic RA, et al. Extracellular vesicle sizing and enumeration by nanoparticle tracking analysis. J Extracell Vesicles. 2013;2: 19671. Epub 2013/ 09/07.

[76] Ghosal A. Importance of secreted bacterial RNA in bacterial-host interactions in the gut. Microb Pathog. 2017;104: 161–163. Epub 2017/ 01/24.

[77] Ghosal A, Upadhyaya BB, Fritz JV, et al. The extracellular RNA complement of Escherichia coli. Microbiologyopen. 2015;4: 252–266. Epub 2015/ 01/23.

[78] Soo CY, Song Y, Zheng Y, et al. Nanoparticle tracking analysis monitors microvesicle and exosome secretion from immune cells. Immunology. 2012;136: 192–197. Epub 2012/ 02/22.

[79] Zabeo D, Cvjetkovic A, Lasser C, et al. Exosomes purified from a single cell type have diverse morphology. J Extracell Vesicles. 2017;6: 1329476. Epub 2017/ 07/19.

[80] Enderle D, Spiel A, Coticchia CM, et al. Characterization of RNA from exosomes and other extracellular vesicles isolated by a novel spin column-based method. PLoS One. 2015;10:e0136133.

[81] Koliha N, Wiencek Y, Heider U, et al. A novel multiplex bead-based platform highlights the diversity of extracellular vesicles. J Extracell Vesicles. 2016;5:29975.

[82] Kowal J, Arras G, Colombo M, et al. Proteomic comparison defines novel markers to characterize heterogeneous populations of extracellular vesicle subtypes. Proc Natl Acad Sci U S A. 2016;113:E968–77.

[83] Gamez-Valero A, Monguio-Tortajada M, Carreras-Planella L, et al. Size-exclusion chromatography-based isolation minimally alters extracellular vesicles' characteristics compared to precipitating agents. Sci Rep. 2016;6:33641.

[84] Zarovni N, Corrado A, Guazzi P, et al. Integrated isolation and quantitative analysis of exosome shuttled proteins and nucleic acids using immunocapture approaches. Methods. 2015;87:46–58.

[85] Lotvall J, Hill AF, Hochberg F, et al. Minimal experimental requirements for definition of extracellular vesicles and their functions: a position statement from the International Society for Extracellular Vesicles. J Extracell Vesicles. 2014;3: 26913. Epub 2014/ 12/30.

[86] Lobb RJ, Becker M, Wen SW, et al. Optimized exosome isolation protocol for cell culture supernatant and human plasma. J Extracell Vesicles. 2015;4: 27031. Epub 2015/ 07/22.

[87] Welton JL, Webber JP, Botos LA, et al. Ready-made chromatography columns for extracellular vesicle isolation from plasma. J Extracell Vesicles. 2015;4:27269.

[88] Baranyai T, Herczeg K, Onodi Z, et al. Isolation of exosomes from blood plasma: qualitative and quantitative comparison of ultracentrifugation and size exclusion chromatography methods. PLoS One. 2015;10: e0145686.

[89] Quek C, Bellingham SA, Jung CH, et al. Defining the purity of exosomes required for diagnostic profiling of small RNA suitable for biomarker discovery. RNA Biol. 2017;14:245–258.

[90] Deregibus MC, Figliolini F, D'Antico S, et al. Charge-based precipitation of extracellular vesicles. Int J Mol Med. 2016;38:1359–1366.

[91] Witwer KW, Soekmadji C, Hill AF, et al. Updating the MISEV minimal requirements for extracellular vesicle studies: building bridges to reproducibility. J Extracell Vesicles. 2017;6: 1396823. Epub 2017/ 12/01.

[92] Arroyo JD, Chevillet JR, Kroh EM, et al. Argonaute2 complexes carry a population of circulating microRNAs independent of vesicles in human plasma. Proc Natl Acad Sci U S A. 2011;108: 5003–5008. Epub 2011/ 03/09.

[93] Mateescu B, Kowal EJ, van Balkom BW, et al. Obstacles and opportunities in the functional analysis of extracellular vesicle RNA – an ISEV position paper. J Extracell Vesicles. 2017;6: 1286095. Epub 2017/ 03/23.

[94] van Eijndhoven MA, Zijlstra JM, Groenewegen NJ, et al. Plasma vesicle miRNAs for therapy response monitoring in Hodgkin lymphoma patients. JCI Insight. 2016;1: e89631. Epub 2016/ 11/25.

Appendix III

Contribution by Stefanie Hermann:

- Project administration
- Manuscript conceptualization
- Writing – original draft
- Investigation – laboratory experiments
- Formal analysis and data curation
- Visualization

Stefanie Hermann

Prof. Dr. Michael W. Pfaffl

Taylor & Francis
Taylor & Francis Group

RESEARCH ARTICLE

🔓 OPEN ACCESS   Check for updates

Transcriptomic profiling of cell-free and vesicular microRNAs from matched arterial and venous sera

Stefanie Hermann [a], Dominik Buschmann [a], Benedikt Kirchner [a], Melanie Borrmann [b], Florian Brandes [b], Stefan Kotschote[c], Michael Bonin[c], Anja Lindemann[d], Marlene Reithmair [d], Gustav Schelling [b] and Michael W. Pfaffl [a]

aDivision of Animal Physiology and Immunology, School of Life Sciences Weihenstephan, Technical University of Munich, Freising, Germany; bDepartment of Anesthesiology, University Hospital, Ludwig-Maximilians-University Munich, Munich, Germany; cIMGM Laboratories GmbH, Planegg, Germany; dInstitute of Human Genetics, University Hospital, Ludwig-Maximilians-University Munich, Munich, Germany

ABSTRACT

Extracellular vesicles (EVs) play central physiological and pathophysiological roles in intercellular communication. Biomarker studies addressing disorders such as cardiovascular diseases often focus on circulating microRNAs (miRNAs) and may, depending on the type of disease and clinic routine, utilise patient specimens sampled from arterial or venous blood vessels. Thus, it is essential to test whether circulating miRNA profiles depend on the respective sampling site. We assessed potential differences in arterial and venous cell-free miRNA profiles in a cohort of 20 patients scheduled for cardiac surgery. Prior to surgery, blood was simultaneously sampled from the radial artery and the internal jugular vein. After precipitating crude EVs, we performed small RNA Sequencing, which failed to detect significantly regulated miRNAs using stringent filtering criteria for differential expression analysis. Filtering with less strict criteria, we detected four miRNAs slightly upregulated in arterial samples, one of which could be validated by reverse transcription real-time PCR. The applicability of these findings to purified arterial and venous EVs was subsequently tested in a subset of the initial study population. While an additional clean-up step using size-exclusion chromatography seemed to reduce overall miRNA yield compared to crude EV samples, no miRNAs with differential arteriovenous expression were detected. Unsupervised clustering approaches were unable to correctly classify samples drawn from arteries or veins based on miRNAs in either crude or purified preparations. Particle characterisation of crude preparations as well as characterisation of EV markers in purified EVs resulted in highly similar characteristics for arterial and venous samples. With the exception of specific pathologies (e.g. severe pulmonary disorders), arterial versus venous blood sampling should therefore not represent a likely confounder when studying differentially expressed circulating miRNAs. The use of either arterial or venous serum EV samples should result in highly similar data on miRNA expression profiles for the majority of biomarker studies.

Abbreviations ACE inhibitors: Angiotensin-converting-enzyme inhibitors; ApoA1: Apolipoprotein A1; CNX: Calnexin; Cv: Coefficient of variation; cDNA: Complementary DNA; CABG: Coronary artery bypass graft; DGE: Differential gene expression; DPBS: Dulbecco's Phosphate Buffered Saline; EVs: Extracellular vesicles; log2FC: Log2 fold change; baseMean: Mean miRNA expression; miRNA: MicroRNA; NTA: Nanoparticle Tracking Analysis; NGS: Next-Generation Sequencing; RT-qPCR: Reverse transcription quantitative real-time PCR; rRNA: Ribosomal RNA; RT: Room temperature; SEC: Size-exclusion chromatography; snoRNA: Small nucleolar RNA; snRNA: Small nuclear RNA; small RNA-Seq: Small RNA Sequencing; SD: Standard deviation; tRNA: Transfer RNA; TEM: Transmission electron microscopy; UA: Uranyl acetate.

Introduction

Recent research has demonstrated the crucial pathophysiological role of extracellular vesicles (EVs) in cell-cell communication in cardiovascular diseases and multiple other disorders. EVs, loaded with signalling molecules such as proteins, lipids and RNA, are involved in numerous physiological and pathological processes [1].

Previous biomarker research has pointed out that arterial and venous blood are not entirely rheologically comparable, and it has therefore been proposed to consistently use either arterial or venous blood samples for biomarker detection [2]. This recommendation has, however, never been systematically tested regarding circulating cell-free microRNAs (miRNAs) or circulating

EVs and their molecular cargo, particularly miRNAs. If applicable to EV research, it would render results of studies using arterial and venous approaches to blood sampling difficult to compare.

When analysing circulating miRNAs derived from porcine whole blood samples by Next-Generation Sequencing (NGS), 12 miRNAs with different arteriovenous expression levels were identified by Bai et al. [3]. Aligning matched arterial and venous rat plasma samples using microarray techniques, altered expression levels of 24 miRNAs were detected in another study [4]. In contrast, identical protein expression was found in paired arterial and venous human samples when comparing serum biomarker levels using ELISA [5]. These data indicate that arterial and venous blood samples may have many similarities regarding protein and miRNA content, but it cannot be ruled out that differences in specific blood components might exist nonetheless.

Blood samples for diagnostic or research purposes are usually drawn using peripheral venous access, whereas arterial lines inserted for monitoring purposes are more convenient and often preferred in critically ill patients undergoing intensive care unit therapy or major surgery. This may result in inherent differences in EV biomarker validity and sensitivity when data from arterial and venous samples are compared within a particular study [6] or in a loss of information when only one type of vascular access is used. Additionally, potential differences in miRNA profiles render comparability of results across studies that are based on either arterial or venous EVs and other carriers of circulating miRNAs difficult. A more detailed analysis of potential differences in EV morphology and non-coding RNA load could provide information on organ-specific effects, as arterial EVs pass through the left ventricle and lungs whereas venous EVs may more closely reflect the total venous return. Therefore, it seems to be of considerable interest to systematically analyse and compare circulating miRNAs sampled from arteries and veins. In this study, we compared circulating miRNA profiles in paired arterial and venous sera from cardiac surgical patients using small RNA Sequencing (small RNA-Seq). After detecting highly similar arteriovenous miRNA expression in crude cell-free preparations, these findings were additionally validated in purified EVs. Subsequent biological characterisation failed to establish systematic differences in characteristics of either crude preparations or purer EVs. The study was performed in accordance with the MISEV guidelines [7]. Sequencing data were deposited with the European Nucleotide Archive (http://www.ebi.ac.uk/ena/data/view/PRJEB33261) and all relevant data of the experiments were submitted to the EV-TRACK knowledgebase (EV-TRACK ID: EV190051) [8]

Materials and methods

Study population

The study population consisted of 20 cardiac surgical patients (n = 18 male and n = 2 female, age: 67.3 ± 10.7 years, BMI: 28.8 ± 5.9) with severe heart disease (Table 1). Out of those patients, fifteen had coronary artery disease requiring coronary artery bypass surgery (CABG) and five patients had combined heart valve disease and were scheduled for CABG and aortic or mitral valve replacement. Fifteen patients had arterial hypertension, seven suffered from non-insulin-dependent diabetes and five presented with mild preoperative renal function impairment. Ten patients received beta-adrenergic antagonists, seven were treated with angiotensin-converting-enzyme inhibitors (ACE inhibitors) and twelve were on statins or combinations of these compounds.

Sample collection

An arterial line (20 G, 8 cm polyethylene catheter, Vygon, Aachen, Germany) was preoperatively introduced into the radial artery. After induction of anaesthesia using the hypnotic agent propofol and the opiate sufentanil, a central venous line (8.5 F, 16 cm, polyurethane catheter with chlorhexidine coating, Arrow International, Teleflex Medical GmbH, Fellbach, Germany) was placed into the internal jugular vein.

Arterial and venous blood were simultaneously sampled from the arterial line and the central venous

Table 1. Demographics and clinical characteristics of the study population.

ID	Sex	Age [y]	Height [cm]	Weight [kg]	BMI	Disease	Intervention
1	M	83	176	80	25.83	CAD	CABG
2	M	81	178	88	27.77	CAD	CABG
3	M	60	180	89	27.47	CAD	CABG
4	M	71	175	90	29.39	CAD	CABG
5	F	75	174	63	20.81	CAD	CABG
6	M	82	168	90	31.89	CAD	CABG
7	M	74	172	85	28.73	CAD	CABG
8	M	58	184	102	30.13	CAD, TAA	CABG + AAR
9	M	67	185	103	30.10	CAD	CABG
10	F	58	158	100	40.06	MR	MVR
11	M	66	183	70	20.90	AS	AVR
12	M	57	186	161	46.54	AI	AVR
13	M	65	177	88	28.09	CAD	CABG
14	M	76	178	85	26.83	CAD	CABG
15	M	82	182	98	29.59	CAD	CABG
16	M	50	172	85	28.73	CAD	CABG
17	M	59	177	88	28.09	MR	MVR
18	M	64	166	65	23.59	CAD	CABG
19	M	48	183	80	23.89	AI	AVR
20	M	70	165	74	27.18	CAD	CABG

BMI: body mass index; CAD: coronary artery disease; CABG: coronary artery bypass grafting; TAA: thoracic aortic aneurysm; AAR: aortic arch replacement; MR: mitral regurgitation; MVR: mitral valve replacement; AS: aortic stenosis; AVR: aortic valve replacement; AI: aortic insufficiency; M: male; F: female.

line. For each patient, blood at both sampling sites was drawn into one 9 ml serum collection tube (S-Monovette, Sarstedt AG&Co, Nümbrecht, Germany) each, allowed to clot for 30 min and subsequently centrifuged at 3,400 x g for 10 min at room temperature (RT). Within 10 min of separation, serum was aliquoted and stored at – 80°C.

Enrichment of crude cell-free RNA

Crude EVs were enriched from 1 ml serum using a polymer-based precipitation method (miRCURY Exosome Isolation Kit-Serum and Plasma, Exiqon, Vedbaek, Denmark). Pellets were resuspended in the provided resuspension buffer for subsequent RNA extraction and downstream characterisation.

Total RNA was extracted from crude EVs with either the miRCURY RNA Isolation Kit-Biofluids (Exiqon, Vedbaek, Denmark) for NGS or the miRNeasy Micro Kit (Qiagen, Venlo, The Netherlands) for reverse transcription quantitative real-time PCR (RT-qPCR), respectively. To increase the yield of these samples, herein referred to as crude cell-free RNA, eluates were reapplied to the membrane for a second elution. Eluates were concentrated to a volume of 8 µl for NGS and 5 µl for RT-qPCR by applying vacuum-induced centrifugal evaporation (Savant SpeedVac SC100, Savant Instruments Inc., Bloomberg, USA). RNA size distribution and yield were assessed by capillary electrophoresis (2100 Bioanalyzer, RNA 6000 Pico Kit, Agilent Technologies, Santa Clara, USA).

Validation of arteriovenous miRNA profiles in purified EV samples

To validate our findings on crude cell-free RNA in EV samples with higher purity, we performed additional experiments using a subgroup of the initial patient population (n = 14). In these experiments, crude EVs were enriched from 1 ml arterial or venous serum using precipitation as described above and further purified by size-exclusion chromatography (SEC, qEVoriginal, Izon Bioscience, Cambridge, UK). Crude EV pellets were resuspended in 500 µl Dulbecco's Phosphate Buffered Saline (DPBS) and loaded onto qEV columns as per the manufacturer's instructions. The EV-containing fractions 7–9 were collected, pooled and pelleted by ultracentrifugation for 2 h at 200,000 x g (Beckman Optima LE-80K Ultracentrifuge, SW60 Rotor, k-factor 84.0, Brea, USA). Total RNA was subsequently extracted from pellets using the miRNeasy Micro Kit (Qiagen, Venlo, The

Netherlands). Preparation of sequencing libraries, sequencing-by-synthesis and differential gene expression (DGE) analyses were performed as described below. For EV characterisation experiments, pellets were resuspended in 30 µl sterile-filtered DPBS or lysed in 1x RIPA buffer (Abcam, Cambridge, UK).

Next-Generation Sequencing

The applied methods were previously described [6]. Briefly, complementary DNA (cDNA) libraries were prepared from 6 µl of total RNA from arterial and venous samples using the NEBNext Multiplex Small RNA Library Prep Set for Illumina (New England Biolabs Inc., Ipswich, USA). To compensate for low RNA input and reduce the formation of primer dimers, all adaptors and primers were diluted 1:2 in nuclease-free water. After amplifying the cDNA products by PCR, the concentration of ligation products corresponding to miRNAs was determined on the 2100 Bioanalyzer using the DNA 1000 Kit (Agilent Technologies, Santa Clara, USA). Whenever available, 8 ng of each bar-coded sample were pooled, and size selection for ligation products equivalent to miRNAs was subsequently performed using 4% agarose gel electrophoresis. For samples with lower concentrations, the total amount of cDNA was used for sequencing. After purification of cDNA libraries (Monarch DNA Gel Extraction Kit, New England Biolabs Inc., Ipswich, USA) and quality control using capillary electrophoresis (2100 Bioanalyzer, DNA High Sensitivity Kit, Agilent Technologies, Santa Clara, USA), small RNA-Seq was performed in 50 cycles of single-end sequencing using the HiSeq2500 (Illumina Inc., San Diego, USA).

Data analysis

Small RNA-Seq data were processed as described previously [6]. In summary, FastQC (version 0.11.5) [9] was used to evaluate sequence quality and length distribution. Using Btrim, adaptor sequences were trimmed [10], and all reads lacking adaptors were discarded. Additionally, reads shorter than 16 nucleotides in length were excluded [11]. Reads that mapped to sequences of ribosomal RNA (rRNA) and transfer RNA (tRNA) obtained from RNAcentral were eliminated from the data set [12]. The remaining reads were aligned to miRNA sequences in the most recent version (22) of miRBase [13] and subsequently to small nucleolar RNA (snoRNA) and small nuclear RNA (snRNA) sequences from RNAcentral. Mapping was accomplished with Bowtie [14] and the "best" alignment

algorithm, allowing one mismatch for alignment to both RNAcentral and miRBase. Subsequently, DGE analyses were performed using the Bioconductor package DESeq2 (version 1.22.1) [15] for R (version 3.5.3) with the included normalisation strategy based on median ratios of mean miRNA expression and the Benjamini–Hochberg method to correct for false discovery. Setting a mean expression of ≥ 50 reads (baseMean), a log2 fold change (log2FC) |log2FC| ≥ 1 and adjusted p-value (padj) ≤ 0.05 as thresholds, no differentially expressed miRNAs were detected. To identify slightly regulated miRNAs, results from DGE analyses were filtered with less stringent criteria (baseMean ≥ 50, |log2FC| ≥ 0.5, padj ≤ 0.1).

Results were tested for normal distribution using the Shapiro-Wilk test. Data that were not normally distributed are reported as median and quartiles (Q25, Q75) and were compared using the non-parametric Mann Whitney U test. Normally distributed data were compared using two-tailed, paired Student's t-test and are reported as mean ± standard deviation (SD). A p-value ≤ 0.05 was regarded as statistically significant.

RT-qPCR

All miRNAs remaining differentially regulated after filtering the crude cell-free NGS data were tested in the same study population by RT-qPCR as described previously [16]. To identify reference candidates, we evaluated the most stably expressed miRNAs from the small RNA-Seq dataset by geNorm [17] and NormFinder [18]. Four μl RNA were used as starting material for reverse transcription (miRCURY LNA RT Kit, Qiagen, Venlo, The Netherlands). After dilution of cDNA (1:30), qPCR was performed using the miRCURY LNA SYBR Green PCR Kit. Individual miRCURY LNA miRNA PCR Assays (Qiagen, Venlo, The Netherlands) were purchased for miR-223-3p, miR-379-5p, miR-493-5p and miR-542-3p as well as two reference miRNAs (miR-30d-5p and miR-30e-5p, Table 2). qPCR reactions were run on a Rotor-Gene Q thermal cycler (Qiagen, Venlo, The Netherlands). Data were normalised using the geometric mean of the reference miRNAs

and quantified relatively with the ΔΔCq method [19]. Statistical significance was tested using two-tailed, paired Student's t-test with a significance level of p ≤ 0.05.

Nanoparticle tracking analysis

Size and concentration of extracellular particles in crude and purified EV samples were determined by Nanoparticle Tracking Analysis (NTA, ZetaView PMX 110, Particle Metrix, Meerbusch, Germany). The optical layout of this device is a 90 ° laser scattering video microscope equipped with a digital camera (640 x 480 px) and a 520 nm diode laser. Two cycles of videos were recorded, each by scanning 11 distinct positions in the cell cross section applying at a frame rate of 30 fps. The temperature was adapted to 21°C for all measurements. Settings were optimised by adjusting the minimum brightness to 20, the shutter to 70 and the sensitivity to 85%. Post-acquisition parameters were set to min size 5 and max size 1000. All samples were diluted to an appropriate concentration for particle measurements in sterile-filtered DPBS. Videos were analysed with the ZetaView 8.04.02 software, tracking at least 500 particles per sample. At maximum three positions per sample were excluded from analysis. Original particle concentrations per ml serum were calculated as described elsewhere [20]. Statistical significance was tested using two-tailed, paired Student's t-test with a significance level of p ≤ 0.05.

Transmission electron microscopy

Two μl of crude and purified EV samples were diluted 1:5 in sterile-filtered DPBS and adsorbed for 20 min onto formvar/carbon-coated 200 mesh nickel grids (Electron Microscopy Sciences, Hatfield, USA). Grids were fixed with 2 % paraformaldehyde for 20 min, washed in sterile-filtered DPBS and fixed with 1% glutaraldehyde for 5 min. Following washing in ultrapure water, negative staining was performed in 0.2 μm filtered 4% uranyl acetate (UA; Sigma-Aldrich, St. Louis, USA) for 5 min. Grids were embedded in 0.4% UA/1.8% methyl cellulose for 10 min in the dark and air-dried. Particle morphology was illustrated by Transmission Electron Microscopy (TEM) using a Zeiss EM900 (Carl Zeiss Microscopy GmbH, Jena, Germany) with a wide-angle dual speed 2KCCD camera at 80 kV.

Table 2. Mean Cq values for RT-qPCR reference genes and statistical testing for arteriovenous differences using two-tailed, paired student's t-test.

	miR-30d-5p [mean Cq ± SD]	miR-30e-5p [mean Cq ± SD]
Arterial	22.40 ± 2.05	24.65 ± 2.83
Venous	22.74 ± 2.12	25.53 ± 2.66
p-value	p = 0.48	p = 0.13

SD: standard deviation.

Western blot analysis

To assess potential differences in EV marker expression, crude EVs were precipitated from arterial and venous sera and purified by SEC as described above. Resulting pellets were subsequently lysed on ice in 30 μl 1x RIPA buffer (Abcam, Cambridge, UK) containing protease inhibitors (cOmplete Mini Protease Inhibitor Cocktail, Roche, Basel, Switzerland) for 15 min. Half the lysate was used for reducing and non-reducing SDS-PAGE, respectively. To enhance the dissolution of EVs, samples were sonicated using an ultrasonic bath three times for 1 min each. Immunoblotting was performed under reducing conditions for syntenin, alix, calnexin (CNX), apolipoprotein A1 (ApoA1) and serum albumin and non-reducing conditions for CD63 and CD81. Lysates were either heated for 10 min at 70°C in reducing Laemmli buffer (Bio-Rad, Hercules, USA) containing β-Mercaptoethanol (Sigma-Aldrich, St. Louis, USA), or incubated for 20 min at RT in non-reducing Laemmli buffer (Bio-Rad, Hercules, USA). After separation on NuPAGE 4–12% Bis-Tris Gels (Invitrogen, Carlsbad, USA), proteins were transferred to 0.45 μm nitrocellulose membranes (GE Healthcare Life Sciences, Chicago, USA). Membranes were blocked with 1% non-fat milk powder in phosphate buffered saline with tween for 1 h at RT and incubated with primary antibodies at 4°C overnight. After triplicate washing with blocking buffer, appropriate horseradish peroxidase coupled secondary antibodies were added to the membranes for 1 h at RT. Following another three washing steps, blots were imaged using the Clarity Western ECL Blotting Substrate Kit (Bio-Rad, Hercules, USA). Primary antibodies were purchased from Abcam (rabbit anti-Syntenin clone EPR8102, 1:5,000, ab57113, 1:250; mouse anti-CD63, clone TS63, ab59479, 1:500; rabbit anti-ALIX clone EPR15314-33, ab186728, 1:1000; mouse anti-CD81, clone M38, ab79559, 1:1000; rabbit anti-ApoA1, clone EP1368Y, ab52945, 1:1000; mouse anti-Human Serum Albumin, clone 1A9, ab37989, 1:2000, Cambridge, UK) and Biomol (goat anti-Calnexin, WA-AF1179a, 1:2,500, Hamburg, Germany). Secondary antibodies were obtained from Abcam (goat anti-Mouse HRP, ab97040, 1:10,000, goat anti-Rabbit, ab97080, 1:10,000, rabbit anti-Goat HRP, ab97105, 1:10,000, Cambridge, UK). HEK293 cell lysate (OriGene, LY500001, Rockville, USA, 10 μg), recombinant human ApoA1 (Abcam, ab50239, Cambridge, UK, 50 ng), and HepG2 cell lysate (Abcam, ab7900, Cambridge, UK, 30 μg) were used as positive controls.

Ethics approval and consent to participate

Approval of the study was granted by the Ethics Committee of the Medical Faculty of the Ludwig-Maximilians-University of Munich under Protocol #551-14. All samples from this study were anonymised during analyses. The study was conducted in accordance with approved guidelines and written informed consent for publication of blinded individual person's data was obtained from each participant.

Results

RNA profiles and sequencing library composition of arterial and venous samples are highly similar

Using capillary electrophoresis to characterise crude cell-free and EV RNA profiles, major differences in RNA quantities between individual patients, but not arterial and venous specimens, were revealed. The median amount of total RNA in crude EVs precipitated from 1 ml serum was 16.32 (10.58–29.95) ng for arterial specimens and 11.95 (9.54–26.2) ng for venous ones, and there was no statistically significant difference between the groups (p = 0.61). In EVs additionally purified by SEC, the median yield was 2.01 (1.40–2.78) ng and 1.53 (0.95–3.14) ng for arterial and venous EVs, respectively. RNA yields from arterial and venous EVs were not significantly different (p = 0.53).

As evidenced by high Phred scores, technical sequencing quality was excellent for all arterial and venous libraries. Phred scores were 38.06 (29.38–38.97) for arterial and 38.02 (28.56–38.98) for venous crude cell-free samples, respectively. In the experiments using additionally purified EVs, Phred scores were 39.12 (39.06–39.15) for arterial EVs and 39.12 (39.02–39.15) for venous EVs. For crude cell-free samples, library sizes as well as proportions of miRNA reads were very similar for specimens from both sampling sites (Figure 1(a)). Arteriovenous differences were not statistically different for either library sizes (p = 0.69) or number of mapped miRNAs (p = 0.90). When comparing library sizes of crude and purified samples, there were no significant differences for arterial (p = 0.88) or venous (p = 0.89) samples. With the caveat that different RNA isolation kits were used for crude and purified EVs, the latter yielded significantly lower numbers of miRNA reads for both arterial (p = 1.14E-6) and venous (p = 4.72E-8) specimens (Figure 1(b)). Within purified EVs, neither library sizes (p = 0.39) nor miRNA reads (p = 0.66) were significantly different between arterial and venous samples.

These apparently sample type-specific differences were further substantiated in the detailed mapping statistics (Figure 2). Purified EVs presented lower
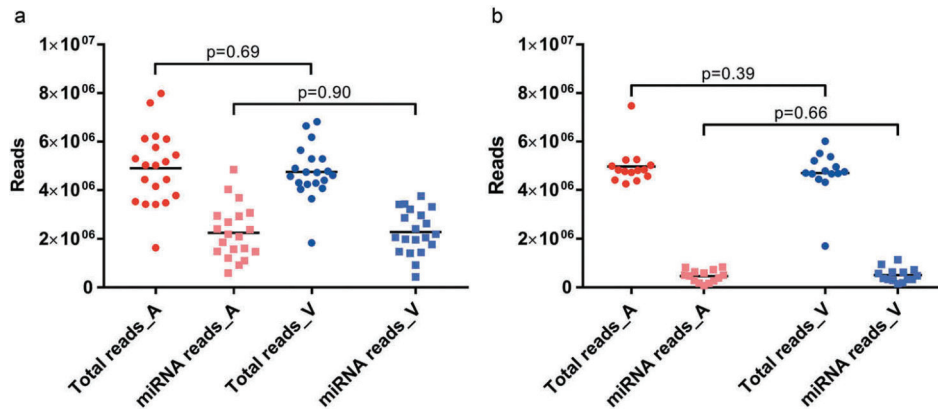
Figure 1. Library sizes (dots) and mapped miRNA reads (squares) for arterial (red) and venous (blue) crude cell-free samples (a) and samples additionally purified by SEC (b). All data are absolute numbers of reads. Lines indicate mean per-group read counts.
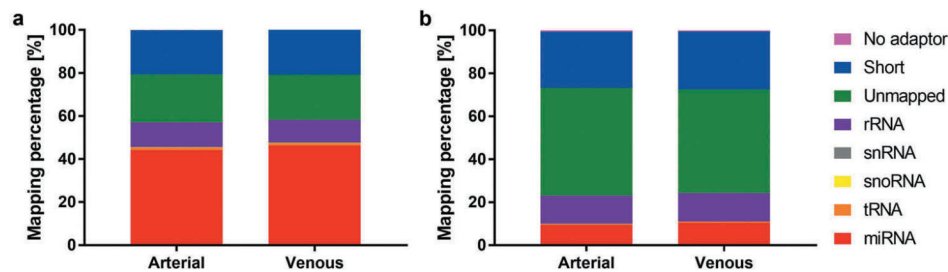

Figure 2. Mapping distribution for crude cell-free samples (a) and samples additionally purified by SEC (b). Statistics of reads mapped to major classes of non-coding RNAs. Read counts are visualised as relative frequencies of total library sizes. Mapping rates for miRNAs were 44.20 ± 9.96% (arterial crude samples), 46.39 ± 11.46% (venous crude samples), 9.51 ± 5.03% (arterial purified EVs) and 10.48 ± 4.55% (venous purified EVs).

frequencies of miRNA mapping and an increased share of reads mapping to rRNA and reads that did not align to any of the major small RNA classes (miRNA, tRNA, snoRNA, snRNA). Relative miRNA frequencies were 44.20 ± 9.96% (arterial crude cell-free samples), 46.39 ± 11.46% (venous crude cell-free samples), 9.51 ± 5.03% (arterial purified EVs) and 10.48 ± 4.55% (venous purified EVs). There were no apparent arteriovenous differences in small RNA mapping for crude cell-free (Figure 2(a)) or purified (Figure 2(b)) samples.

Arterial and venous miRNA profiles overlap significantly in crude and purified samples

Overall miRNA expression was first assessed in exploratory data analysis. In both sample types, arterial and venous miRNA profiles correlated extremely well (Figure 3). Coefficients of determination for all detected miRNAs were 0.9923 and 0.9992 in crude (Figure 3(a)) and purified (Figure 3(c)) samples, respectively. The same stringent correlation was observed for miRNAs with lower expression levels (<

1E4 reads) in both crude (0.9948, Figure 3(b)) and purified (0.9943, Figure 3(d)) samples.

Unsupervised clustering of miRNA expression further highlighted similarities between arterial and venous samples. As visualised by principal component analysis (Figure 4(a and c)), expression profiles in arterial and venous specimens overlapped considerably for both crude cell-free samples and purified EVs. In hierarchical clustering analysis, arterial and venous samples did not cluster systematically. While crude EVs clustered by patient ID rather than sampling site, this trend was less pronounced for additionally purified samples (Figure 4(b and d)), still indicating that individual person-to-person variation might be more pronounced than the variability introduced by sampling arterial or venous blood. This hypothesis was further strengthened as the variability of highly expressed miRNAs in arterial and venous samples within patients was generally lower than their variability in arterial and venous samples across patients for both crude cell-free samples and purified EVs (Figure 5).

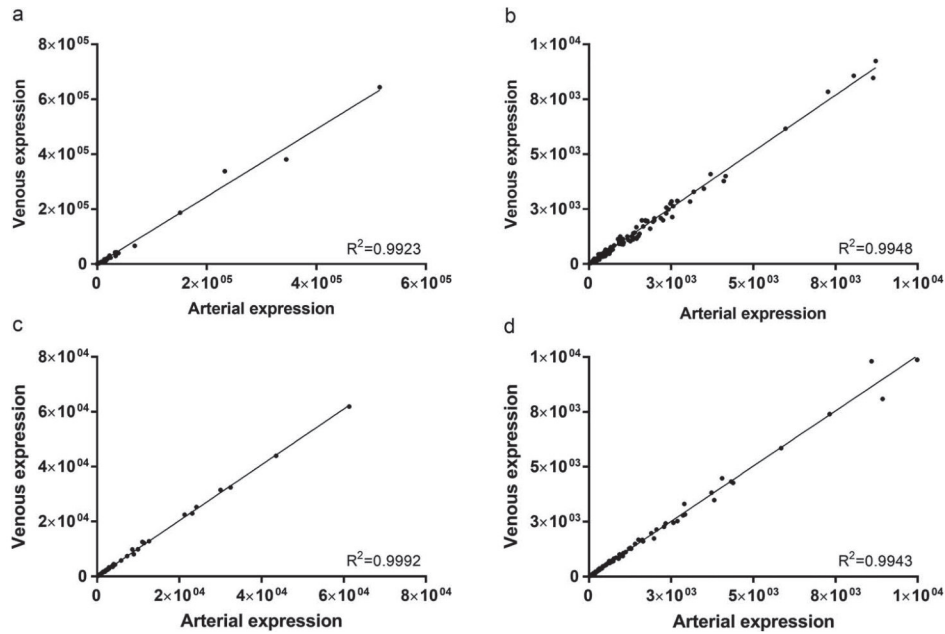Applying our standard stringent DGE filtering criteria (baseMean ≥ 50, |log2FC| ≥ 1 and padj ≤ 0.05) to

Figure 3. Correlation of arterial and venous miRNA expression in crude cell-free samples for all miRNAs (R^2 = 0.9923, a) and miRNAs with a mean expression < 1E4 reads (R^2 = 0.9948, b). Similarly, in samples purified by SEC, correlation of arterial and venous miRNA expression was extremely high for all miRNAs (R^2 = 0.9992, c) and miRNAs with a mean expression < 1E4 reads (R^2 = 0.9943, d). All data are mean DESeq2-normalised read counts for arterial and venous samples (n = 20 for crude and n = 14 for purified samples, respectively).

expression profiles in crude cell-free samples, no significantly regulated miRNAs were detected. Only with less stringent filtering criteria (baseMean ≥ 50, |log2FC| ≥ 0.5, padj ≤ 0.1) could we identify a subset of four miRNAs (miR-223-3p, miR-379-5p, miR-493-5p, miR-542-3p) to be differentially expressed (Figure 6(a)). Although all four miRNAs displayed an overall trend towards higher arterial expression, contradictory higher venous expression was detected in individual specimens. With an upregulation of 1.60-fold in arterial samples, miR-493-5p displayed the largest regulation of all miRNAs. Out of the four upregulated miRNAs, only miR-493-5p was significantly (p = 1.4E-3) higher expressed in arterial specimens (fold change 2.37) in the subsequent RT-qPCR validation (Figure 6(b)). In SEC-purified EVs, no miRNAs with significant arteriovenous differences were detected using either set of filtering criteria detailed above. Additionally, none of the other non-coding RNA classes assessed in this study (rRNA, snRNA, snoRNA, tRNA) displayed any significant expression differences between samples from arterial and venous sera for either crude or purified EVs. In summary, patient-specific inter-sample variation was high, while overall differences in arterial versus venous samples were marginal. This implies that in our cohort, small RNA-Seq data from both crude and purified EVs were not able to distinguish between arterial and venous serum samples.

Extracellular particles and EVs in arterial and venous sera display eminently comparable physiochemical characteristics

The concentration, size and morphology of extracellular particles in crude preparations and purified EVs were assessed to investigate potential arteriovenous differences. Nanoparticle tracking analysis revealed that arterial crude and purified EVs were marginally smaller, albeit with size differences bordering on the margin of error for NTA technologies [21]. Extracellular particles in crude arterial and venous samples had mean diameters of 113.20 ± 8.30 nm and 117.15 ± 6.20 nm and median diameters of 97.85 ± 8.02 nm and 101.27 ± 6.20 nm, respectively (Figure 7(a)). Particle concentrations were 6.71E11 ± 4.53E11 particles/ml serum in arterial and 7.27E11 ± 4.33E11 particles/ml serum in venous crude specimens (Figure 7(c)). Purified EVs had mean diameters of 138.54 ± 10.18 nm (arterial) and 147.54 ± 6.84 nm (venous) and median diameters of 123.78 ± 9.72 nm (arterial) and 132.00 ± 6.22 nm (venous, Figure 7(b)). NTA of purified EVs revealed overall lower particle concentrations compared to crude preparations. Arterial and venous purified EVs had particle concentrations of 1.30E+09 ± 1.13E+09 particles/ml serum and 1.38E+09 ± 8.18E+08 particles/ml serum, respectively (Figure 7(d)). Using electron microscopy, we detected EV-like particles
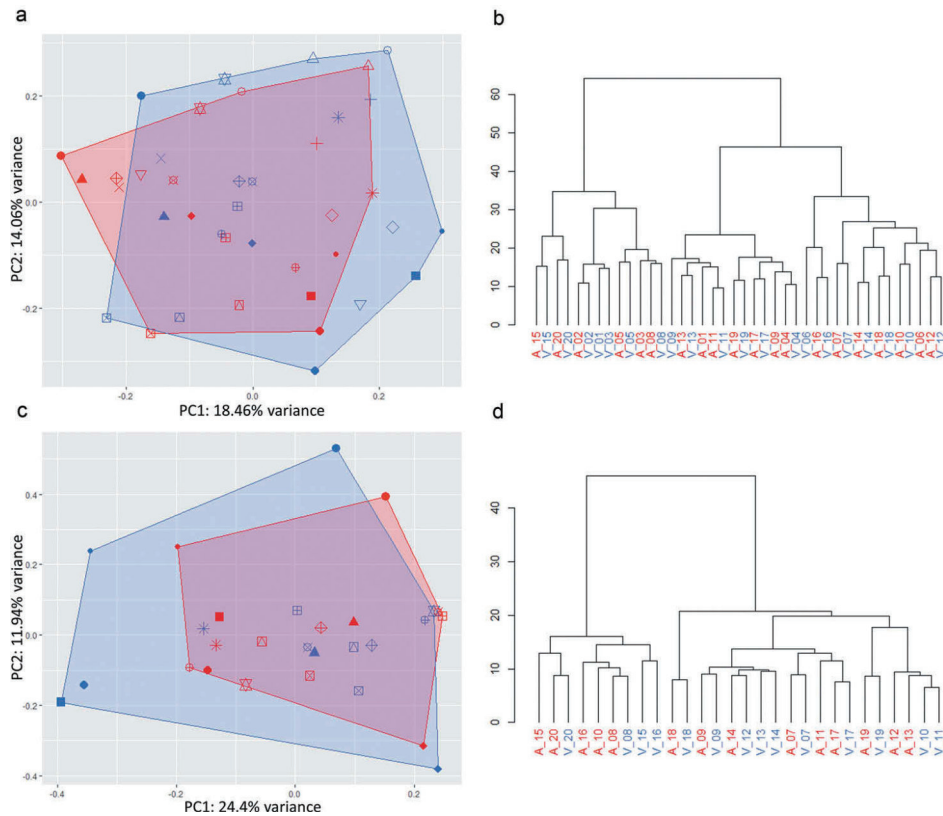
Figure 4. Unsupervised clustering of miRNA expression in crude (top panel) and SEC-purified (bottom panel) samples. Samples are colour-coded in red (arterial) and blue (venous). Patients are displayed by individual symbols. In principal component analysis, arterial and venous expression profiles of crude (a) and purified (c) samples displayed significant overlap. In hierarchical clustering, individual specimens in crude samples generally clustered by patient ID rather than sampling site (b), while purified EVs clustered by patient ID to a lower degree (d).
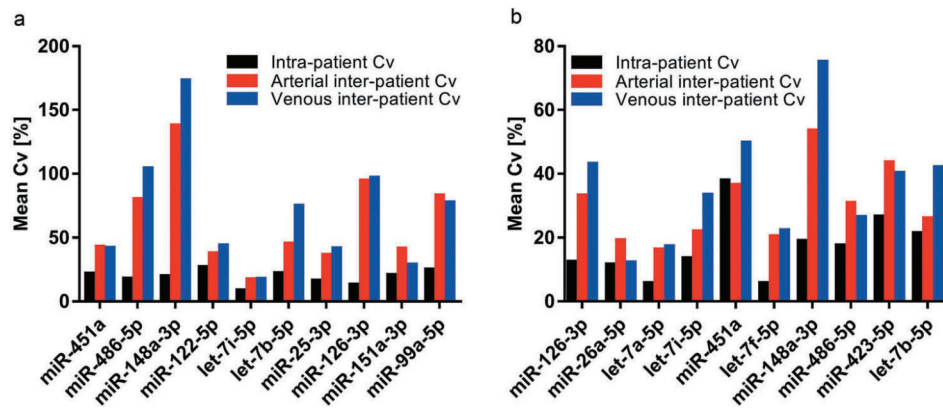
Figure 5. Variability of the top ten most abundant miRNAs within and across patients for crude cell-free samples (a) and additionally purified samples (b). Black bars: Mean intra-patient coefficient of variation (Cv) of arterial and venous samples. Red and blue bars: Mean Cv of all arterial and venous samples across patients, respectively.

with diameters of approximately 100 nm in arterial and venous samples for both isolation protocols (Figure 7(e and f)). SEC-purified samples were analysed by immunoblotting to substantiate potential arteriovenous differences in EV protein markers (Figure 7(g)). While the commonly used EV protein markers alix, CD63, syntenin and CD81 were equally detected in arterial and venous samples, the negative marker CNX was not detected, indicating the absence of contamination with cellular fragments. However, contaminations of by SEC-purified
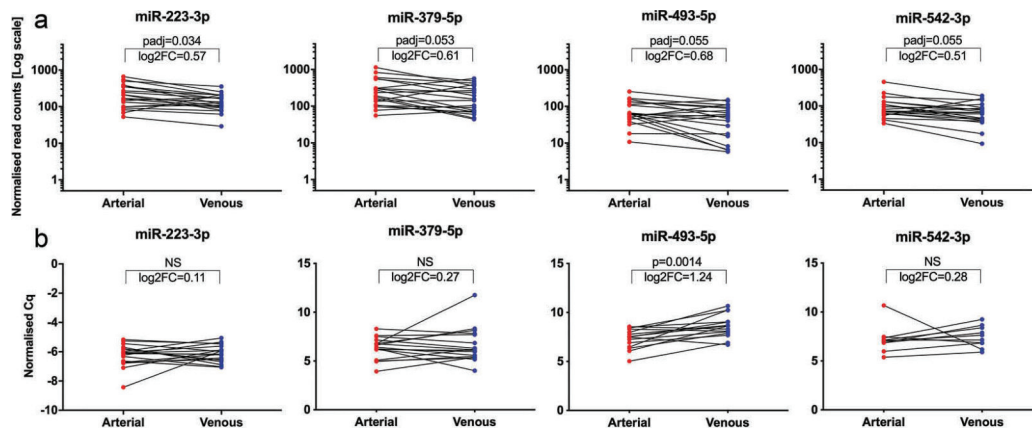
Figure 6. Significantly regulated miRNAs from NGS and validation by RT-qPCR. Illustration of four miRNAs differentially regulated between arterial and venous crude samples from NGS (a). Normalised read counts were plotted for each paired arterial and venous specimen. Individual changes in miRNA expression are indicated by lines. All miRNAs displayed a slight overall tendency of higher expression in arterial samples, albeit with reversed trends for some patients. padj: adjusted p-value; log2FC: log2 fold change. Illustration of normalised Cq values from the subsequent RT-qPCR validation (b). Only miR-493-5p showed significantly higher expression in arterial samples. Specimens which did not proper amplify during RT-qPCR were removed from the data set, and only matched arterial and venous samples were included for analyses. miR-223-3p, n = 19; miR-379-5p, n = 17; miR-493-5p, n = 15; miR-542-3p, n = 10; NS: not significant.

samples with high-density lipoproteins (ApoA1) and highly abundant serum proteins (albumin) were present to the same extent in EVs isolated from arterial and venous blood. Since SDS-PAGE input was normalised to serum volume (instead of EV protein amount), differently pronounced protein bands were detected due to varying levels of marker proteins across individual patients. Our data indicate that specimens from arterial and venous sera have highly similar biological characteristics on both the level of overall extracellular particles and the level of purified EVs.

Discussion

As central players in liquid biopsies, EVs hold great promise for diagnosis, prognosis and therapeutic guidance. However, the isolation, study and characterisation of EVs is often challenging, as they are small-sized, and only limited quantities can usually be obtained from patient-derived samples [22]. To avoid the influence of confounding variables on blood miRNA profiles, collection tubes, preparation, handling and storage of samples should be standardised [23]. The formation of platelet-derived EVs was shown to occur as a response to platelet activation [24] induced by surface contact, pressure and high shear stress [25,26] during blood sampling. Therefore, it is recommended to standardise needle bore size, diameter, length of the sampling system and sampling site [26]. Since a significant impact on miRNA expression profiles has been shown for different EV isolation methods

[6] and sequencing methodologies [27], these parameters should also be considered, especially when combining multiple datasets. While cell-free miRNAs that robustly indicate disease states are still valuable biomarker candidates regardless of their association with EVs, and impurities in EV preparations were shown to have little impact on downstream nucleic acid quantification [28], specific diseases and clinical questions might require additional validation using more EV-specific isolation methods such as density gradient centrifugation. As demonstrated previously, serum EV precipitates contain a significant amount of cell-free proteins, which might include well-known carriers of circulating miRNAs such as argonaute 2 or lipoprotein particles [29–31]. We therefore characterised miRNA profiles in both crude and additionally purified samples to assess potential carrier-specific arteriovenous differences. As some lipoproteins overlap in size with EVs [32], samples purified by SEC still contain a certain amount of contamination [33], which was also shown in the current study. Despite previously reported variables that can influence the diagnostic potential of EVs, only minor differences between paired arterial and venous miRNA profiles were observed in samples with lower and higher purity, and extracellular particles from both compartments appeared to have highly similar biological properties.

Since blood flows from pulmonary to systemic circulation, it is conceivable that arterial blood is enriched with biomolecules from lung cells or the left ventricle when compared to venous blood. In our study,
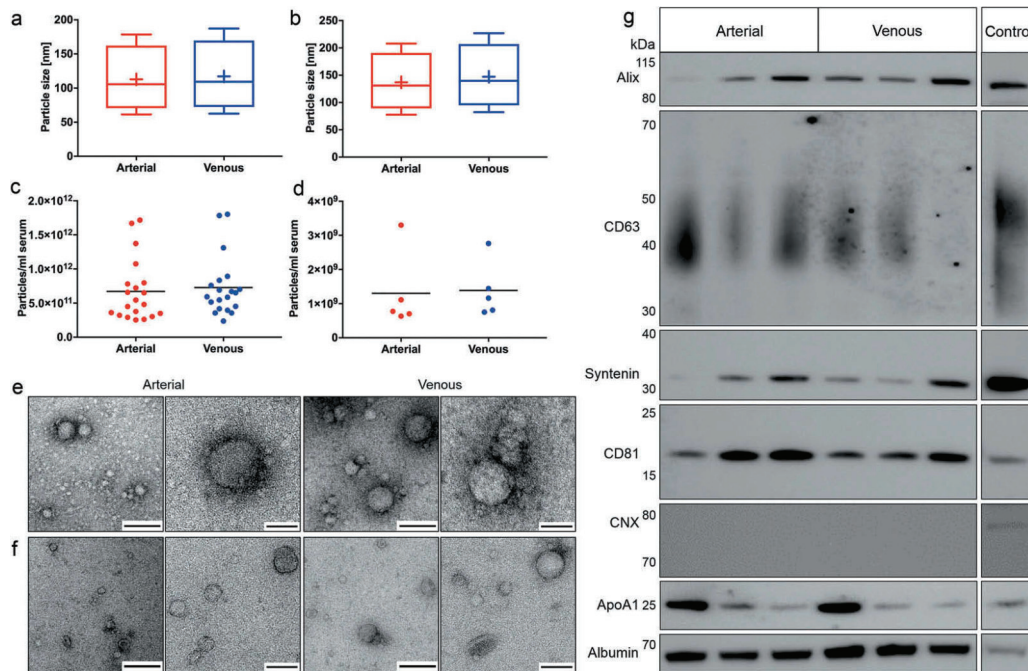
Figure 7. Biological characterisation of crude and purified EVs. Characterisation of particle size distributions by NTA in crude (n = 20, a) and purified samples (n = 5, b). Data are displayed as boxplots from the 10th to the 90th percentile, showing median (line) and mean (+) particle diameters. Median diameters of crude EVs from arterial and venous serum did not differ significantly (p = 0.056), while mean diameters of arterial particles were significantly smaller (p = 0.040). Particle diameters in additionally purified samples were also significantly smaller for arterial samples (median: p = 0.034, mean: p = 0.031). Depiction of particle concentrations/ml serum by NTA in crude (n = 20, c) and purified samples (n = 5, d). No significant changes in particle numbers could be detected for arterial and venous crude (p = 0.059) and purified EVs (p = 0.650). Lines indicate mean. Illustration of spherical EV-like extracellular particles with a size of about 100 nm by TEM for crude (e) and purified samples (f). Matched specimens from n = 3 individuals were imaged for both isolation protocols. Scale bar 1st and 3rd column: 250 nm; Scale bar 2nd and 4th column: 100 nm. Immunoblot profiling of SEC-purified samples (g). Arterial and venous samples were positive for EV-specific protein markers (alix, CD63, syntenin and CD81). CNX could not be detected in any of the samples. All samples were positive for non-EV-enriched proteins ApoA1 and serum albumin. Results are depicted for three paired arterial and venous biological replicates. HEK293 cell lysate was used as a positive control for alix, CD63, syntenin, CD81 and CNX. Recombinant ApoA1 and HepG2 cell lysate served as a positive control for ApoA1 and serum albumin, respectively.

however, we only found a minor subset of slightly differentially expressed miRNAs, while the majority of arterial miRNAs matched the expression levels in venous samples. The fact that different RNA extraction kits were used for NGS and RT-qPCR in the experiments on crude samples might have resulted in divergent miRNA recovery [34], and therefore could have affected results for the technical validation of candidate miRNAs.

As light scattering-based methods of EV quantification are prone to detecting nonvesicular particles such as lipoproteins, which outnumber circulating EVs by orders of magnitude, they most likely overestimate EV concentrations [32]. In accordance with previous findings by our group [6], the reduced frequencies of miRNA mapping in SEC-EVs observed in this study might therefore be due to the removal of nonvesicular miRNA carriers or larger EVs by the additional purification step. While it seems likely that lower miRNA

yields in purified samples stem from the fact that the less specific precipitation method also captured miRNAs not associated with EVs, it needs to be mentioned that different RNA extraction kits were used in experiments on crude preparations and SEC-EVs. Technical biases brought about by the respective extraction chemistry might therefore have partly contributed to the quantitative miRNA differences between the two sample types used in this study.

Emphasis should also be put on the fact that we only studied serum, but not plasma samples. As a by-product of coagulation, it has been shown that serum RNA concentrations might be higher, and that sera are enriched in cell-free platelet-derived miRNAs when compared to the corresponding plasma samples [35]. Therefore, performing the same experiments using platelet-free plasma might result in arterial and venous differences, which possibly have been obscured due to high platelet-derived RNA content in the serum samples from our study.

Another limitation of our study results from the fact that we only studied patients with severe heart disease, and this conclusion may not be applicable to all individuals and all disorders. Additional arteriovenous comparisons need to be performed in patients showing specific pathologies (e.g. patients with severe pulmonary disease). Nevertheless, it seems feasible to use either arterial or venous serum in the majority of miRNA-based EV biomarker studies with comparable results.

ORCID

Stefanie Hermann http://orcid.org/0000-0002-6274-5919
Dominik Buschmann http://orcid.org/0000-0003-0460-6459
Benedikt Kirchner http://orcid.org/0000-0003-3878-0148
Melanie Borrmann http://orcid.org/0000-0002-0741-616X
Florian Brandes http://orcid.org/0000-0003-3741-287X
Marlene Reithmair http://orcid.org/0000-0002-9113-9643
Gustav Schelling http://orcid.org/0000-0002-6538-0652
Michael W. Pfaffl http://orcid.org/0000-0002-3192-1019

References

[1] Shah R, Patel T, Freedman JE. Circulating extracellular vesicles in human disease. N Engl J Med. 2018;379:958–966.

[2] Mokken FC, van der Waart FJM, Henny CP, et al. Differences in peripheral arterial and venous hemorheologic parameters. Ann Hematol. 1996;73:135–137.

[3] Bai L, Ma J, Wang Y, et al. MicroRNAomes of porcine arterial and venous blood. J Anim Vet Adv. 2014;13:21–27.

[4] Xu W, Zhou Y, Xu G, et al. Transcriptome analysis reveals non-identical microRNA profiles between arterial and venous plasma. Oncotarget. 2017;8:28471–28480.

[5] Kelly E, Owen C, Abraham A, et al. Comparison of arterial and venous blood biomarker levels in chronic obstructive pulmonary disease. F1000 Research. 2013;2:114.

[6] Buschmann D, Kirchner B, Hermann S, et al. Evaluation of serum extracellular vesicle isolation methods for profiling miRNAs by next-generation sequencing. J Extracell Vesicles. 2018;7:1481321.

[7] Thery C, Witwer KW, Aikawa E, et al. Minimal information for studies of extracellular vesicles 2018 (MISEV2018): a position statement of the international society for extracellular vesicles and update of the MISEV2014 guidelines. J Extracell Vesicles. 2018;7:1535750. Epub 2019/ 01/15.

[8] Consortium E-T, Van Deun J, Mestdagh P, et al. EV-TRACK: transparent reporting and centralizing knowledge in extracellular vesicle research. Nat Methods. 2017;14:228.

[9] Andrews S. FastQC: a quality control tool for high throughput sequence data. 2010. Available online at: http://www.bioinformatics.babraham.ac.uk/projects/fastqc

[10] Kong Y. Btrim: a fast, lightweight adapter and quality trimming program for next-generation sequencing technologies. Genomics. 2011;98:152–153.

[11] Buschmann D, Haberberger A, Kirchner B, et al. Toward reliable biomarker signatures in the age of liquid biopsies - how to standardize the small RNA-Seq workflow. Nucleic Acids Res. 2016;44:5995–6018.

[12] RN C, Petrov AI, Kay SJE, et al. RNAcentral: an international database of ncRNA sequences. Nucleic Acids Res. 2015;43:D123–D9.

[13] Kozomara A, Griffiths-Jones S. miRBase: annotating high confidence microRNAs using deep sequencing data. Nucleic Acids Res. 2014;42:D68–D73.

[14] Langmead B, Trapnell C, Pop M, et al. Ultrafast and memory-efficient alignment of short DNA sequences to the human genome. Genome Biol. 2009;10:R25.

[15] Love MI, Huber W, Anders S. Moderated estimation of fold change and dispersion for RNA-seq data with DESeq2. Genome Biol. 2014;15:550.

[16] Reithmair M, Buschmann D, Marte M, et al. Cellular and extracellular miRNAs are blood-compartment-specific diagnostic targets in sepsis. J Cell Mol Med. 2017;21:2403–2411.

[17] Vandesompele J, De Preter K, Pattyn F, et al. Accurate normalization of real-time quantitative RT-PCR data by geometric averaging of multiple internal control genes. Genome Biol. 2002;3:Research0034.

[18] Andersen C, Jensen J, TF O. Normalization of real-time quantitative reverse transcription-PCR data: a model-based variance estimation approach to identify genes suited for normalization, applied to bladder and colon cancer data sets. Cancer Res. 2004;64:5245–5250.

[19] Livak K, Schmittgen T. Analysis of relative gene expression data using real-time quantitative PCR and the 2 (-Delta Delta C(T)) method. Methods. 2001;25:402–408.

[20] Eitan E, Green J, Bodogai M, et al. Age-related changes in plasma extracellular vesicle characteristics and internalization by leukocytes. Sci Rep. 2017;7:1342.

[21] Bachurski D, Schuldner M, Nguyen PH, et al. Extracellular vesicle measurements with nanoparticle tracking analysis - an accuracy and repeatability

comparison between NanoSight NS300 and ZetaView. J Extracell Vesicles. 2019;8: 1596016. Epub 2019/ 04/17.

[22] Ramirez MI, Amorim MG, Gadelha C, et al. Technical challenges of working with extracellular vesicles. Nanoscale. 2018;10:881–906.

[23] Glinge C, Clauss S, Boddum K, et al. Stability of circulating blood-based MicroRNAs - Pre-Analytic methodological considerations. PLoS One. 2017;12:e0167969.

[24] Cauwenberghs S, Feijge MA, Harper AG, et al. Shedding of procoagulant microparticles from unstimulated platelets by integrin-mediated destabilization of actin cytoskeleton. FEBS Lett. 2006;580:5313–5320.

[25] Reininger AJ, Heijnen HF, Schumann H, et al. Mechanism of platelet adhesion to von Willebrand factor and microparticle formation under high shear stress. Blood. 2006;107:3537–3545.

[26] Lance MD, Henskens YM, Nelemans P, et al. Do blood collection methods influence whole-blood platelet function analysis? Platelets. 2013;24:275–281.

[27] Coenen-Stass AML, Magen I, Brooks T, et al. Evaluation of methodologies for microRNA biomarker detection by next generation sequencing. RNA Biol. 2018;15: 1133–1145. Epub 2018/ 09/19.

[28] Quek C, Bellingham SA, Jung CH, et al. Defining the purity of exosomes required for diagnostic profiling of small RNA suitable for biomarker discovery. RNA Biol. 2017;14:245–258.

[29] Arroyo JD, Chevillet JR, Kroh EM, et al. Argonaute2 complexes carry a population of circulating microRNAs independent of vesicles in human plasma. Proc Natl Acad Sci U S A. 2011;108: 5003–5008. Epub 2011/ 03/ 09.

[30] Vickers KC, Palmisano BT, Shoucri BM, et al. MicroRNAs are transported in plasma and delivered to recipient cells by high-density lipoproteins. Nat Cell Biol. 2011;13: 423–433. Epub 2011/ 03/23.

[31] Turchinovich A, Weiz L, Langheinz A, et al. Characterization of extracellular circulating microRNA. Nucleic Acids Res. 2011;39:7223–7233.

[32] Sodar BW, Kittel A, Paloczi K, et al. Low-density lipoprotein mimics blood plasma-derived exosomes and microvesicles during isolation and detection. Sci Rep. 2016;6:24316. Epub 2016/ 04/19.

[33] Karimi N, Cvjetkovic A, Jang SC, et al. Detailed analysis of the plasma extracellular vesicle proteome after separation from lipoproteins. Cell Mol Life Sci. 2018;75: 2873–2886. Epub 2018/ 02/15.

[34] Tan GW, Khoo AS, Tan LP. Evaluation of extraction kits and RT-qPCR systems adapted to high-throughput platform for circulating miRNAs. Sci Rep. 2015;5:9430.

[35] Wang K, Yuan Y, Cho JH, et al. Comparing the MicroRNA spectrum between serum and plasma. PLoS One. 2012;7:e41561.

Appendix IV

Contribution by Stefanie Hermann:

- Project administration
- Manuscript conceptualization
- Writing – original draft
- Investigation – laboratory experiments
- Formal analysis and data curation
- Visualization

Stefanie Hermann

Prof. Dr. Michael W. Pfaffl

ORIGINAL ARTICLE

WILEY

Diagnostic potential of circulating cell-free microRNAs for community-acquired pneumonia and pneumonia-related sepsis

Stefanie Hermann[1] [iD] | Florian Brandes[2] [iD] | Benedikt Kirchner[1] [iD] | Dominik Buschmann[1] [iD] | Melanie Borrmann[2] | Matthias Klein[3] | Stefan Kotschote[4] | Michael Bonin[4] | Marlene Reithmair[5] [iD] | Ines Kaufmann[6] | Gustav Schelling[2] | Michael W. Pfaffl[1]

[1]Division of Animal Physiology and Immunology, School of Life Sciences Weihenstephan, Technical University of Munich, Freising, Germany

[2]Department of Anesthesiology, University Hospital, Ludwig-Maximilians-University Munich, Munich, Germany

[3]Department of Neurology, University Hospital, Ludwig-Maximilians-University of Munich, Munich, Germany

[4]IMGM Laboratories GmbH, Planegg, Germany

[5]Institute of Human Genetics, University Hospital, Ludwig-Maximilians-University Munich, Munich, Germany

[6]Department of Anesthesia, Klinikum Neuperlach, Munich City Hospitals, Munich, Germany

Correspondence
Stefanie Hermann, Animal Physiology & Immunology, Technical University Munich, Weihenstephaner Berg 3, 85354 Freising-Weihenstephan, Germany.
Email: stefanie.hermann@tum.de

Abstract

Cell-free microRNAs (miRNAs) are transferred in disease state including inflammatory lung diseases and are often packed into extracellular vesicles (EVs). To assess their suitability as biomarkers for community-acquired pneumonia (CAP) and severe secondary complications such as sepsis, we studied patients with CAP (n = 30), sepsis (n = 65) and healthy volunteers (n = 47) subdivided into a training (n = 67) and a validation (n = 75) cohort. After precipitating crude EVs from sera, associated small RNA was profiled by next-generation sequencing (NGS) and evaluated in multivariate analyses. A subset of the thereby identified biomarker candidates was validated both technically and additionally by reverse transcription quantitative real-time PCR (RT-qPCR). Differential gene expression (DGE) analysis revealed 29 differentially expressed miRNAs in CAP patients when compared to volunteers, and 25 miRNAs in patients with CAP, compared to those with sepsis. Sparse partial-least discriminant analysis separated groups based on 12 miRNAs. Three miRNAs proved as a significant biomarker signature. While expression levels of miR-1246 showed significant changes with an increase in overall disease severity from volunteers to CAP and to sepsis, miR-193a-5p and miR-542-3p differentiated patients with an infectious disease (CAP or sepsis) from volunteers. Cell-free miRNAs are potentially novel biomarkers for CAP and may help to identify patients at risk for progress to sepsis, facilitating early intervention and treatment.

KEYWORDS
biomarker signature, cell-free microRNAs, community-acquired pneumonia, extracellular vesicles, sepsis, small RNA sequencing

Stefanie Hermann and Florian Brandes should be considered joint first author.

1 | INTRODUCTION

According to the World Health Organization's global health estimates, lower respiratory infections are the fourth leading global cause of deaths and the most deadly communicable disease, causative for three million deaths worldwide in 2016.[1] With the current SARS-CoV-2 pandemic, this fact has very recently been brought to worldwide attention. Data from a prospectively followed multicentre trial revealed an overall mortality of 17.3% for patients with CAP within an 18 months follow-up.[2] Despite the introduction of antibiotic therapies in the 1950s, pneumonia mortality has not decreased substantially,[3] and sepsis, septic shock or acute pulmonary failure (eg acute respiratory distress syndrome, ARDS) are frequent secondary complications.[4,5]

At present, initial pneumonia diagnosis is based on suggestive clinical features such as fever, shortness of breath, sputum production, cough and leukocytosis supplemented by evidence of pulmonary consolidation found in chest X-rays or computed tomography (CT) if required in order to arrive at a final diagnosis. To improve management and treatment of pneumonia, supporting microbiological and virological tests from throat swabs, sputum or blood cultures might be indicated to identify the responsible pathogen(s) and to allow targeted antimicrobial or antiviral therapy. This can be supported by urine antigen tests, molecular assays, serology or bronchoscopy in selected cases. Blood biomarkers such as procalcitonin (PCT), C-reactive protein (CRP), Interleukin-6 (IL-6), white blood cell count and lactate[6,7] are commonly used to differentiate between patients with pneumonia and individuals with pneumonia at risk for sepsis. Scoring systems including the *Confusion, Blood Urea, Respiratory Rate, Blood Pressure, Age ≥ 65* (CURB-65) score [8] are applied in patients with pneumonia to simplify site-of-care decisions such as outpatient treatment *vs.* hospital and intensive care unit (ICU) admission and to facilitate the decision whether to prescribe antibiotics or not.[6] However, the sensitivity and specificity of these scoring systems are limited.[9] The reliable diagnosis of pneumonia can be a time-consuming and complex process. It is particularly challenging in high-risk groups[10] such as the elderly or infants, which often present with atypical symptoms and are at an increased risk for sepsis or acute pulmonary failure as secondary complications.

At present, there are no valid and reliable biomarkers allowing an on-site diagnosis and the identification of high-risk patients.

Circulating EVs are a heterogeneous group of small-sized membranous vesicles that are loaded with biomolecules, particularly proteins, lipids and diverse types of nucleic acids and are exchanged in cell-cell signalling during various physiological and pathological processes.[11] EV-associated miRNAs are key regulators in the pathogenesis of infectious and non-infectious pulmonary disorders.[12-15] Therefore, differential miRNA expression in EV samples from liquid biopsies may indicate the presence of an inflammatory lung disease and discriminate between different disease stages or even predict the course of the disease.[16,17] miRNAs might reflect progression from physical health, to mild and more severe forms of pneumonia.[18] Additionally, EVs from sepsis patients contain miRNAs and messenger RNAs (mRNAs) related to disease-associated pathways, such as inflammatory response, oxidative stress and cell cycle regulation.[19]

Therefore, extracellular miRNAs might be attractive diagnostic biomarkers for pulmonary inflammation and prognostic indicators for disease progression.

In the present study, we identified cell-free miRNA biomarker candidates by high-throughput small RNA sequencing (small RNA-seq) to differentiate between patients with CAP and healthy volunteers, and to distinguish CAP patients from those with sepsis. The candidate biomarker signature was first technically validated by RT-qPCR in the same training cohort of individuals and subsequently confirmed in a second, independent validation cohort.

2 | METHODS

2.1 | Study population

A total of 142 individuals were studied. Of those, 30 patients had CAP, 65 had sepsis and 47 healthy volunteers served as controls. The samples were subdivided into a training and a validation cohort. The training cohort included 67 individuals: twelve had CAP, 28 had sepsis (23 patients were in septic shock) and 27 were volunteers. The validation cohort consisted of 75 individuals: 18 with CAP, 37 with sepsis (30 patients were in septic shock) and 20 were volunteers. Patients with CAP were recruited consecutively from the emergency room of the Munich University academic centre located at the Ludwig-Maximilians-Universität (LMU) hospital. Sepsis patients were enlisted serially from the ICUs of the LMU hospital and the Neuperlach Community Hospital of Munich. Healthy volunteers were enrolled by advertisement and from hospital staff. Inclusion and exclusion criteria for the study subgroups are presented in detail in Table S1 of the online supplement.

CAP was defined as the presence of clinical symptoms such as fever, cough and respiratory impairment in addition to a CURB-65 score for pneumonia severity ≥1[8] and the demonstration of pulmonary infiltrates on chest X-rays or CT scans according to the *Clinical Practice Criteria of the American Thoracic Society of America* (2019 version).[20] Sepsis was defined in agreement to the updated consensus definition of the *Third International Task Force for Sepsis and Septic Shock* (Sepsis-3)[21] and diagnosed by using all available information (including imaging, antibiotic response and surgical findings). The final diagnosis of sepsis was made by experienced ICU and emergency room clinicians without prior knowledge of the results of the molecular studies.

The PCT plasma concentration was measured using a commercially available ELISA test (Brahms Procalcitonin Assay, Thermo Fisher Diagnostics GmbH, Hennigsdorf, Germany). IL-6 levels, neutrophil gelatinase-associated lipocalin (NGAL) and CRP were quantified using the Multiplex Hybcell Technology (Cube Dx GmbH, 4300 St. Valentin, Austria).

2.2 | Blood sampling

Blood from ICU patients was drawn from 20 gauge catheters within the radial artery (8 cm polyethylene catheter, Vygon, Aachen, Germany) on the day of admission to the ICU, while patients with CAP and healthy volunteers were sampled by venipuncture using 21-gauge needles (Safety-Multifly, Sarstedt AG & Co, Nümbrecht, Germany). We recently showed, that arterial *vs.* venous blood sampling has insignificant effects on EV miRNA expression.[22] Blood was drawn into 9 ml serum collection tubes (S-Monovette, Sarstedt AG&Co, Nümbrecht, Germany) each, allowed to clot for 30 minutes and centrifuged at 3400 g for 10 minutes at room temperature (RT). Within 10 minutes of separation, serum was aliquoted and immediately stored at −80°C.

2.3 | Sample preparation

Samples were processed according to the manufacturer's protocols. Crude EVs were precipitated (miRCURY Exosome Isolation Kit-Serum and Plasma, Qiagen, Venlo, the Netherlands) from either 1 ml (small RNA-seq in the training cohort and additional RT-qPCR confirmation in the validation cohort) or 0.75 ml (technical RT-qPCR validation in the training cohort) of serum, respectively. As previously shown by our group, in contrast to other EV isolation methods, precipitation allows for reliable separation of sepsis patients and healthy volunteers in small RNA-seq analyses.[23] As precipitation co-isolates cell-free non-EV miRNA carriers, such as high- and low-density lipoproteins, argonaute-2 protein complexes and others,[24,25] it should be noted that miRNAs from this study are not exclusively EV-derived. Samples were therefore designated as crude EVs. After extracting cell-free total RNA, size distribution and yield were assessed by capillary electrophoresis using the RNA 6000 Pico Kit on the 2100 Bioanalyzer (Agilent Technologies, Santa Clara, USA). The miRNeasy Serum/Plasma Advanced Kit (Qiagen, Venlo, The Netherlands) was used for small RNA-seq, whereas the NucleoSpin miRNA Plasma Kit (Macherey-Nagel GmbH & Co. KG, Düren, Germany) was applied for RT-qPCR experiments. Elution steps were performed twice to increase RNA yields. After vacuum-induced centrifugal evaporation, RNA was diluted in 8 µl of nuclease-free water for small RNA-seq and 9 µl for RT-qPCR experiments, respectively. Differences in RNA concentrations were tested with the non-parametric Mann-Whitney U test using Graphpad Prism (version 8.3.0) and were reported as median values and quartiles (interquartile range, IQR).

2.4 | Small RNA sequencing

As described previously,[23] libraries were prepared with the NEBNext Multiplex Small RNA Library Prep Set for Illumina (New England Biolabs Inc, Ipswich, USA). Six ng of each cDNA library, as well as total libraries for samples with lower concentrations were pooled.

Single-end sequencing ran in 50 cycles on the HiSeq2500 (Illumina Inc, San Diego, USA).

Quality control of small RNA-seq data, trimming of adaptor sequences and alignment of reads was performed as described before.[22] Only samples with a minimum of 1 million reads altogether and 15% of miRNA reads in relation to total library size were included for analyses. DGE analysis was conducted by DESeq2 (version 1.22.1)[26] for R (version 3.5.1) with the implemented normalisation strategy based on library size correction and the Benjamini-Hochberg method to correct for the false discovery rate (FDR). miRNAs were filtered by setting a mean expression across all samples of ≥50 reads (baseMean), a minimum twofold up- or down-regulation (log2 fold change, log2FC ≥1 or log2FC ≤ −1) and adjusted *P*-value padj ≤ 0.05. miRNAs that failed to be detected in more than one sample per group were removed prior to selecting the most drastically dysregulated miRNAs based on log2FC. Unsupervised clustering was performed by principal component analysis (PCA). Additionally, after filtering small RNA-seq data for baseMean ≥500, supervised clustering was performed by sparse partial-least-squares discriminant analysis (sPLS-DA) with four components and maximum five features each using mixOmics[27] to assess the minimal number of miRNAs required to separate groups. Combining data from both, DGE analysis and sPLS-DA, a subset of candidate miRNAs serving as a whole biomarker signature was selected. Statistical significance of RNA mapping was tested with the non-parametric Kruskal-Wallis test followed by Dunn's multiple comparison test using Graphpad Prism (version 8.3.0). Relative mapping frequencies were reported as mean values ± standard deviation.

2.5 | RT-qPCR validation

The most stably expressed miRNAs among all groups were evaluated from the NGS data set as potential reference miRNAs by NormFinder.[28] Validations of the biomarker signature were performed by RT-qPCR using the LNA-optimized miRNA PCR system (miRCURY LNA RT kit, miRCURY LNA SYBR Green PCR kit, Qiagen, Venlo, the Netherlands). For reverse transcription, 6.5 µl of cell-free total RNA was used as template for cDNA synthesis. qPCR reactions were prepared according to the manufacturer's recommendation with the appropriate miRCURY LNA miRNA PCR Assays (Qiagen, Venlo, the Netherlands) for the biomarker candidates and the reference miR-30d-5p. The UniSp6 assay (Qiagen, Venlo, the Netherlands) was used as control for cDNA synthesis and PCR amplification. qPCR reactions were run in triplicates on a ViiA 7 Real-Time PCR System (Thermo Fisher Scientific, Waltham, USA) with the low ROX reference dye (Qiagen, Venlo, the Netherlands). Amplification plots and melting curves were analysed using the QuantStudio Real-Time PCR Software (version 1.3, Applied Biosystems, Waltham, USA). Assays with insufficient signal detection were excluded. Only samples with Cq (cycle quantification) values lower than 38 cycles in at least two replicates were included for analyses. Mean Cq values were quantified relatively with the ΔΔCq method.[29] Statistical analyses of data were performed by Graphpad

Prism (version 8.3.0) using the non-parametric Kruskal-Wallis test followed by Dunn's multiple comparison test. miRNA expression levels from small RNA-seq and RT-qPCR experiments were compared by Spearman's rank-order correlation. Spearman's r and 95% confidence intervals were reported. Additionally, group classification of RT-qPCR data from the independent validation cohort was performed based on partial-least-squares discriminant analysis (PLS-DA) of RT-qPCR data from the training cohort. Expression values of validated miRNAs were depicted as median and IQR.

2.6 | Statistical analysis of demographics and clinical data

Demographic characteristics and clinical data were compared using the non-parametric Mann-Whitney U test or in case of more than two groups by ANOVA on Ranks followed by Dunn's post hoc test. The chi-square or Fisher's exact test was used for comparison of categorical variables. Expression levels of significantly regulated miRNAs from the NGS and the qPCR confirmation analysis were correlated with demographic and clinical data from CAP and sepsis patients of the training and validation cohorts by calculating the non-parametric Spearman's Rank Order correlation.

Data analysis was performed using Python version 3.7 (Python Software Foundation, Beaverton, USA) and SPSS (IBM SPSS Statistics for Windows, version 25; IBM Corp., Armonk, NY, USA). Data in the text and in tables are reported as median and IQR. All statistical tests were two-tailed, and a P-value <0.05 was considered statistically significant.

2.7 | Identification of pathways relevant to community-acquired pneumonia

Ingenuity Pathway Analysis (IPA, Spring version 2020, Qiagen Bioinformatics, Redwood, USA) was used for the in silico identification of gene targets and causal networks from the high-throughput miRNA expression data of the training set (n = 67 patients). Only the 29 miRNAs meeting the predefined cut-off values (baseMean ≥50, log2FC ≥1 or log2FC ≤ −1 and padj ≤0.05) were entered into IPA, and only experimentally confirmed relationships were considered for the identification of miRNA targets and the characterisation of regulatory effects. Possible gene targets were identified using the IPA 'microRNA Target Filter' to identify target genes and to construct networks of relevance to CAP. Disease filtering was set to 'infectious disease', and the network for 'cellular and humoral immune response' was selected.

2.8 | Ethics approval and consent to participate

Approval of the study was granted by the Ethics Committee of the Medical Faculty of the Ludwig-Maximilians-University of Munich

under Protocol #551-14. All samples were anonymised during analyses. The study was conducted in accordance with approved guidelines, and written informed consent to participate was obtained from each participant or the patient's legal representative.

3 | RESULTS

3.1 | Study population

Demographic data of patients with CAP were comparable to healthy volunteers with regard to Body Mass Index, but healthy individuals were significantly younger than patients with CAP (50.0, 45.5-53.0 years vs. 73.0, 63.2-81.0 years, $P < 0.001$). Patients with CAP and sepsis from the training and validation cohorts were comparable with no significant differences in demographic and treatment data (see Tables S2 and S3 of the supporting information). Patients with sepsis were significantly younger and had significantly higher plasma concentrations of the inflammatory markers PCT, CRP, NGAL and IL-6 at ICU admission and a significantly longer duration of hospital stay than patients with CAP (see Table S4 of the online supplement for details).

3.2 | RNA yield, sequencing quality and mapping distribution

As different RNA isolation kits might influence miRNA recovery and composition of RNA,[30,31] yields of crude EVs precipitated from 1 ml serum diverged with respect to individual variation and the isolation method. With 22.30 (8.18-56.28) ng, the median amount of total RNA across all groups was significantly higher ($P = 0.003$) in the validation cohort, when compared to the 11.45 (4.67-24.10) ng of the training cohort. The median amount of total RNA extracted from the training cohort using the miRNeasy Serum/Plasma Advanced Kit (Qiagen, Venlo, the Netherlands) was 7.26 (1.00-11.45) ng for volunteers, 11.26 (2.73-30.71) ng for CAP patients and 20.04 (11.94-64.60) ng for patients with sepsis. With the NucleoSpin miRNA Plasma Kit (Macherey-Nagel GmbH & Co. KG, Düren, Germany) total RNA yields from the validation cohort were 8.13 (5.83-16.38) ng for volunteers, 21.97 (8.79-54.27) ng for patients with CAP and 45.66 (27.16-95.22) ng for sepsis patients.

FastQC[32] evaluated high per-base sequence quality (base 1-30) for all samples with median Phred scores of either 38 or 40. Across all samples, 1894 different miRNAs were detected with at least one read in one sample. Out of these, 225 miRNAs showed an expression level of baseMean ≥50 reads, corresponding to the filter, that was set as the expression minimum during DGE analysis.

Library sizes (Figure 1A), as well as numbers of mapped miRNAs (Figure 1B) tended to be higher in volunteers when compared to patients, while no apparent difference was present between both patient groups. Relative miRNA frequencies were 40.9 ± 11.3% for volunteers, 28.0 ± 9.3% for CAP patients and 31.5 ± 14.4% for

patients with sepsis. Additionally, patient groups had higher frequencies of short sequences < 16 nucleotides in size (CAP: 20.3 ± 15.6%, sepsis: 15.0 ± 12.3%) when compared to volunteers 8.5 ± 8.4%, which probably represent degradation products from longer coding and non-coding RNA species (CAP vs. volunteers: $P = 0.012$, sepsis vs. volunteers: $P = 0.061$, CAP vs. sepsis: $P = 0.831$). The mapping distribution is visualised by relative mean frequencies (Figure 1C).

3.3 | Small RNA sequencing data analyses

When performing unsupervised clustering based on the 500 miRNAs with highest variance, different patient groups overlapped, but could be distinctly separated from volunteers (Figure 2A). Patients with CAP and lower overall disease severity tended to reflect the miRNA profiles of volunteers more closely than sepsis patients, who were more distinctly separated.

Analysing DGE data, the comparison of CAP patients with volunteers revealed 29 significantly up- or down-regulated miRNAs (see Table S5 of the supporting information).

Among these cell-free miRNAs, expression levels of several transcripts correlated with indicators of disease severity in CAP patients including the CURB-65 score as assessment score for pneumonia and the associated risk of mortality,[8] total duration of hospital stay, and plasma levels of NGAL (see Table 1 for details). Only miR-127-3p was related to demographic variables of CAP patients (age: $r = 0.627$, $P = 0.029$) but none of the other miRNAs appeared to be influenced by demographics.

Comparing patients with CAP to those with sepsis, we detected 25 miRNAs with altered expression (see Table S5 of the supporting information). A number of these miRNAs correlated significantly with treatment variables, indicating face validity of these transcripts. In particular, expression values of miR-1-3p were related to plasma

concentrations of the inflammatory markers IL-6, NGAL and vasopressor requirements in sepsis (see Table 2 for details).

In order to establish an integrated biomarker signature, the three most drastically dysregulated miRNAs were selected from each DESeq2 comparison (CAP vs. volunteers: miR-582-3p, miR-432-5p, miR-542-3p; CAP vs. sepsis: miR-1246, miR-1-3p, miR-4433b-3p).

Based on sPLS-DA, group separation was achieved on the basis of twelve miRNAs as discriminators (Figure 2B). Out of these, four miRNAs (miR-182-5p, miR-193a-5p, miR-215-5p, miR-93-5p) were also detected using DESeq2 with log2FC ≥1 or log2FC ≤ −1 (see Table S5 of the supporting information for comparison), while all other miRNAs showed no regulation according to our threshold settings for DGE analysis.

Combining the respective miRNAs from both multivariate analyses, a subset of eighteen miRNAs (miR-432-5p, miR-542-3p, miR-582-3p, miR-1246, miR-1-3p, miR-4433b-3p, miR-181b-5p, miR-182-5p, miR-186-5p, miR-193a-5p, miR-199a-3p = miR-199b-3p, miR-21-5p, miR-215-5p, miR-30e-5p, miR-340-5p, miR-425-5p, miR-93-5p, miR-941) was identified as potential biomarker signature.

3.4 | RT-qPCR validation

The eighteen candidate miRNAs were quantified by RT-qPCR, as a supplementary method, in the same cohort that was used for high-throughput sequencing and additionally confirmed in an independent second cohort of individuals. After quality control of RT-qPCR data, twelve miRNAs remained for analyses.

By reading in RT-qPCR data of all twelve miRNAs measured in the training cohort to PLS-DA, groups were separated and equally distributed compared to the small RNA-seq data (Figure 3A). According to findings from PLS-DA, samples in the validation cohort could be correctly classified using principal components 1-10 and displayed
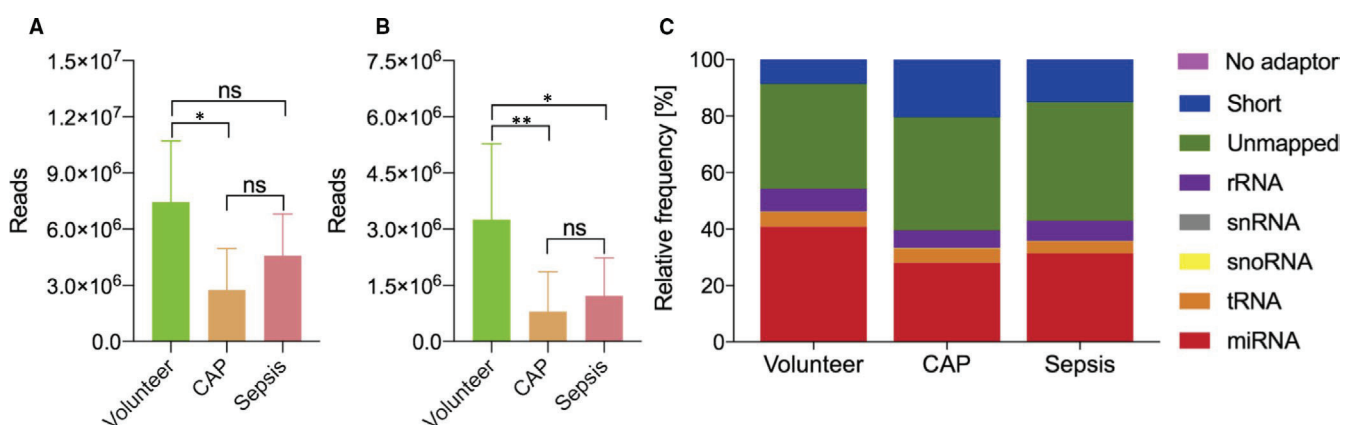

FIGURE 1 Library sizes (A) and mapped miRNA reads (B) are depicted for volunteers, patients with community-acquired pneumonia (CAP) and sepsis as median values and 95% confidence intervals. Library sizes, as well as numbers of mapped miRNA reads tended to be higher in volunteers compared to patients, with no apparent difference between patient groups. Read counts in the mapping distribution (C) are visualised as mean relative frequencies. Volunteers have higher relative miRNA frequencies, as well as fewer incidences of short sequences (<16 nucleotides) when compared to patient groups. No adaptor: sequence lacking adaptors; short: sequence < 16 nucleotides; unmapped: sequence did not align to any of the mapped RNA classes; rRNA: ribosomal RNA; snoRNA: small nucleolar RNA; snRNA: small nuclear RNA; tRNA: transfer RNA; miRNA: microRNA; * $P < 0.05$; ** $P < 0.005$; ns: not significant
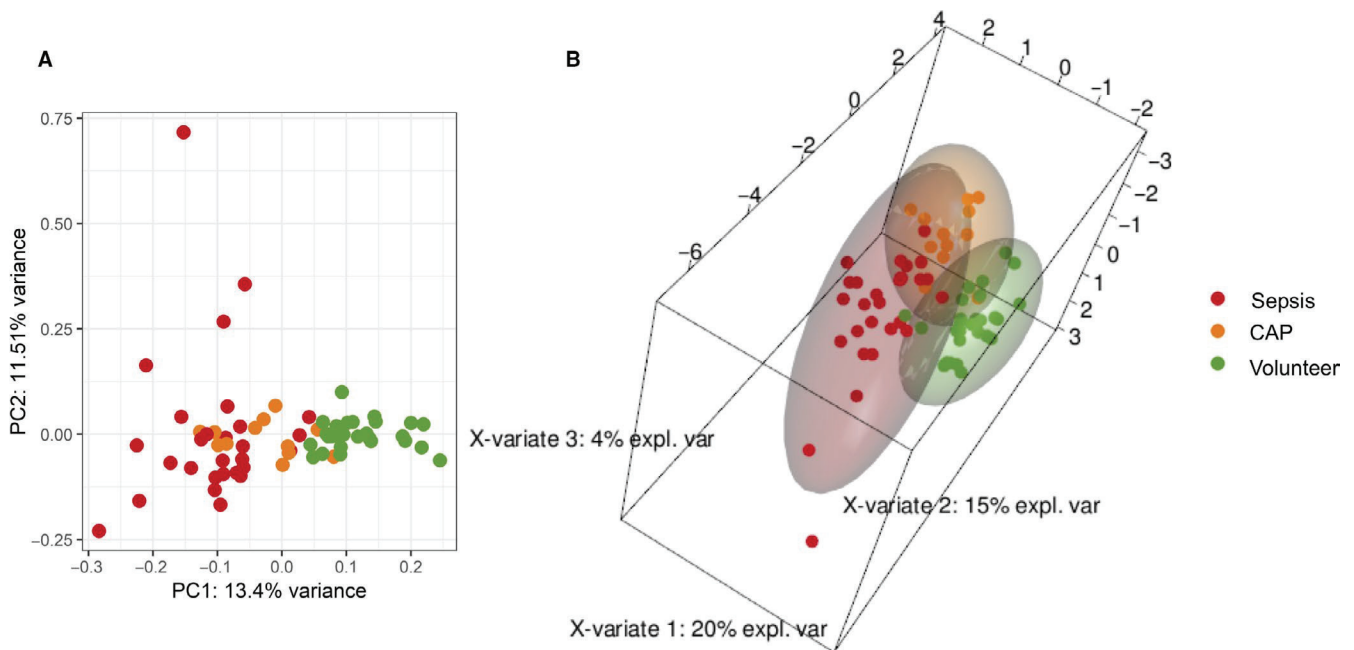
FIGURE 2 Multivariate analyses of small RNA-sequencing data. Unsupervised clustering (A) by principal component analysis based on the 500 miRNAs with highest variance. Volunteers clustered separately from patient groups. Sepsis patients were separated more distinctly from volunteers than patients with community-acquired pneumonia (CAP). Sparse partial-least-squares discriminant analysis for components 1-3 (B) discriminated different groups by twelve miRNAs. PC: principal component; expl. var: explained variance

TABLE 1 Correlational matrix showing the relationship between demographic and treatment variables and expression values of significantly regulated miRNAs from the NGS training set comparing patients with community-acquired pneumonia and healthy volunteers. Data are Spearman's correlational coefficients/P-value. miRNAs were derived from Table S5 presented in the online supplement

miRNA	Age	CURB-65[a] Score	Total hospital stay	Leucocyte count	NGAL[b]
miR-127-3p	0.627/0.029	0.587/0.045	-	-	−0.664/0.018
miR-193b-5p	-	0.667/0.018	-	-	−0.832/0.001
miR-193a-5p	-	-	0.789/0.002	-	-
miR-215-5p	-	−0.613/0.034	-	-	-
miR-450b-5p	-	-	-	0.636/0.035	-
miR-452-5p	-	-	-	−0.800/0.003	-
miR-320d	-	-	-	-	−0.636/0.026
miR-338-5p	-	-	-	-	0.699/0.011
miR-379-5p	-	-	-	-	−0.860/<0.001

[a]Confusion, Urea, Respiratory Rate, Blood Pressure and Age score for pneumonia severity.
[b]Neutrophil gelatinase-associated lipocalin.

high discriminatory power with 73.3% of correctly assigned samples for reduced models from principal components 1-6 or 1-8, respectively (Figure 3B).

Out of these miRNAs, some transcripts showed the same expression pattern for both group comparisons independent of cohort and approach used for analysis, albeit with reversed trends (Figure 4A and C). With one exception, Spearman's rank-order correlation of miRNA expression from the NGS and RT-qPCR data sets showed an overall significant positive relationship (Figure 4B and D). The three most drastically dysregulated miRNAs (CAP *vs.* volunteers: miR-193a-5p, miR-542-3p and miR-1246; CAP *vs.* sepsis: miR-1246) with

equal expression pattern for both approaches and cohorts of individuals were selected as candidate biomarkers for further analysis.

3.5 | Expression levels of candidate miRNAs according to subgroups

When analysing miRNA expression levels in all individuals from both the training and validation cohort together (Figure 5), normalised ΔCq values of miR-193a-5p in patients with CAP were significantly lower (ΔCq = 1.41, 0.57-3.21) than in healthy volunteers

TABLE 2 Correlational matrix showing the relationship between demographic, treatment variables, inflammatory markers (lower part of the table) and expression values of significantly regulated miRNAs from the NGS training set comparing patients with community-acquired pneumonia and those with sepsis. Data are Spearman's correlational coefficients/P-value. miRNAs were derived from Table S5 presented in the online supplement

miRNA	Age	APACHE II-Score	Duration of ICU-treatment	Total hospital stay	Duration of mechanical ventilation
miR-1246	−0.529/0.004	-	-	0.418/0.042	-
miR-1-3p	−0.447/0.017	-	-	-	-
miR-18a-3p	0.436/0.013	-	−0.411/0.046	−0.433/0.024	−0.400/0.035
miR-150-3p	-	0.390/0.044	0.475/0.019	-	-
miR-92a-3p	-	-	−0.473/0.019	-	-
miR-93-5p	-	-	−0.496/0.014	−0.413/0.045	-
miR-511-5p	-	-	-	0.425/0.038	-

miRNA	PCT[a]	CRP[b]	IL-6[c]	NGAL[d]	Vasopressor requirement[e]
miR-150-3p	−0.483/0.009	-	-	-	-
miR-4433b-3p	−0.452/0.016	-	-	-	-
miR-1228-5p	-	−0.494/0.009	-	-	-
miR-1-3p	-	-	0.460/0.014	0.423/0.028	0.577/0.002
miR-500a-3p	-	-	-	-	0.458/0.016
miR-95-3p	-	-	-	-	0.493/0.009
miR-660-5p	-	-	-	-	0.469/0.014

[a]Procalcitonin.

[b]C-reactive protein.

[c]Interleukin-6.

[d]Neutrophil gelatinase-associated lipocalin.

[e]Vasopressor requirements are represented by the required dosage of norepinephrine to achieve an adequate mean arterial pressure to maintain organ perfusion in sepsis.

(ΔCq = 3.93, 2.83-5.22, $P < 0.001$) with no significant difference to patients with sepsis (ΔCq = 1.53, 0.24-2.39). For miR-542-3p, a similar pattern was observed. Normalised ΔCq values were again significantly lower in patients with CAP (ΔCq = 4.33, 3.46-5.02) than in healthy individuals (ΔCq = 5.72, 5.19-6.13, $P < 0.001$) with no significant difference to sepsis (ΔCq = 4.66, 3.31-5.71). Normalised Cq values of miR-1246 showed a significant decrease from healthy individuals (ΔCq = 2.54, 2.00-3.05) to patients with CAP (ΔCq = 0.41, −0.22-1.68, $P < 0.001$) to those with sepsis (ΔCq=−1.14, −2.10-0.07, $P = 0.005$). Overall, these findings indicate higher expression values of the respective miRNAs with higher disease severity.

3.6 | 'The cellular and humoral immune response' in community-acquired pneumonia

When IPA target filtering was set to '*cellular and humoral immune response*', the resulting canonical network in CAP patients was primarily affected by 6 of the 29 significantly regulated miRNAs with 42 possible target mRNA transcripts. Figure S1 in the online supplement shows a simplified network of the two validated and up-regulated miRNAs miR-193a-5p and miR-542-3p, their possible mRNA targets

and their interaction. Possible molecular targets identified by applying the IPA '*microRNA Target Filter*' module for the candidate miRNA miR-193a-5p were IL-10 (Interleukin-10), IL2RG (Interleukin-2 receptor subunit gamma) and mTOR (mechanistic Target of Rapamycin). One of the identified molecular targets of miR-542-3p was inflammatory mediator PTGS2 (prostaglandin G/H synthase 2).

4 | DISCUSSION

Our study outlines the possibility of using cell-free miRNA biomarkers to discriminate patients with CAP from healthy volunteers and from those with sepsis as a severe secondary complication. We characterised a subset of twelve miRNAs as a potential biomarker for this purpose, technically validated miR-193a-5p, miR-542-3p and miR-1246 and confirmed our findings in an independent cohort.

When analysing relative miRNA expression, miR-1246 showed significant increases with more severe overall disease from volunteers to patients with CAP and to those with sepsis, whereas miR-193a-5p and miR-542-3p differentiated patients with an infectious disease (CAP or sepsis) from healthy individuals.

The miR-193a/b-5p family was previously shown to be a possible indicator for CAP, as expression of miR-193b-5p was related
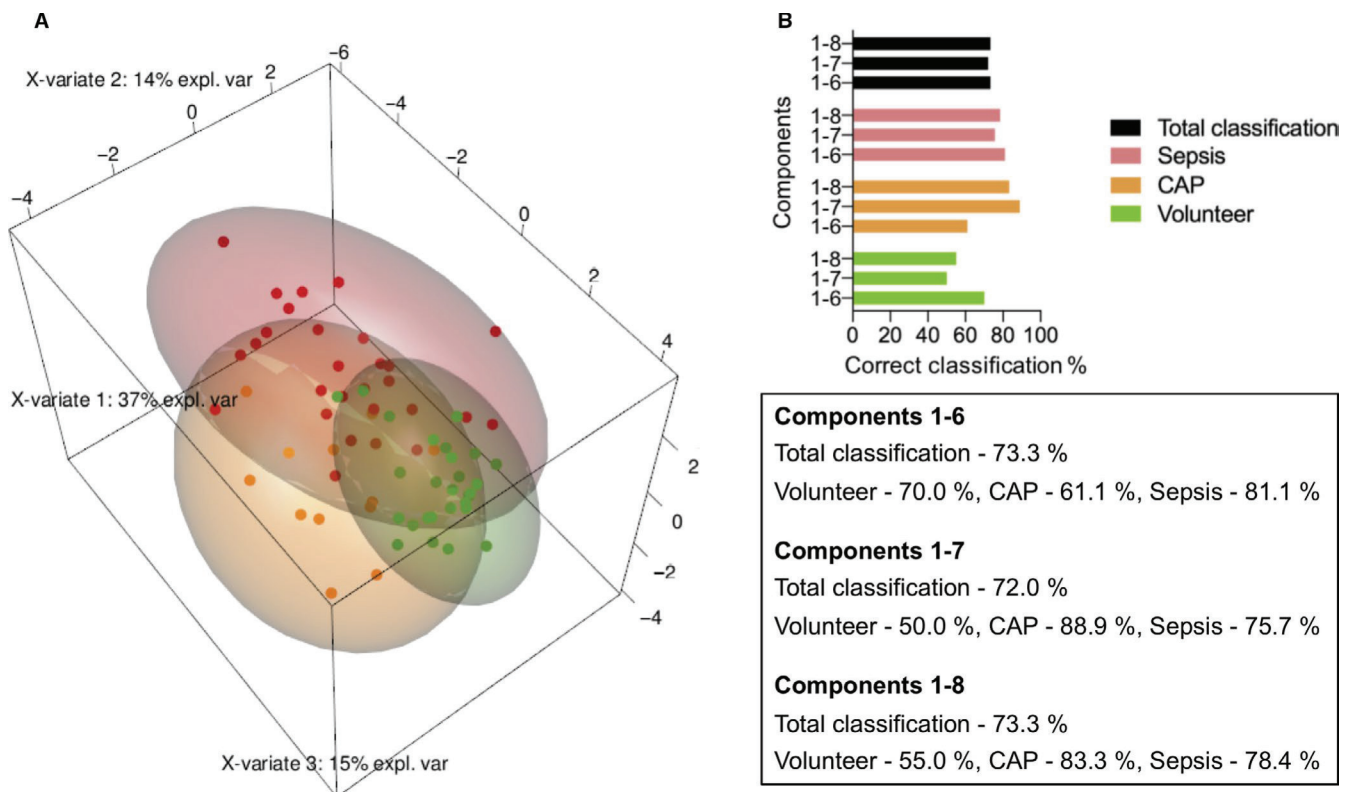
A

B

FIGURE 3 Multivariate analyses of reverse transcription quantitative real-time PCR (RT-qPCR) data. Partial-least-squares discriminant analysis for components 1-3 (A). Based on expression levels (ΔCq) of the twelve miRNAs from the RT-qPCR validation in the training cohort, groups were separated. Correct total classification of the validation cohort based on expression (ΔCq) of the twelve miRNAs from the training cohort and assignment for each individual group (B). expl. var: explained variance

to the CURB-65 score, a validated clinical prediction score for pneumonia and the associated risk of mortality[8] and also to NGAL plasma levels. NGAL has recently been described as a useful biomarker for lower respiratory tract infections[33] and the associated mortality[34] and may also serve as an indicator of an ongoing risk for renal injury,[35] which is common in patients with pulmonary disorders.[36] Moreover, expression levels of miR-193a-5p were related to the duration of the required hospital stay in our study. Identified molecular targets of miR-193a-5p included IL-10, which is known to correlate with the CURB-65 score and is associated with increased mortality in patients with CAP[37] and mTOR, which has been shown to be down-regulated in sepsis due to CAP.[38] Our group previously showed the positive correlation of cell-free miR-193a-5p expression with disease severity in sepsis patients.[17] Expression levels of miR-193 in serum were also associated with death from sepsis in recent studies.[39] miR-542-3p was shown to be a causal mediator of mitochondrial dysfunction in muscle tissue of patients with sepsis.[40] In our study, one of the molecular targets of miR-542-3p was PTGS2, a pro-inflammatory mediator, which is known to be responsible for the production of prostaglandins that are involved in the inflammatory response.[41] Moreover, elevated miR-1246 levels have been shown to mediate lipopolysaccharide-induced apoptosis of pulmonary endothelial cells and acute lung injury.[42] In conclusion, our findings indicate that these three cell-free miRNAs may be

valuable for the diagnosis of CAP and sepsis as a severe secondary complication.

The fact that these miRNAs were also associated to EVs isolated from the peripheral circulation suggests a possible role of these vesicles in mediating inflammatory signals from the lung to the periphery including blood cells or *vice versa* by acting as a transport media for non-coding RNAs and other signalling molecules. A recent study in animals with experimental bacterial pulmonary infection clearly demonstrated the existence of a subpopulation of EVs in bronchoalveolar lavage fluid that contained high concentrations of pro-inflammatory miRNAs and was likely derived from alveolar epithelial type-I cells.[43] These EVs could theoretically reach the peripheral circulation, but the responsible mechanisms for transport of EVs within the lung and to the periphery are poorly understood.[44] Our observation that the expression values of some of the differentially expressed miRNAs isolated from crude EVs clearly correlated with clinical indicators of pneumonia severity points to this possibility but does not prove it.

A limitation of our study results from the fact that two different RNA extraction methods were used for small RNA-seq and RT-qPCR. As miRNA composition might vary with the respective RNA isolation method,[30,31] and different approaches were used, our data might be biased partially. Given the fact that individual biological properties and different miRNA analysing platforms
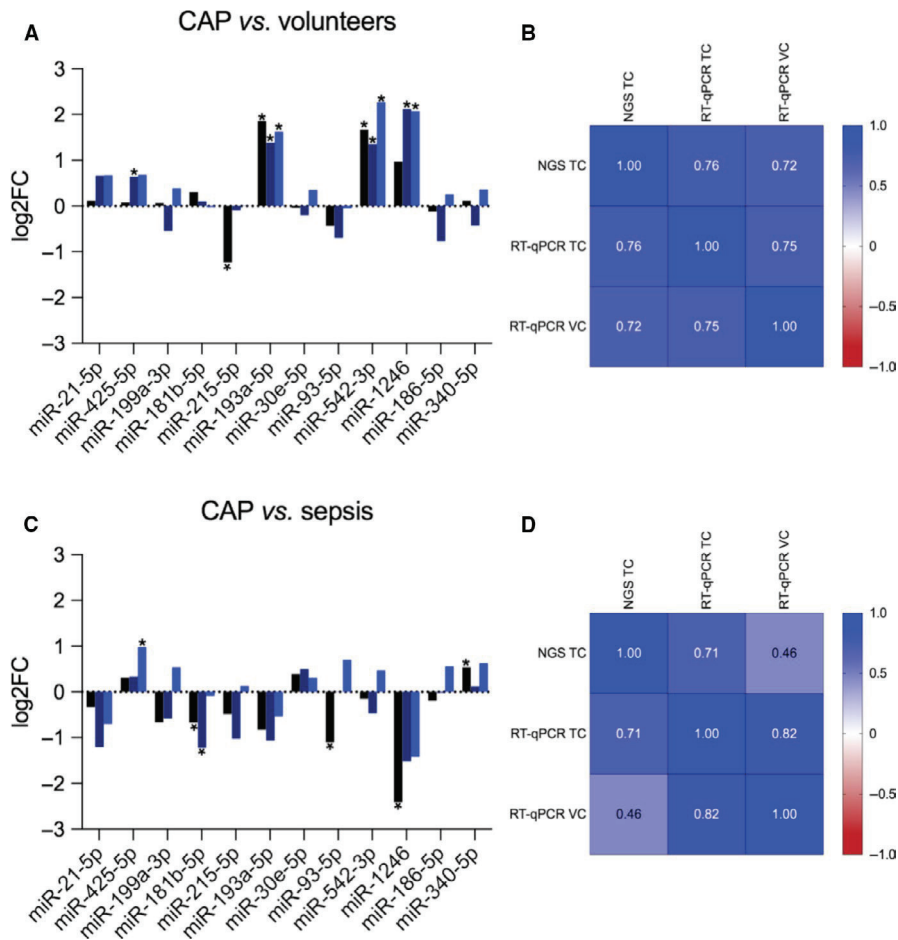
FIGURE 4 Log2 fold changes (log2FC) for CAP vs. volunteers (a), and CAP vs. sepsis (c) calculated from next-generation sequencing (NGS, black) and reverse transcription quantitative real-time PCR (RT-qPCR) data in the training (TC, dark blue) and validation cohort (VC, light blue). Significant changes are marked by asterisks. Spearman's correlation matrix of expression levels (log2FC) from NGS and RT-qPCR data sets shown as heatmaps for CAP vs. volunteers (b) and CAP vs. sepsis (d). CAP vs. volunteers: NGS TC vs. RT-qPCR TC, $r = 0.76$ (0.32-0.93), $P = 0.006$; NGS TC vs. RT-qPCR VC, $r = 0.72$ (0.23-0.92), $P = 0.011$; RT-qPCR TC vs. RT-qPCR VC: $r = 0.75$ (0.29-0.93), $P = 0.007$; CAP vs. sepsis: NGS TC vs. RT-qPCR TC, $r = 0.71$ (0.22-0.92), $P = 0.012$; NGS TC vs. RT-qPCR VC, $r = 0.46$ (−0.17 − 0.82), $P = 0.13$; RT-qPCR TC vs. RT-qPCR VC: $r = 0.82$ (0.45-0.95), $P = 0.002$; CAP: community-acquired pneumonia
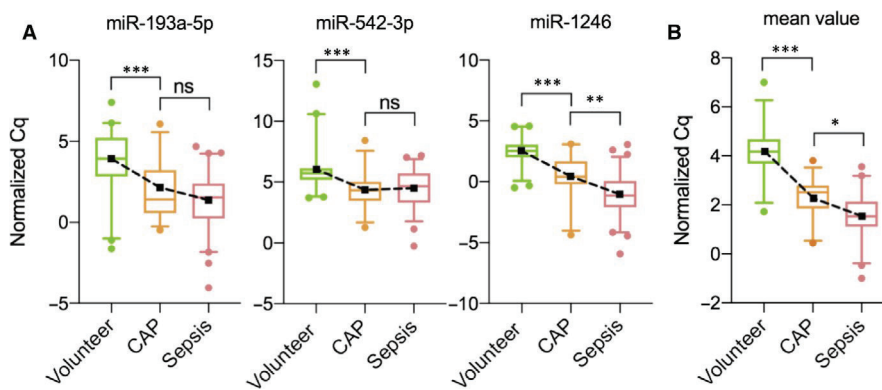
FIGURE 5 Merge of technically and additionally validated miRNAs from reverse transcription quantitative real-time PCR experiments for each miRNA separately (A), and mean values of all three miRNAs (B). Data are displayed as boxplots from the 5th to the 95th percentile, showing median (line) and mean (square) values. Dots represent samples outside the percentile range. Changes in mean miRNA expression among groups are indicated by dashed lines. Lower values of ΔCq indicate higher expression levels of the respective miRNAs. Cq: cycle quantification; *$P < 0.05$; **$P = 0.005$; ***$P < 0.001$; ns: not significant

(NGS and RT-qPCR) are associated with miRNA expression profiles,[45,46] this might have contributed to reversed trends in miRNA regulation seen with some of the miRNAs identified in our study. However, the fact that our final biomarker signature has been confirmed for two different RNA extraction methods (1), miRNA analysing platforms (2) and individual cohorts (3) might represent additional proof of its stability.

In conclusion, our findings indicate that in patients with suspected CAP, cell-free miR-193a-5p, miR-miR-542-3p and miR-1246 may serve as indicators for CAP, whereas a further increase in miR-1246 may suggest an increased risk to develop sepsis. For the successful use of these miRNAs as biomarkers, studies in larger patient cohorts with both conditions will be required to confirm our data of this novel diagnostic approach.

CONFLICT OF INTEREST

The authors confirm that there are no conflicts of interest.

AUTHORS' CONTRIBUTION

Stefanie Hermann: Conceptualization (supporting); Data curation (lead); Formal analysis (lead); Visualization (lead); Writing-original draft (lead). Florian Brandes: Conceptualization (supporting); Data curation (lead); Formal analysis (lead); Writing-original draft (lead). Benedikt Kirchner: Conceptualization (supporting); Formal analysis (supporting); Visualization (supporting); Writing-review & editing (equal). Dominik Buschmann: Conceptualization (supporting); Formal analysis (supporting); Writing-review & editing (equal). Melanie Borrmann: Conceptualization (supporting); Formal analysis (supporting); Writing-review & editing (equal). Matthias Klein: Conceptualization (supporting); Writing-review & editing (equal). Stefan Kotschote: Conceptualization (supporting); Funding acquisition (lead); Writing-review & editing (equal). Michael Bonin: Conceptualization (supporting); Funding acquisition (lead); Writing-review & editing (equal). Marlene Reithmair: Conceptualization (lead); Funding acquisition (lead); Project administration (lead); Writing-review & editing (equal). Ines Kaufmann: Conceptualization (supporting); Writing-review & editing (equal). Gustav Schelling: Conceptualization (lead); Data curation (lead); Formal analysis (lead); Writing-original draft (lead). Michael W Pfaffl: Conceptualization (lead); Funding acquisition (lead); Project administration (lead); Writing-review & editing (equal).

DATA AVAILABILITY STATEMENT

Small RNA-seq data were deposited with the European Nucleotide Archive (http://www.ebi.ac.uk/ena/data/view/PRJEB35757). RT-qPCR data are available from the corresponding author upon reasonable request.

ORCID

Stefanie Hermann https://orcid.org/0000-0002-6274-5919
Florian Brandes https://orcid.org/0000-0003-3741-287X
Benedikt Kirchner https://orcid.org/0000-0003-3878-0148
Dominik Buschmann https://orcid.org/0000-0003-0460-6459
Marlene Reithmair https://orcid.org/0000-0002-9113-9643

REFERENCES

1. Global Health Estimates 2016. Disease burden by Cause, Age, Sex, by Country and by Region, 2000–2016. Geneva, World Health Organization; 2018.
2. Guertler C, Wirz B, Christ-Crain M, et al. Inflammatory responses predict long-term mortality risk in community-acquired pneumonia. *Eur Respir J.* 2011;37:1439-1446.
3. Aliberti S, Dela Cruz CS, Sotgiu G, et al. Pneumonia is a neglected problem: it is now time to act. *Lancet Resp Med.* 2019;7:10-11.
4. Thompson K, Venkatesh B, Finfer S. Sepsis and septic shock: Current approaches to management. *Intern Med J.* 2019;49:160-170.
5. Thompson BT, Chambers RC, Liu KD. Acute respiratory distress syndrome. *N Engl J Med.* 2017;377:562-572.
6. Mandell LA, Wunderink RG, Anzueto A, et al. Infectious diseases society of America/American thoracic society consensus guidelines on the management of community-acquired pneumonia in adults. *Clin Infect Dis.* 2007;44(Suppl 2):S27-72.
7. Sungurlu S, Balk RA. The role of biomarkers in the diagnosis and management of pneumonia. *Clin Chest Med.* 2018;39:691-701.
8. Lim WS, van der Eerden MM, Laing R, et al. Defining community acquired pneumonia severity on presentation to hospital: an international derivation and validation study. *Thorax.* 2003;58:377-382.
9. Ranzani OT, Taniguchi LU, Torres A. Severity scoring systems for pneumonia: current understanding and next steps. *Curr Opin Pulm Med.* 2018;24:227-236.
10. Musher DM, Thorner AR. Community-acquired pneumonia. *N Engl J Med.* 2014;371:1619-1628.
11. Yáñez-Mó M, Siljander P-M, Andreu Z, et al. Biological properties of extracellular vesicles and their physiological functions. *J Extracell Vesicles.* 2015;4:27066.
12. Lee H, Abston E, Zhang D, et al. Extracellular vesicle: An emerging mediator of intercellular crosstalk in lung inflammation and injury. *Front Immunol.* 2018;9:924.
13. Raeven P, Zipperle J, Drechsler S. Extracellular vesicles as markers and mediators in sepsis. *Theranostics.* 2018;8:3348-3365.
14. Bartel S, La Grutta S, Cilluffo G, et al. Human airway epithelial extracellular vesicle miRNA signature is altered upon asthma development. *Allergy.* 2019;75(2):346-356.
15. Jung AL, Møller Jørgensen M, Bæk R, et al. Surface proteome of plasma extracellular vesicles as biomarkers for pneumonia and acute exacerbation of chronic obstructive pulmonary disease. *J Infect Dis.* 2020.221(2):325–335.
16. Lin J, Wang Y, Zou Y-Q, et al. Differential miRNA expression in pleural effusions derived from extracellular vesicles of patients with lung cancer, pulmonary tuberculosis, or pneumonia. *Tumour Biol.* 2016;37(12):15835-15845.
17. Reithmair M, Buschmann D, Märte M, et al. Cellular and extracellular miRNAs are blood-compartment-specific diagnostic targets in sepsis. *J Cell Mol Med.* 2017;21:2403-2411.
18. Huang S, Feng C, Zhai Y-Z, et al. Identification of miRNA biomarkers of pneumonia using RNA-sequencing and bioinformatics analysis. *Exp Ther Med.* 2017;13:1235-1244.
19. Real JM, Ferreira LRP, Esteves GH, et al. Exosomes from patients with septic shock convey miRNAs related to inflammation and cell cycle regulation: new signaling pathways in sepsis? *Crit Care.* 2018;22:68.
20. Metlay JP, Waterer GW, Long AC, et al. Diagnosis and treatment of adults with community-acquired pneumonia. an official clinical practice guideline of the American thoracic society and infectious diseases society of America. *Am J Respir Crit Care Med.* 2019;200:e45–e67.
21. Shankar-Hari M, Phillips GS, Levy ML, et al. Developing a new definition and assessing new clinical criteria for septic shock: For the third international consensus definitions for sepsis and septic shock (Sepsis-3). *JAMA.* 2016;315:775-787.
22. Hermann S, Buschmann D, Kirchner B, et al. Transcriptomic profiling of cell-free and vesicular microRNAs from matched arterial and venous sera. *J Extracell Vesicles.* 2019;8:1670935.
23. Buschmann D, Kirchner B, Hermann S, et al. Evaluation of serum extracellular vesicle isolation methods for profiling miRNAs by next-generation sequencing. *J Extracell Vesicles.* 2018;7:1481321.

24. Arroyo JD, Chevillet JR, Kroh EM, et al. Argonaute2 complexes carry a population of circulating microRNAs independent of vesicles in human plasma. *Proc Natl Acad Sci USA*. 2011;108:5003-5008.

25. Karttunen J, Heiskanen M, Navarro-Ferrandis V, et al. Precipitation-based extracellular vesicle isolation from rat plasma co-precipitate vesicle-free microRNAs. *J Extracell Vesicles*. 2019;8:1555410.

26. Love MI, Huber W, Anders S. Moderated estimation of fold change and dispersion for RNA-seq data with DESeq2. *Genome Biol*. 2014;15:550.

27. Rohart F, Gautier B, Singh A, et al. mixOmics: an R package for 'omics feature selection and multiple data integration. *PLoS Comput Biol*. 2017.13(11):e1005752–.

28. Andersen C, Jensen J, Ørntoft TF. Normalization of real-time quantitative reverse transcription-PCR data: A model-based variance estimation approach to identify genes suited for normalization, applied to bladder and colon cancer data sets. *Cancer Res*. 2004;64:5245-5250.

29. Livak K, Schmittgen T. Analysis of relative gene expression data using real-time quantitative PCR and the 2(-Delta Delta C(T)) Method. *Methods*. 2001;25:402-408.

30. Tan GW, Khoo AS, Tan LP. Evaluation of extraction kits and RT-qPCR systems adapted to high-throughput platform for circulating miRNAs. *Sci Rep*. 2015;5:9430.

31. Guo Y, Vickers K, Xiong Y, et al. Comprehensive evaluation of extracellular small RNA isolation methods from serum in high throughput sequencing. *BMC Genom*. 2017;18:50.

32. Andrews S. FastQC: A quality control tool for high throughput sequence data. 2010.

33. Liu C, Wang F, Cui L, et al. Diagnostic value of serum neutrophil gelatinase-associated lipocalin, interleukin-6 and anti-citrullinated alpha-enolase peptide 1 for lower respiratory tract infections. *Clin Biochem*. 2020;75:30-34.

34. Kim JW, Hong DY, Lee KR, et al. Usefulness of plasma neutrophil gelatinase-associated lipocalin concentration for predicting the severity and mortality of patients with community-acquired pneumonia. *Clin Chim Acta*. 2016;462:140-145.

35. Zhang AN, Cai Y, Wang P-F, et al. Diagnosis and prognosis of neutrophil gelatinase-associated lipocalin for acute kidney injury with sepsis: a systematic review and meta-analysis. *Crit Care*. 2016;20:41.

36. Sorino C, Scichilone N, Pedone C, et al. When kidneys and lungs suffer together. *J Nephrol*. 2019;32:699-707.

37. Pinargote-Celorio H, Miralles G, Cano M, et al. Cytokine levels predict 30-day mortality in octogenarians and nonagenarians with community-acquired pneumonia: a retrospective observational study. *Eur J Clin Microbiol Infect Dis*. 2020;39:299-307.

38. Davenport EE, Burnham KL, Radhakrishnan J, et al. Genomic landscape of the individual host response and outcomes in sepsis: A prospective cohort study. *Lancet Resp Med*. 2016;4:259-271.

39. Wang H, Zhang P, Chen W, et al. Serum microRNA signatures identified by Solexa sequencing predict sepsis patients' mortality: A prospective observational study. *PLoS One*. 2012;7:e38885.

40. Garros RF, Paul R, Connolly M, et al. MicroRNA-542 promotes mitochondrial dysfunction and SMAD activity and is elevated in intensive care unit-acquired weakness. *Am J Respir Crit Care Med*. 2017;196:1422-1433.

41. Clària J. Cyclooxygenase-2 biology. *Curr Pharm Des*. 2003;9:2177-2190.

42. Yue Fang FG, Hao J, Liu Z. microRNA-1246 mediates lipopolysaccharide-induced pulmonary endothelial cell apoptosis and acute lung injury by targeting angiotensin-converting enzyme 2. *Am J Transl Res*. 2017;9:1287-1296.

43. Lee H, Groot M, Pinilla-Vera M, et al. Identification of miRNA-rich vesicles in bronchoalveolar lavage fluid: Insights into the function and heterogeneity of extracellular vesicles. *J Control Release*. 2019;294:43-52.

44. Haggadone MD, Peters-Golden M. Microenvironmental influences on extracellular vesicle-mediated communication in the lung. *Trends Mol Med*. 2018;24:963-975.

45. Git A, Dvinge H, Salmon-Divon M, et al. Systematic comparison of microarray profiling, real-time PCR, and next-generation sequencing technologies for measuring differential microRNA expression. *RNA*. 2010;16:991-1006.

46. Ameling S, Kacprowski T, Chilukoti RK, et al. Associations of circulating plasma microRNAs with age, body mass index and sex in a population-based study. *BMC Med Genomics*. 2015;8:61.

SUPPORTING INFORMATION

Additional supporting information may be found online in the Supporting Information section.

How to cite this article: Hermann S, Brandes F, Kirchner B, et al. Diagnostic potential of circulating cell-free microRNAs for community-acquired pneumonia and pneumonia-related sepsis. *J Cell Mol Med*. 2020;24:12054–12064. https://doi.org/10.1111/jcmm.15837